UNIVERSITY OF CALIFORNIA
SANTA CRUZ

UNRAVELING STEELHEAD LIFE HISTORY COMPLEXITY THROUGH MATHEMATICAL MODELING

A dissertation submitted in partial satisfaction of the
requirements for the degree of

DOCTOR OF PHILOSOPHY

in

STATISTICS AND APPLIED MATHEMATICS

by

Juan Lopez Arriaza

December 2015

The Dissertation of Juan Lopez Arriaza
is approved:

Professor Marc Mangel, Chair

Professor Athanasios Kottas

Professor Stephan Munch

Dr. David Boughton

Tyrus Miller
Vice Provost and Dean of Graduate Studies

Table of Contents

List of Figures

List of Tables

Abstract

Unraveling Steelhead Life History Complexity Through Mathematical Modeling

by

Juan Lopez Arriaza

Steelhead trout exhibit highly variable population dynamics that are driven by the vast life history variability of individuals that results in a complex system with highly non-linear dynamics for both individuals and populations. In this dissertation, I consider three different projects with the aim of understanding both individual processes and population dynamics using mathematical and statistical tools. In each chapter I develop new mathematical and statistical methodology that incorporates the biological knowledge about steelhead life history in order to answer different questions about the individual and population dynamics observed in nature.

The first project focuses on the development and application of methodology to better explain the observed adult returns in the Carmel River. To do this, I incorporate knowledge about conditional migration strategies into a life history model. In this work, I discover a decreasing trend in mean stream temperature that is coupled with a decreasing trend in mean length of individuals. One of the primary goals of this chapter is to test the scientific hypothesis that the inclusion of life history attributes would improve the predictions of adult returns. I demonstrate that the mechanistic inclusion of life history attributes into the mathematical model does significantly improve the ability to predict adult returns.

In the second project, I develop a Physiologically Structured Population Model (PSPM) for steelhead trout. The PSPM framework allows me to account for the biological processes driving the life history of steelhead through their entire lifetime. A benefit of this framework is that the resultant population dynamics arise solely from the interactions between individuals and their environment. The model captures the wide variability of life histories that are observed in nature. With this model, I explore the effects that size-dependent mortality and competition have on the population dynamics. I also explore the effects of three different temperature regimes on the population dynamics, highlighting the non-linear nature of the system.

The last project is the development of a Bayesian Semi-parametric model that describes the relationship between temperature and individual consumption that determines growth. Developing a state-space model that incorporates a Gaussian Process prior for the temperature-consumption relationship allows the data to determine the shape of the relationship and account for both measurement error and process stochasticity. I first test the model with simulated data with different levels of data availability, measurement error and process stochasticity. This application demonstrates that the total number of temporal measurements affects the performance of the model more than the number of individuals. I then apply the model to experimental data from a growth experiment of steelhead trout. The results demonstrate the ability of the model to describe the growth of individuals as well as to capture individual consumption. The model shows agreement between the shape of the temperature-consumption function that I predict and the relationship that is commonly used for steelhead.

Acknowledgments

The work that I have completed wouldn't have been possible without the support of a number of people. First and foremost, I thank my adviser, Marc Mangel, for his support and guidance throughout my Ph.D. He has taught me to refine my intuition about the projects I have undertaken. Marc has allowed me to explore interesting problems and helped me grow as a scientist through guidance rather than dictation. For that, I am forever grateful. His vast knowledge has served as an essential tool in my success and without the doors he has opened for me, I wouldn't be where I am.

The rest of my committee, Steve Munch, David Boughton and Thanos Kottas have been essential in my growth as a scientist and have provided me with interesting projects to work on. Without their guidance and insight, this dissertation wouldn't have been possible. Thank you also to André de Roos for allowing me to visit his group in the Netherlands and guide me through the work we undertook together.

I am in debt to the entire AMS department for the vast knowledge about Math, Statistics and life you have taught me and for incubating my scientific curiosity. Especial thanks to Tony Pourmohamad for the many discussions over coffee and cards we have had. My work has been greatly improved due to your criticisms and personal insights.

Thanks to my family for all they have done to get me to this point. Thank you to my parents for instilling a value for education and for allowing me to explore my curiosity in the natural world at a young age. Thanks to my brother for his support, discussions and guidance throughout my life.

Last but not least, thank you to my wife, Samantha, for being next to me through

these years. You were patient during the rough times and long nights. The days when my work consumed me, you were able to keep me grounded and stopped me from burning out. Above all, thank you for your love, patience and support.

Chapter 1

Introduction

Steelhead trout, *Oncorhyncus mykiss*, exhibit high levels of variability in their life history strategies. The life history of individuals can be approximately described as emergence from the redd (nest) into the stream, a period of growth in freshwater ranging from months to years, and an annual decision to migrate to the ocean or remain in the stream. The ability to migrate to the ocean before reproduction (anadromy) results in individuals being classified as either in-stream maturing (resident, rainbow) or ocean-maturing (anadromous, steelhead); with resident individuals typically being smaller in size than the ocean-maturing counterparts. The choice to undertake the ocean migration is controlled by three mechanisms: genetics, internal condition, and the environment. More specifically, during a particular period in the year, an individual makes the decision to begin the smolting process to migrate to salt water based on a genetic response to its physiological condition (e.g. weight, length, fat reserves) and its environment (e.g. temperature, food availability). This migration strategy balances the benefits of high marine growth that results in high

reproductive output, but also, the higher mortality levels experienced in the ocean. The option of residency, anadromy and the variable possibilities for age at ocean migration and time spent in the ocean results in a large number of life history choices (Table 1.1).

Freshwater Age	0	1	2	3	4	5	6
Ocean Age							
0	–	x	x	x	x	–	–
1	–	x	x	x	x	x	x
2	–	x	x	x	x	x	–
3	–	x	x	x	x	–	–
4	–	–	x	x	x	–	–
5	–	–	x	–	–	x	–
6	–	–	–	?	–	–	–

Table 1.1: Possible combinations of maturation ages based on freshwater and ocean age for migrating steelhead. Redrawn from Thorpe (1998)

In light of this complexity, in order to understand the resultant population dynamics, it is necessary to accurately describe the dynamics of the individuals within the population. Since the ultimate life history of individuals is highly influenced by their individual condition, properly describing their growth provides insight into an individual's ultimate fate. Therefore, to understand the population dynamics, in the following chapters, I employ bioenergetic models to describe the growth of individuals. Bioenergetic models provide a thermodynamically consistent way to balance the energy gained through consumption with metabolic costs and growth. Steelhead are ectotherms, so that temperature plays an important role in both consumption and metabolism; therefore in the following chapters, I explicitly account for the temperature that individuals experience and focus specifically on how it affects individual consumption in Chapter 4.

The aim of this dissertation is to understand life history complexity of individual

steelhead and connect it to the complex population dynamics that are exhibited as a result. Experimental approaches are essential to understanding many aspects of these two questions, but the scale of the problem both spatially and temporally makes understanding this complex system solely through experimental approaches infeasible. To bypass these limitations, I apply both mathematical and statistical methods to explore three distinct questions regarding both individual and population dynamics. In Chapter 2, I attack the applied problem of trying to understand the population dynamics that have been observed in the Carmel River, a watershed in the Central Coast of California. One of the goals of this chapter is to highlight the inclusion of biological mechanisms that drive different aspects of an individual's life history within a mathematical framework to provide insight into the currently unexplained population dynamics in terms of adult returns. The exposition of the work in this chapter focuses on the application and the mathematics are primarily explained in the appendices. In Chapter 3, I turn my attention to developing a mathematical model that incorporates the vast amount of knowledge about steelhead life history. I utilize the Physiologically Structured Population Models (PSPM) framework that allows me to mechanistically model the entire life history of an individual.

This is the first application of PSPMs to describe an anadromous species; I mechanistically model size-dependent competitive interactions between individuals in the population. Finally, in Chapter 4, I investigate the temperature-consumption relationship that is commonly used to model the growth of individuals. To do this I employ Bayesian Semi-parametric modeling to the consumption-temperature relationship within a Bayesian state-space framework. This modeling approach has two important benefits: first it provides

a flexible approach to handle the complex structure of the bioenergetic models used for the growth of individuals while accounting for multiple sources of uncertainty; second it allows me to forgo the use of a specific functional form for the temperature-consumption relationship.

Chapter 2

The Roles of Rearing and Rescue in Maintaining the Anadromous Life History, With Application to Steelhead in the Carmel River*

2.1 Motivation and Background

The prediction of population dynamics is in general a difficult task due to the interdependencies of physiological, genetic, and environmental processes that drive them. The first step in developing methodology to understand and describe the observed dynamics of a population is to understand the dynamics of the individual constituents of that popu-

*This chapter will be converted to a journal article by Lopez, Boughton, Urquhart, Williams, Rundio and Mangel entitled "The Roles of Rearing and Rescue in Maintaining the Anadromous Life History, With Application to Steelhead in the Carmel River" for *The North American Journal of Fisheries Management.*

lation. Due to their variable life histories, broad use of different habitats with considerable environmental heterogeneity and the influence that the environment has on an individual's life history, the challenges posed by predicting the population dynamics of anadromous salmonids epitomize the challenges in predicting population dynamics in general. This is particularly true for Steelhead trout (*Oncorhynchus mykiss*), which demonstrate arguably the highest level of life history complexity among all Pacific salmonids (Thorpe et al., 1998; Thorpe, 1998; Quinn, 2005; Pavlov et al., 2008). Steelhead are able to reproduce multiple times and can either be anadromous and migrate from fresh water to the ocean and return to fresh water to spawn; or resident, and stay in fresh water their entire lifetime. Furthermore, migrating individuals exhibit high levels of plasticity in the timing of both out and return migration, which results in a large number of different life history trajectories available to individuals, with at least 32 being observed. The choice of life history trajectory is at least partially genetically programmed to respond to the environment, primarily through an individual's body size and growth at specific decision windows (Mangel, 1994; Thorpe, 1998; Satterthwaite et al., 2010).

The maintenance of anadromy is a topic of particular importance for populations in California. California steelhead are divided into five Distinct Population Segments (DPSs), which are the anadromous component of Evolutionarily Significant Units. Due to both natural and anthropogenic factors, four of these DPSs are listed as threatened and one as endangered (Waples, 1991). The occurence of anadromy has important implications on a population through its influence on the abundance, genetic diversity and resilience of the population. The presence of migratory individuals often leads to larger population

sizes due to the higher fecundity that is achieved from growth in the ocean (Quinn et al., 2011). Straying by anadromous individuals between watersheds and reproduction between migratory and resident phenotypes increases the level of genetic diversity in a population (Garza & Pearse, 2008; Pearse et al., 2009). In addition to the higher abundance and greater genetic diversity induced by the presence of anadromous individuals, life history diversity in the form of anadromy acts as a buffering mechanism by spreading risk over space and time (Moore et al., 2014; Boughton et al., 2006). While there have been efforts to understand both individual-level and population dynamics of steelhead, there is still much uncertainty about the specific mechanisms that drive these dynamics. Furthermore, although there is a consensus that individual condition is a major determinant in the ultimate life history of an individual, the mechanistic way to incorporate this knowledge into the prediction of population dynamics is less clear.

In this study, I develop a framework that accounts for individual growth, partial migration strategies, ocean survival and in-stream temperature to make predictions of the number of returning adults. I then apply this framework to Steelhead in the Carmel River in California, a complex system in which describing population dynamics is further complicated by a variety of anthropogenic and environmental factors. I demonstrate the applicability of this framework by determining the relative contribution of Young-of-the-Year (YOY) individuals to the adult returns observed in the past 15 years. Throughout the development and implementation of this framework I ask three primary questions: (i) How has the Carmel River system changed over time? (ii) How have mitigation activities in the Carmel River impacted the population? (iii) What benefits can be gained by accounting for individual

life history attributes when predicting adult returns?

2.2 Study Area

The Carmel River Watershed is a 660 km^2 drainage in the Central Coast of California originating at the Santa Lucia Mountains (Figure 2.1). The construction of two dams, the San Clemente Dam and the Los Padres Dam, in 1921, and 1949 respectively, as well as an increase in legal and illegal water pumping has caused tremendous alterations to the landscape. These alterations include dewatering, broadening of the channel, loss of riparian habitat, and alterations to the substrate. These changes have important implications for steelhead habitat and population structure. As a result, there has been a drastic reduction in the production of steelhead: the population declined to 25% of historical levels by 1975 (Snider, 1983). In 1976 and 1977 there were no returning adults observed at the fish ladders due to a drought and from 1988-1990 the river never reconnected with the ocean, making it inaccessible to adults. The streamflow alterations have the potential of stranding individuals within the stream network and blocking migration of individuals to the ocean, leading to higher mortality and therefore reducing the number of returning adults. In light of these threats to the population, each year multiple organizations including the Monterey Peninsula Water Management District (MPWMD) and the Carmel River Steelhead Association (CRSA) carry out a number of monitoring, mitigation and restoration activities. While these activities were based on the goal of the recovery of the population, there continues to be a downward trend in the number of returning adults that remains unexplained.

2.3 Methods

In the following section, I describe the data available for the Carmel River system and the methodology used to analyze it (Section 2.3.1), the modeling approach that I employ to describe the life history of an individual (Section 2.3.2), and a description on how I combined the data with the life history model (Section 2.3.3). I conclude with a description of a naive model that only accounts for abundance for comparison (Section 2.3.3). In the present work, I focus the analysis on modeling the life history and ultimate fate of YOY individuals.

2.3.1 Data

Monitoring Data

Juvenile Abundance

The MPWMD carries out a variety of activities to annually monitor the status of the juvenile and adult steelhead population in the Carmel River. In order to assess the status of the juvenile population, in terms of abundance and distribution, the MPWMD has conducted annual surveys of 11 sites in the 17 miles of the river below the San Clemente Dam. In this chapter, I use data from the 9 sites that have been most consistently sampled (Figure 2.2). The surveys of these sites are composed of depletion electrofishing in order to estimate local population density and recordings of length-frequency data to estimate the population composition (Figures 2.3 and 2.4).

The focus of this study is to determine the contributions from YOY individuals to the overall adult run, therefore; both the population size and the relative abundance of

YOY individuals must be estimated from the survey data. To determine the composition of the different age classes present at a given site in a given year, I assume that the length frequency of individuals follows a mixture of normal distributions. That is, the length of individual i in year t and site j, $l^i_{t,j}$ follows the mixture distribution

$$l^i_{t,j} \sim \sum_{k=1}^{k=K} \alpha_k N(\mu_k, \sigma_k) \tag{2.1}$$

where $\alpha_k N(\mu_k, \sigma_k)$ represents a weighted normal distribution with mean μ_k and variance σ_k and weight α_k. I assume that there are a possible K different age classes present in the population. Since both the total number of age classes, relative proportion of age classes, mean length of each age class and variance of the length of each age class are unknown *a priori*, I fit models with one to four age classes to the data available for each site to determine these parameters, and select the model that yields the lowest BIC value (Figure 2.5, see Appendix A.2 for more details).

Since the length-frequency data for the I individuals that were captured during the electrofishing events only represent a subsample of the population, I estimate the total population abundance, N_0 for a site. For the site-year combinations in which at least 3 passes of depletion electrofishing were conducted, I estimate local abundance estimates following Carle & Strub (1978), while in the years in which only two depletion passes were conducted I estimate the local population abundance following Seber & Le Cren (1967) (see Appendix A.1 for more details of these methods).

With an estimate for the total population abundance I impute the length values for the $N_0 - I$ individuals in the population that were not captured by drawing random samples from Equation 2.1. Finally, all of the individuals in the population are assigned to

different age categories based on the posterior probability of having come from cluster k in Equation 2.1.

Adult Returns

The MPWMD operates a fish counter at the San Clemente Dam (Figure 2.6). Although this count is not a total census of the returning migrants, I assume that it serves as a good descriptor of the population trends.

Temperature

The MPWMD monitors river temperatures continuously (Optic StowAway temperature data loggers from the Onset Computer Corporation) at six locations throughout the watershed to determine the habitat suitability for juvenile steelhead. In order to model the growth of individuals within the specific sites, I derive daily temperature profiles at the 9 locations where the juvenile surveys are conducted by linearly interpolating between the four continuously logging locations.

Mitigation Activity Data

The MPWMD and CRSA conduct a variety of mitigation activities to prevent mortality of stranding juveniles in the drying sections of the river. Individuals who are threatened by stranding are relocated to upstream sections of the watershed with perennial flow, the estuary-lagoon, directly to the ocean or to the Sleepy Hollow Steelhead Rearing Facility (SHSRF).

The mission of the SHSRF is to hold the fish during times in which the river's

quality is inadequate for survival. The majority of the fish in the SHSRF are reared in a 13 bay, 800-foot long, artificial rearing channel that emulates a natural stream (including riffles and pools, cobbled bottom, boulders, logs, etc). Although the original goal of the facility was to match the growth of fish to what would be observed in the wild, individuals within the facility experience higher than natural growth due to increased feeding with high quality food, which is done to prevent cannibalism. Prior to the release of individuals back into the stream, the MPWMD counts the total number of individuals and subsamples the lengths and weights of a portion of the individuals from the different sections of the rearing channel in order to assess their condition (Figures 2.7, 2.8). When in-stream survival conditions are considered adequate (normally when the river reconnects with the ocean), the individuals in each section of the rearing facility are transplanted back to the stream.

As with the lengths from the juvenile population surveys, the lengths of the individuals reared in the SHSRF are samples of the entire population. In a similar fashion as the in-stream reared individuals, the lengths of the unmeasured individuals are imputed by fitting a normal distribution to the known sample of the population in each portion of the rearing channel and drawing random samples from the fits for the lengths of the unmeasured individuals.

2.3.2 Modeling individual life history

Modeling Growth

I model the weight of an individual, W_i, as a balance of consumption and metabolic costs.

$$\frac{dW_i}{dt} = \Phi_c\left(T\right) A(t,l) c_1 \; W_i^{c_2} - \Phi_m\left(T\right) m_1 W_i^{m_2} \tag{2.2}$$

Basal catabolism is the product of two terms: catabolic costs that are described by an allometric relationship with weight, $m_1 W_i^{m_2}$, and the effect of temperature on catabolism, $\Phi_m\left(T\right)$. Anabolism is the product of four terms: relative energy density of food to fish tissue, c_1, the allometric relationship of consumption and fish weight, $W_i^{c_2}$, the functional relationship of maximum consumption and temperature, $\Phi_c(T(t))$ and a term accounting for competition between individuals $A(t,l)$ that will be described below. This model formulation, with the exception of the competition term, is the same as that described in the bioenergetics literature (Hanson et al., 1997; Railsback & Rose, 1999; Satterthwaite et al., 2010). For the allometric relationships between weight and catabolism and anabolism I use parameter values for Scott Creek steelhead in the Central California Coast from Satterthwaite et al. (2010). For the temperature scalings of catabolism and anabolism I follow Brett (1952) and Thornton & Lessem (1978), reparametrized for California steelhead by Railsback & Rose (1999) from data analyzed by Myrick & Cech (2004), Van Winkle et al. (1998) and From & Rasmussen (1984).

Modifications of bionergetic models such as the competition term in Equation 2.2 have been used to include additional sources of variability in growth (e.g. activity requirements) (Mangel & Munch, 2005; Satterthwaite et al., 2010; Boughton et al., 2015).

In Equation 2.2, $A(t, l)$ accounts for competitive interactions, which have been demonstrated to be driven by size hierarchies in many species, including salmonids (Elliott, 2002; Metcalfe, 1986; de Roos et al., 2003). This term allows us to investigate the effects juvenile abundance and density dependent effects on overall population dynamics. It modulates the individual's consumption through the competitive interactions between the focal individual and every other individual in the population. These competitive interactions are often driven by individuals attempt to access common resources (e.g. food or habitat).

Specifically, I model the size-dependent competition for resources between an individual of size l and a competitior of size λ as:

$$C(l|\lambda) = \exp(\beta(\lambda - l)) \tag{2.3}$$

where the parameter β determines the asymmetry of size-dependent competition that occurs (for a more detailed discussion see Chapter 3). Increasing values of β result in increasing competitive dominance of larger individuals over smaller individuals. Individuals of different lengths will experience their environment in different manners depending on the rest of the population. I describe this as the effective population density function $\eta(t, l)$:

$$\eta(t, l) = \int_{l_b}^{l_M} C(l|\lambda) n(t, \lambda) \lambda^2 d\lambda \tag{2.4}$$

This function effectively describes the cumulative competitive effects that are imposed on an individual by a population with a size distribution, $n(t, \lambda)$, that ranges from lengths l_b to l_M. The λ^2 term accounts for our assumption that competition scales with the surface area of an individual. I connect the effective population density experienced by an

individual and its access to the resources in the environment, $A(t,l)$:

$$A(t,l) = \frac{\eta_H}{\eta_H + \eta(t,l)} \tag{2.5}$$

Here the half-saturation constant, η_H, scales the population density and describes the total amount of resources in the environment. As $\eta(t,l)$ increases, an individual's access to the resources decreases, with the converse being true for decreasing values of $\eta(t,l)$.

Modeling Adult Production

The production of returning adult steelhead relies on two size-dependent mechanisms, transition to ocean entry (smolt transformation) and subsequent ocean survival. I model the smolting decision as being a function of an individual's length at the time of emigration (nominally April 1). In particular, the probability that an individual will smolt and migrate to the ocean is

$$P_{smolting}(l) = \frac{1}{1 + \exp\left(-\frac{l-l_s}{\sigma_s}\right)} \tag{2.6}$$

where l_s is the length threshold at which the probability that individual smolts is 0.5 and σ_s characterizes the dispersion around this threshold. I set the baseline value of the threshold at $l_s = 120\,mm$ and the variance around this threshold at $\sigma_s = 10\,mm$ based on data from Beakes et al. (2010) and Doctor et al. (2014).

In order to return as adults, individuals have to survive the subsequent entry to sea as well as the marine phase of their life. Although the presence of inter-annual variability in marine growth and survival conditions may have significant effects on adult production, the lack of knowledge about the oceanic phase of an individual's life history makes it difficult

to accurately incorporate it (McGurk, 1996; Kendall et al., 2015). Rather, I model the size-dependent expected marine survival of emigrating smolts as:

$$P_{survival}(l) = \max\left\{0.35, 0.84 \times \frac{1}{1+\exp(8.657 - 0.0369l)}\right\} \tag{2.7}$$

as determined by Satterthwaite et al. (2009) from data from Bond et al. (2008) and Shapovalov (1967) to match survival in Scott Creek.

Given these descriptions for the probability of smolting and the probability of survival, conditional on smolting; the probability that an individual will smolt, survive the marine phase and return as an adult is simply the product of these two probabilities

$$P_{\text{adult}} = P_{\text{smolting}} \times P_{\text{survival|smolting}} \tag{2.8}$$

In addition to the variability exhibited in the decision for emigration or residency, steelhead demonstrate variability in return rates, with individuals typically spending between 1 and 3 years in the ocean. Due to the lack of data on the return timing of individuals for the Carmel River, I assume that the run of returning adults in a given year (R_t) is composed of individuals that migrated 1 and 2 years prior (M_{t-1}, M_{t-2} respectively), with their relative composition based on data from Shapovalov & Taft (1954). Specifically

$$R_t = 0.53M_{t-1} + 0.47M_{t-2} \tag{2.9}$$

Subsequently, I use this return composition in calculating the weighted mean length of the migrants that make up the returning adults in a given year ($\mathcal{R}_t$) based on the length at ocean entry of individuals L_t in year t such that

$$\mathcal{R}_t = 0.53L_{t-1} + 0.47L_{t-2} \tag{2.10}$$

2.3.3 Combining the Model with Data

In-stream Adult Production

To determine the total contribution of adults from in-stream rearing juveniles, I parametrize the YOY life history model described in section 2.3.2 with the juvenile survey data described in section 2.3.1. By parametrizing the model uniquely at multiple sites each year, I can at least partially capture the heterogenous growing conditions present throughout the river. Using the length-frequency data estimated for the YOY individuals at each individual site also allows me to determine the growing conditions for that site.

I characterize the annual growth potential at each site by modeling the growth of each YOY individual at a given site from spring "birth" to the time of the fall juvenile surveys. Since I don't have data for the weights of individuals at birth, I assume their individual lengths are distributed following a truncated normal distribution with a lower and upper bounds of 28 mm and 39 mm respectively and mean and standard deviation values of 34 mm and 5 mm, and also that immediately following the spawning season all newborn individuals disperse homogeneously throughout the watershed (Snider & Titus, 2000) (Figure 2.9). With the total population of YOY individuals and their lengths for every site-year combination, I can use the temperature profile for any specific location and solve Equation 2.2 backwards in time to find the parameter combinations for β and η_H that result in the assumed distribution for the initial weights of individuals. In particular, I assess the similarity between back-calculated initial weight distribution from Equation (2.2), $\vec{W}_0^*$, and the assumed initial weight distribution, W_0, via the Kolmogrov-Smirnov test (K-S test) and find the parameter combination for β and η_H that yields a satisfactory

fit. Rather than attempting to precisely recreate the initial distribution, I am interested in reconstructing a biologically meaningful back-calculated initial size-distribution. In order to achieve this, I set a satisfactory threshold of $p > 0.01$ for the K-S test. Using this parameter set, and assuming that competition and food conditions remain constant in a given site, I then project the fate of the individuals forward to the time of smolting and emigration. I then use size-specific smolting rate ($P_{smolting}(l)$, Equation 2.6) and size-specific ocean survival ($P_{survival}(l)$, Equation 2.7) to estimate adult production from the projected size distribution. I then estimate the stream-wide adult production by using the mean annual adult production density (adults/foot) and extrapolating it to the portion of the river between Los Padres Dam (river mile 25) and the estuary (Figure 2.1).

SHSRF Adult Production

Without knowledge of the in-stream growing conditions for the locations that individuals from the SHSRF were realeased I am not able to make forward growth projections to the time of emigration for individuals reared in the SHSRF. I therefore assume that the length at emigration time will be the same as the length at the time of release from the facility, essentially assuming that all individuals released from the rearing facility experience maintenance conditions or move quickly to the ocean. Given this length at emigration I am able to calculate the expected adult production from the rearing facility in the same fashion as that of the in-stream reared individuals following Equations 2.6 and 2.7 for smolting and survival respectively.

Abundance Based Model

One of the goals of this study is to determine the benefits of including life history attributes in the predictive models for the number of returning anadromous adults. To accomplish this, I compare the full model (life history+ abundance) to a simpler, abundance-based model that assumes that the total number of migrants any given year is simply proportional to the total number of YOY individuals in the population (both in-stream abundance and SHSRF releases). The returning number of adults then follows the same relationship as described by Equation 2.9. This approach is equivalent to saying that all individuals would have equal probability of smolting and ocean survival regardless of their length. In order to optimize the predictive ability of this model, I determine the constant of proportionality by minimizing the root-mean-square error (RMSE) between the predicted (R_t) and observed number of adults (R_t^{obs}).

$$c^* = \min_c \sqrt{\frac{\sum_{t=1}^{T}(cR_t - R_t^{obs})^2}{T}} \tag{2.11}$$

2.4 Results

I present the results in three different parts; 1) trends and patterns for both biotic and abiotic factors in the Carmel River that emerged from the data analysis, 2) predictions from the life history model and 3) comparison between the life history model and the abundance based model. To analyze the trends and patterns that emerged between different measured variables, I employ Bayesian linear regression with standard diffuse priors (see Appendix A.3 for more details).

2.4.1 General Patterns

A number of general trends emerge from the analysis of the historical data collected by the MPWMD. The stream-wide mean length of YOY individuals has declined (Figure 2.10). Of the 9 sites for which data were available, 4 show a statistically significant decline, while the other 5 have had no significant change in mean length. The 5 sites that didn't experience a significant change in mean length were historically composed of smaller individuals, and so had less scope for decline. In addition to a general decline, the length of individuals appears to display an oscillatory pattern with a 3 year period. To test a potential explanation for these apparent oscillations, I looked at the relationship between the mean observed length for all individuals in the stream and the Southern Oscillation Index (SOI), which is often used as an indicator of the El Niño (negative SOI) and La Niña (positive SOI) cycles. There is noticeable negative correlation between both 1 year and 2 year lags of the SOI and the mean length of all individuals in the stream (Figure 2.11). La Niña conditions tended to be associated with smaller YOY individuals 1 or two years later. I also discovered a decreasing trend in the mean in-stream temperature of the river ($\hat{\beta} = -0.1652$) (Figure 2.12).

The complexity and interdependencies between the different processes driving the ecology of Steelhead in the Carmel river does not allow us to directly discern the effects of the relocations performed. However, I found some important general relationships. There is a notable negative relationship between the total number of relocations that take place in a given year and the mean YOY length of individuals (Figure 2.13), as well as between the total number of relocations and mean YOY abundance (Figure 2.14). However, there is no

discernible relationship between the mean YOY abundance and mean YOY length (Figure 2.15). This implies that years that are good for the survival of individuals (large population abundances at the fall surveys) are also good years for the growth of individuals. Most importantly, there is a very significant positive relationship between the weighted (by the coefficients in Equation 2.9) mean length of smolts that make up the returning adults in a given year (Equation 2.10) and the number of returning adults (Figure 2.16, Table 2.1).

		β	
y	x	Mean	95% C.I.
TR	YOYL	-4.460×10^{-4}	$(-8.891 \times 10^{-4}, -1.810 \times 10^{-7})$
TR	YA	-2.216	$(-0.728, 3.676)$
YA	YOYL	-6.903×10^{-5}	$(-2.080 \times 10^{-4}, 7.158 \times 10^{-5})$
ML	RA	24.207	$(9.256, 16.776)$

Table 2.1: Posterior mean and 95% posterior C.I. for β in the different linear regression models as described in the 2.4.1 section. TR=Total Relocations, YOYL= mean YOY length, YA= mean YOY abundance, ML=mean migrant length, RA=Total returning adults.

Predictions of Adult Returns

The model that included life history information significantly outperformed the abundance based model. While perfect prediction was not expected, the inclusion of life history attributes allows us to capture the general quantitative behavior of observed adult returns (Figure 2.17). The inclusion of life history attributes in the model for the number of returning adults allows us to increase the Pearson-correlation between the prediction and the observed values to $\rho = 0.42$, a markedly increase from the abundance based model $\rho = 0.025$. Figure 2.18 (A) demonstrates this increase with the increased slope between

predicted and observed adult returns (note that the negative values of Figure 2.18 are artifacts of the linear regression and are admittedly impossible). Accounting for life history attributes also yields a lower RMSE (202) when compared to the abundance model (220). There is also a clear shift in the returning adult composition between the years of 2004 and 2005. In the years prior to 2004, the majority of the predicted adult returns are composed of wild produced individuals, while after 2005, the composition is predominantly composed of individuals reared in the SHSRF (Figure 2.19).

Sensitivity Analysis

Since there are high levels of uncertainty about the precise smolting threshold and ocean survival for the Carmel River, and steelhead populations in general, I performed a numerical sensitivity analysis to asses the effects that the baseline assumptions have on the predictions of adult returns. I reanalyze the predictions under the combination of scenarios for smolting threshold values ranging from 90 mm to 150 mm and ocean survival from 85% to 115% of the baseline value (Equation 2.7, Figure 2.20). Exploring the effects that different parameter combinations have on the results allows me to quantify the effect of the assumptions that were required for the model. I expect that decreases (increases) of the smolting threshold and increases (decreases) in ocean survival will result in higher (lower) numbers of returning adults. However, the interactions between these parameters are non-linear and the effects on the prediction of adult returns is complex. Different parameter combinations of ocean survival and smolting threshold result in both different quantitative and qualitative predictions than that of baseline values. The counteracting effects of a high (low) smolting threshold and a low (high) ocean survival level create a

region that yields the same level of RMSE between the observed and predicted number of returning adults (Blue band in Figure 2.21 A). While the RMSE level between the number of observed and predicted returning adults depends on both the smolting threshold and ocean survival, the Pearson correlation between the observed values and predicted values is seemingly independent of ocean survival (Figure 2.21 B). The combination of a low smolting threshold and low ocean survival leads to both the lowest RMSE and highest Pearson correlation between the predicted and observed number of returning adults. This combination of values significantly increases the Pearson correlation between the predicted and observed adult returns but it does not drastically reduce the RMSE. The exploration of different parameter combinations leads to increases of error and decreases of error with the amount of change dependent on the year (Figure 2.22). The direction of the error in terms of under or over predictions is also not significally affected by the changes in parameters with a significant patter of over (under) prediction present after (before) 2007 (Figure 2.22). Ultimately, the changes in these parameters only have minor effects on the predictions. While in some years, changes in parameter values may yield better prediction of adult returns, changes in parameter values generally do not drastically affect the ability to predict the number of adult returns (Figure 2.23).

2.5 Discussions and Conclusions

Since length plays a key role in many of the mechanisms driving the life history of an individual (e.g. resource acquisition, survival and migratory decision), the observed decline in mean size of YOY has important implications for population dynamics. The

decline of the in-stream temperature may be partially responsible for the decline in length due to the strong dependence of growth on temperature regimes. During a 10 year Benthic MacroInvertebrate (BMI) study of the Carmel river, King (2010) found that there has been a decline in the biotic integrity in portions of the stream which may also be driving the decline in individual length. While I demonstrate there is a close relationship between the SOI and the oscillations in length (Figure 2.11), describing the precise mechanism driving this relationship is beyond the scope of this study. The model suggests that there has been a shift in composition of returning adults from wild-dominant to heavily reliant on the adult production from the SHSRF. Since YOY abundance has remained relatively stable during the years studied, this shift is at least partially attributed to the decline in length. This result is of particular interest since this decline in wild production of returning adults is occurring during the same period in which stream restoration efforts are being conducted. This may partially signify that the current restoration efforts to increase the number of returning adults could be better directed to maximize their impact.

One of the primary goals of this study was to determine what benefit, if any, the inclusion of life history considerations in the prediction of adults would yield. The results show that the inclusion of growth, conditional migration theory, and environmental factors allows us to gain substantial improvement on the prediction or adult returns. Even in light of the many assumptions and the use of data that were not collected specifically for this study, I am able to capture qualitative patterns such as the peaks of adult returns with relatively high fidelity (Figure 2.18). Furthermore, while the predictions of returning adults were made independently of the observed returns, the quantitative estimates are generally

similar to the observed returns. Conversely, the predictions based solely on the abundance of YOY individuals show no significant relationship with the observed returns and generally predict vastly different values for the number of observed returns.

The sensitivity analysis demonstrates a general robustness of the estimates for adult returns in both RMSE and correlation from deviations in assumptions about smolting threshold and ocean survival. Furthermore, Figure 2.21 illustrates the dependence of predictions on ocean survival and smolting threshold. Figure 2.21 (A) also illustrates the compensatory relationship between smolting probability and ocean survival. Namely, while a higher smolting threshold yields a lower number of individuals migrating, a higher value of ocean survival can offset the effects on the ultimate number of returning adults. While the same response is not true for the correlation between the prediction and the observed number of adults, the correlation value is substantially higher throughout the entire range when compared to the correlation value achieved by the abundance based model. Even the parameter values that yielded the lowest correlation between the predictions and the observed returns outperform the correlation found by the abundance based model.

The prediction error does not appear to be random. I generally under-predict in the years where I estimate the wild contribution to be dominant while I over-predict in the years that the SHSRF contribution is predicted to be dominant. A possible cause of the over predictions in the latter scenario is the assumption that all returning adults produced by the SHSRF migrate past the San Clemente Dam fish counter. Since the individuals reared in the SHSRF were all rescued from regions below the dam, it is highly likely that at least some of the returning adults spawn below the dam and are never counted. Another

mechanism that may be driving the over-predictions is the exclusion of early maturation caused by rapid growth in the model. It is feasible that the rapid growing conditions within the SHSRF may be producing some fish that mature in freshwater and thus never smolt, which could also lead to the over-prediction of adult counts. The reasons for the under-prediction in the years that the contribution from wild-production dominates the returning run is less apparent. *

Here I have presented a methodology that incorporates knowledge about the life history of individuals in order to better understand the dynamics of a population. The model was driven primarily by data on single annual snapshot of abundance and length-frequency of juveniles, I therefore had to make a wide range of assumptions about other characteristics describing the life history of individuals in the Carmel River. Even under these uncertainties and assumptions, the process-based methodology utilized to connect the growth and condition of YOY individuals to the number of returning adults allows us to make both qualitatively and quantitatively reasonable predictions of the returning adults. It also allows us to gain further insight into the mechanisms that may be driving the dynamics of the population while raising new questions about the patterns that are more difficult to explain. The methodology that I develop and utilize in this study is not population specific, that is, while I demonstrate the application specifically to the Carmel River, the prediction of population dynamics of steelhead is a topic of broad interest. Finally, the results highlight the benefit of connecting data with process in order to increase insight.

*Estimates omit prediction from above Los Padres Dam, and also from important tributaries.

2.6 Acknowledgements

I thank the entire MPWM team for the use of their data as well as their comments and guidance on the work. Particularly, Cory Hamilton, Beverly Channey and Kevan Urqhart have given me unprecedented access to the data they have collected over the years. This work couldn't have been completed without the help, advice and comments of Colin Nicol, Lea Bond, David Boughton, Tommy Williams and Dave Rundio.

2.7 Figures

Figure 2.1: Map of the Carmel River watershed showing streams, dams and current and historical distribution from the Nature Conservancy.

(http://www.casalmon.org/salmon-snapshots/location/carmel-river)

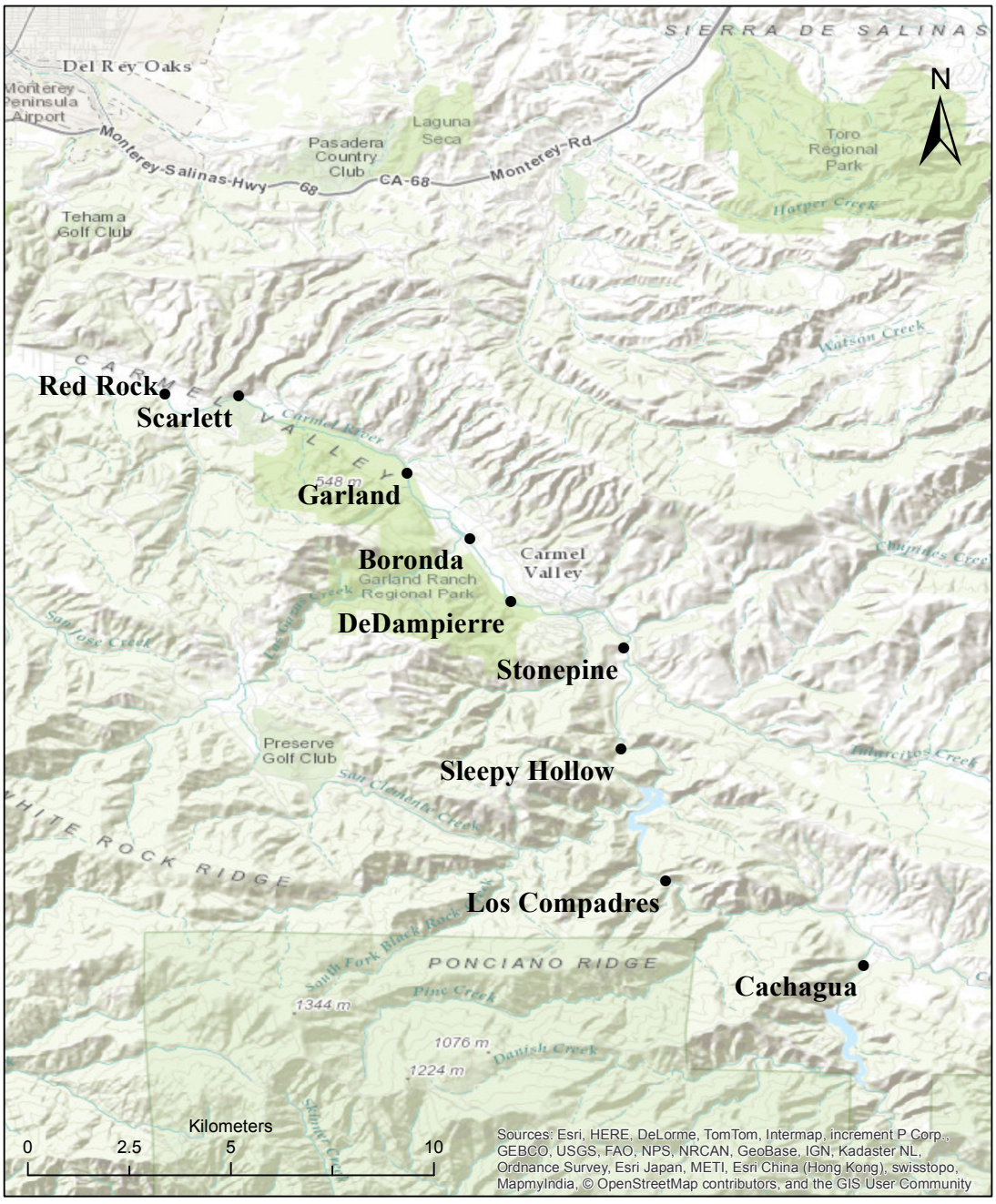

Figure 2.2: The locations of the 9 different sampling sites in the Carmel River.

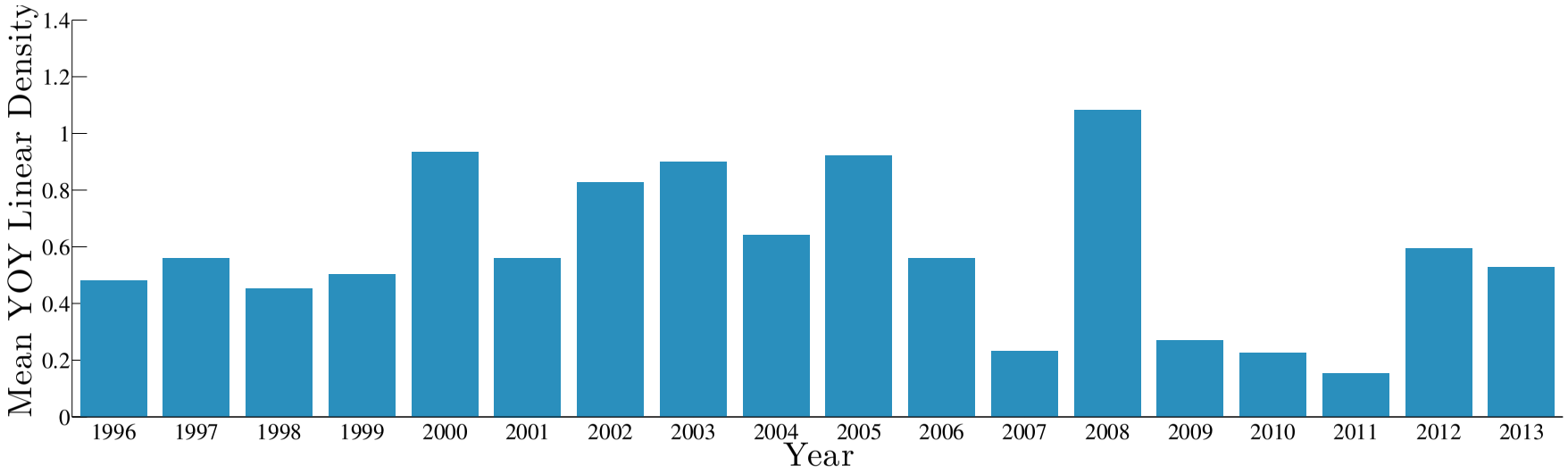

Figure 2.3: Mean observed annual Young-of-Year (YOY) density as calculated in section Appendix 2.3.1.

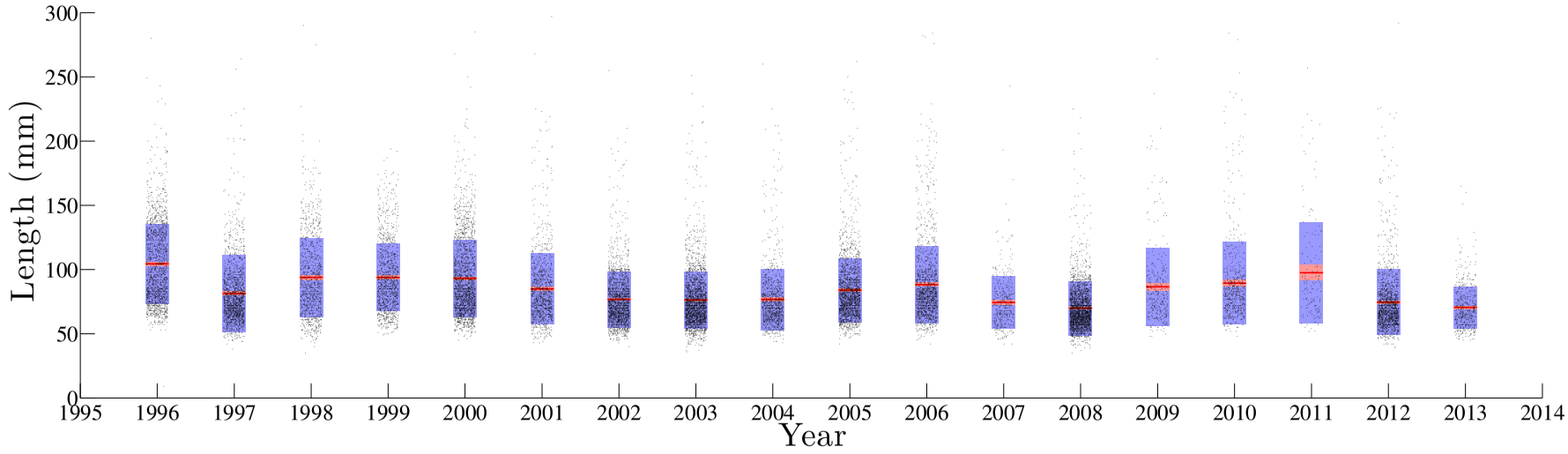

Figure 2.4: Lengths of all individuals measured during the fall population surveys by the MPWMD. Each point represents an individual and red line represent mean value for a given year, red shaded region is the Standard Error of the Mean (SEM) and purple region is 1 standard deviation.

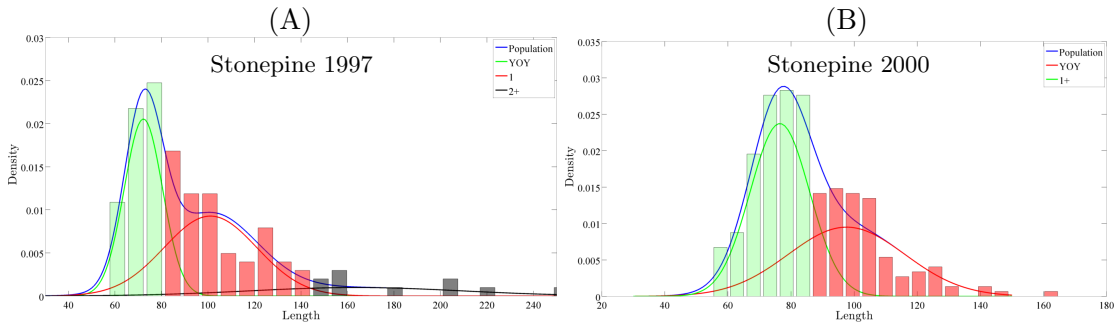

Figure 2.5: Illustration of the fitting procedure for the length distribution data from the MPWMD juvenile surveys. Blue curve is the probability density of the Gaussian mixture distribution fit the data from the entire population (bars). Green, red and black curves are the individual components from the Gaussian mixture distribution corresponding to YOY and 1 and 2+ individuals respectively. The shading of the bars represents which component each individual was assigned to. Note the different axis and presence of 3 year classes in panel (A) but not panel (B).

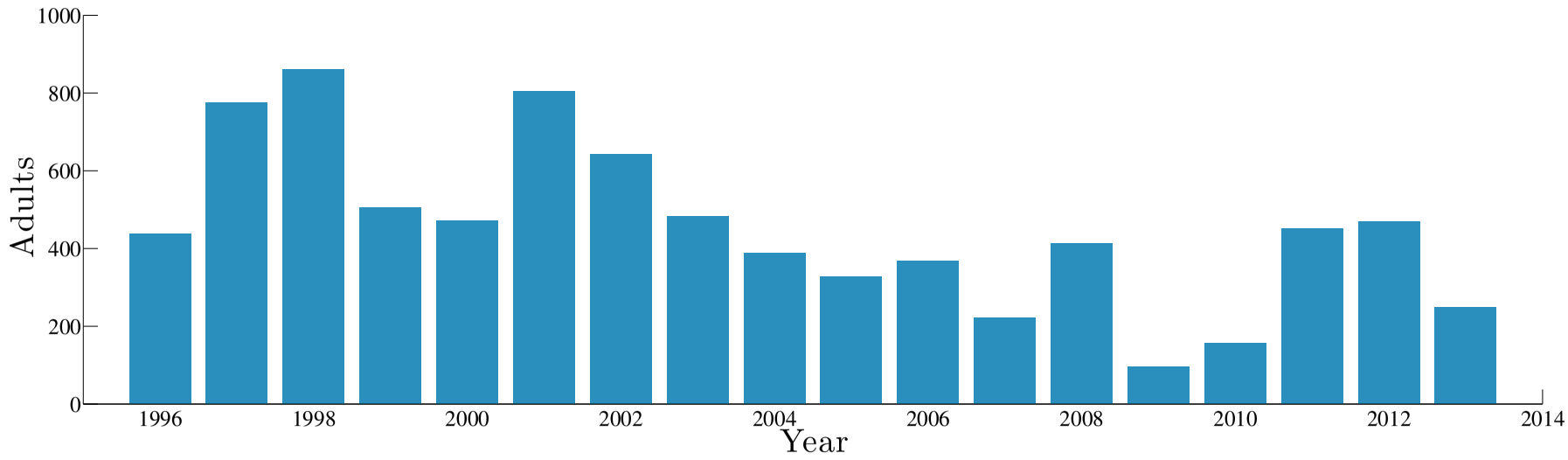

Figure 2.6: The annual total number of returning adults observed at the San Clemente Dam fish counter based on data from the MPWMD.

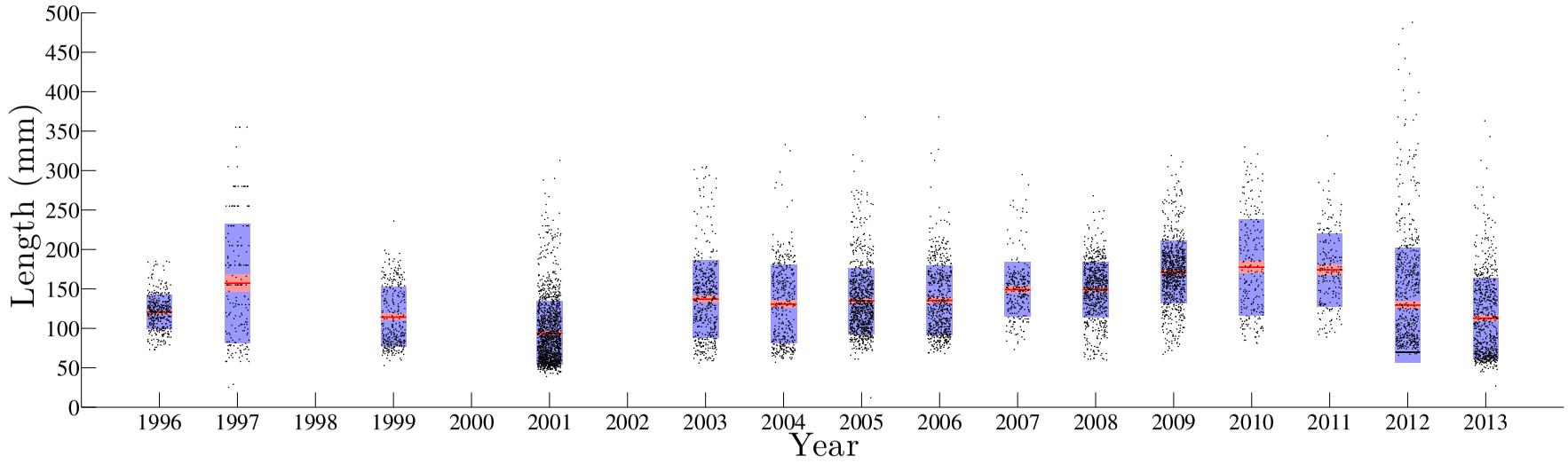

Figure 2.7: Lengths of sampled individuals at the time of release from the SHSRF based on data from the MPWMD. Each point represents an individual and red line represent mean value for a given year, red shaded region is the Standard Error of the Mean (SEM) and purple region is 1 standard deviation.

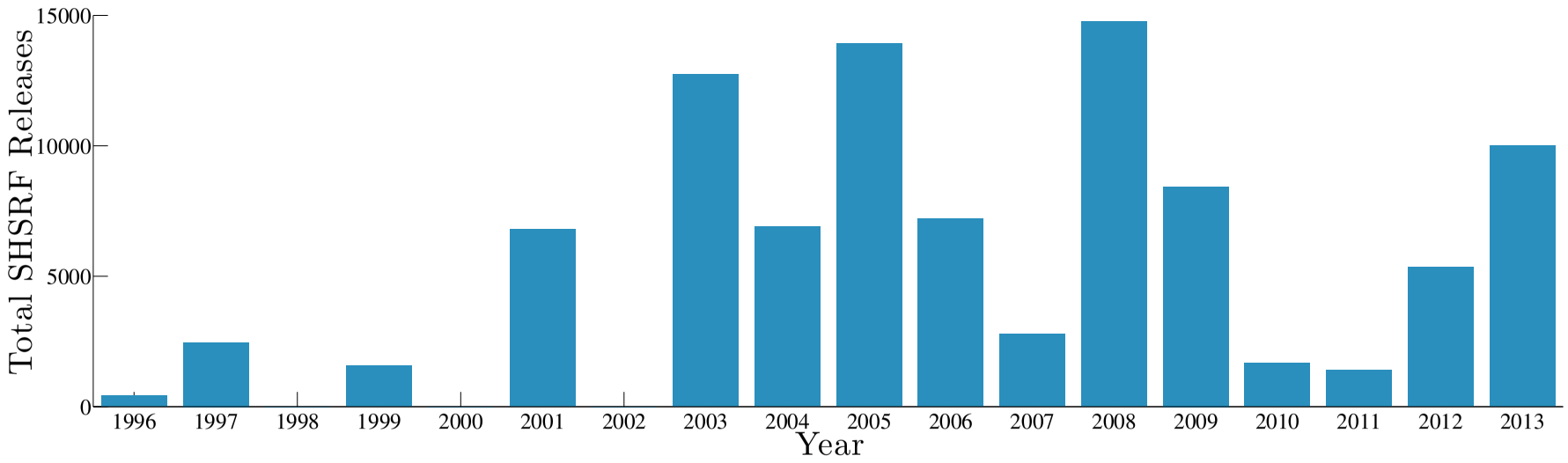

Figure 2.8: Total number of individuals annually released from the SHSRF for which sample lengths could be inferred from data provided by the MPWMD.

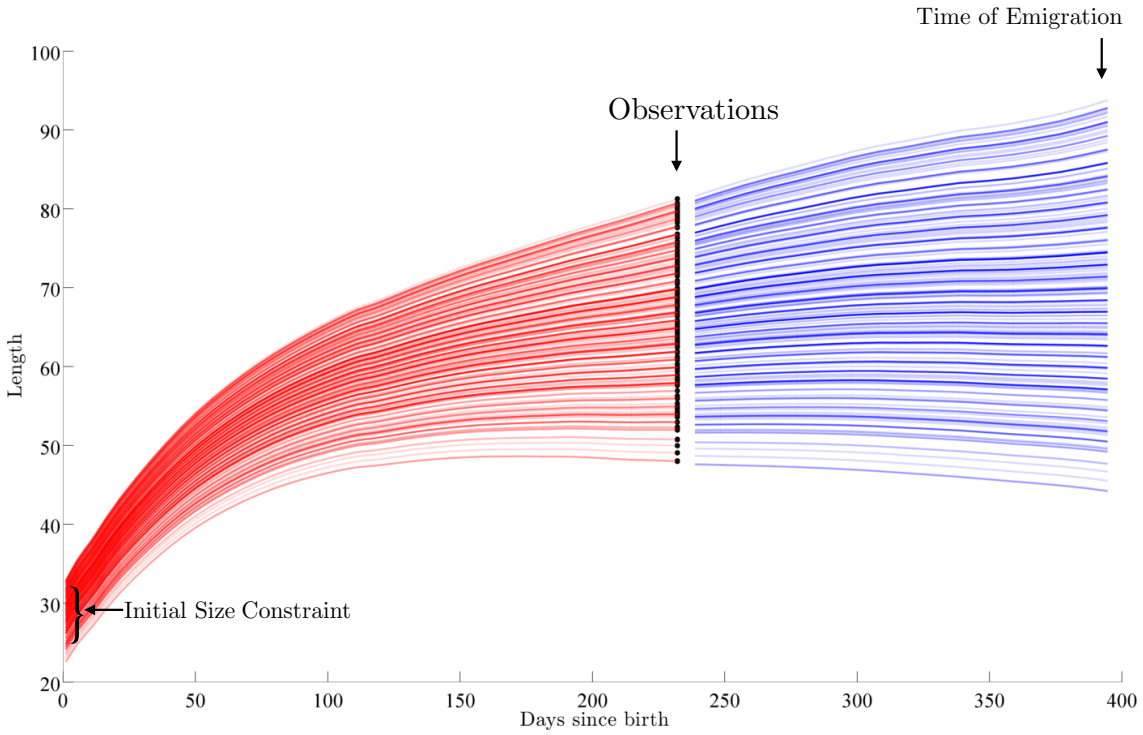

Figure 2.9: Example of the growth fitting procedure as described in section 2.3.3. The red portions of the curves represents the back calculated growth of individuals based on the length-frequency distribution during the juvenile surveys (black circles). The blue portion of the curve is the projected growth trajectories based on the parameters of best fit from the K-S test.

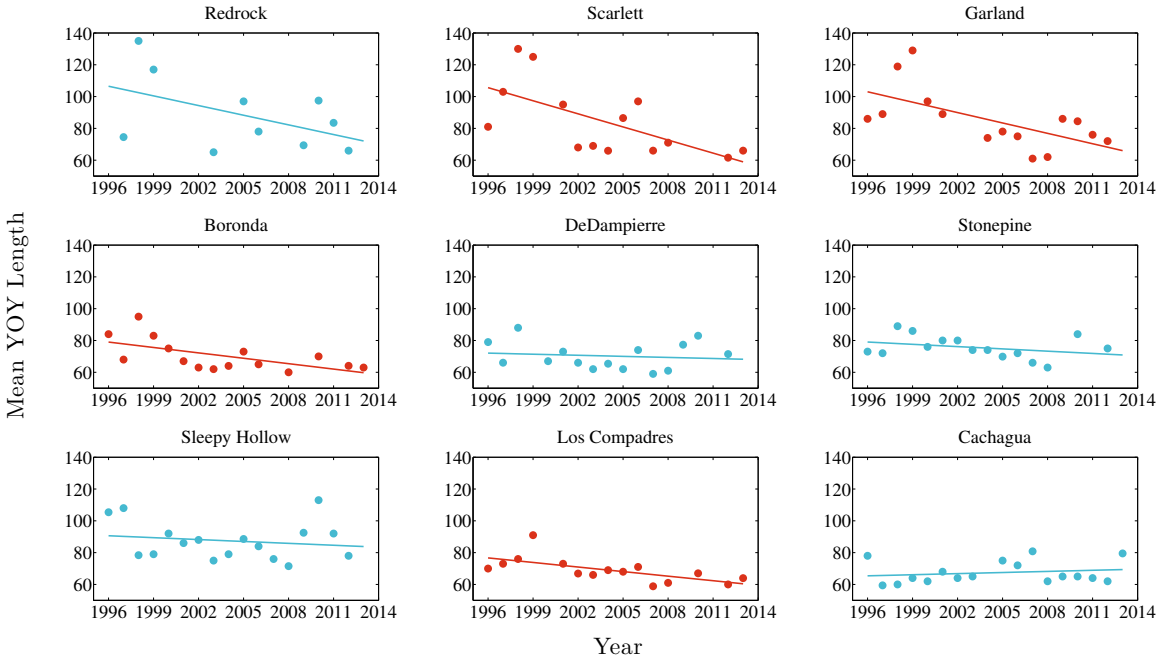

Figure 2.10: The trend in mean length for YOY individuals for the 9 different YOY lengths with regression lines based on the median parameter estimate for the slope of the regression based on the Bayesian linear regression. Red indicates that 95% CI quantiles did not include 0.

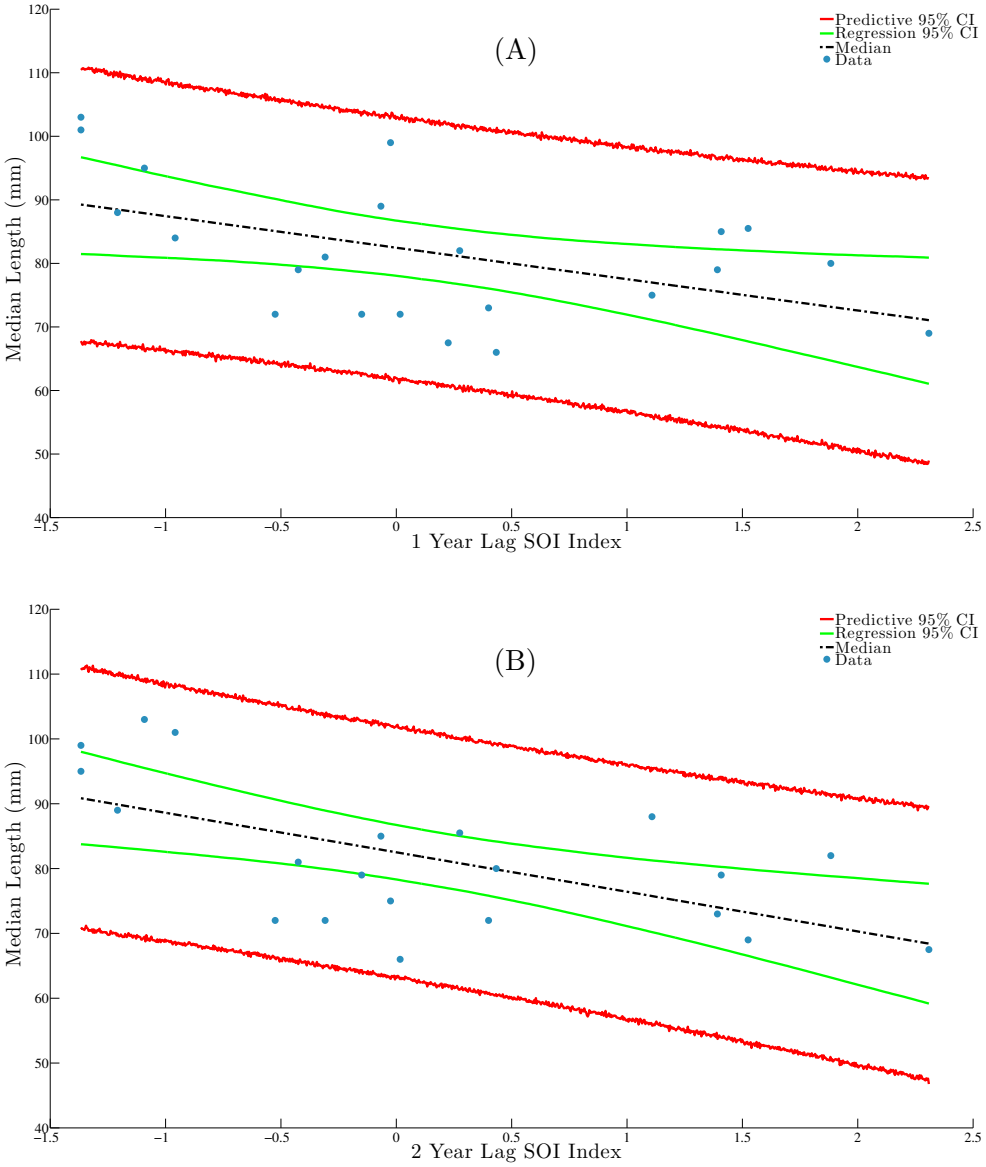

Figure 2.11: Observed relationships between mean individual length and the 1 year lag SOI (A) and 2 year lag SOI (B) with 95% C.I. intervals for both inference and prediction. Each data point represents one year of data.

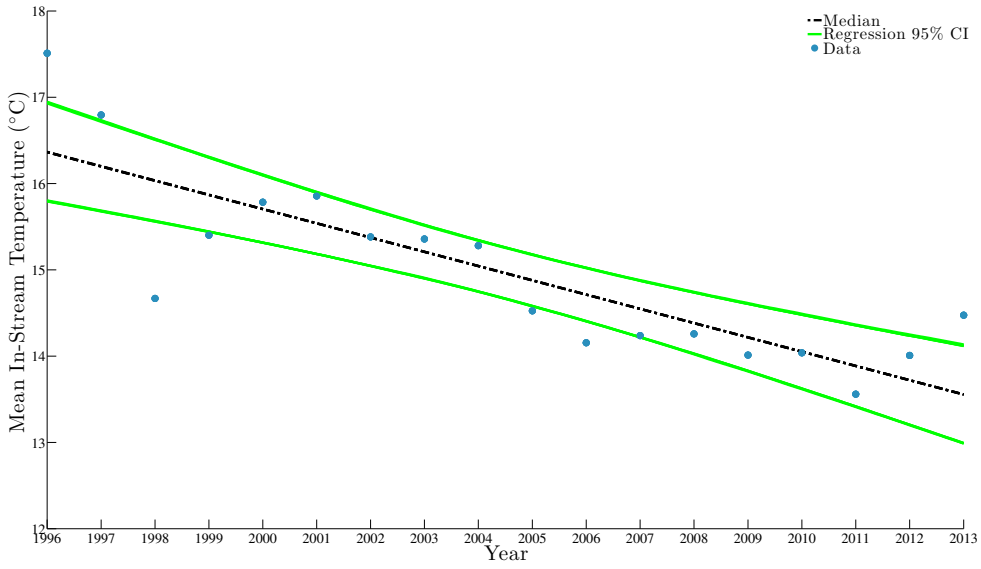

Figure 2.12: The Bayesian linear regression fit and 95% C.I. demonstrating the decline in mean in-stream temperature in the Carmel River.

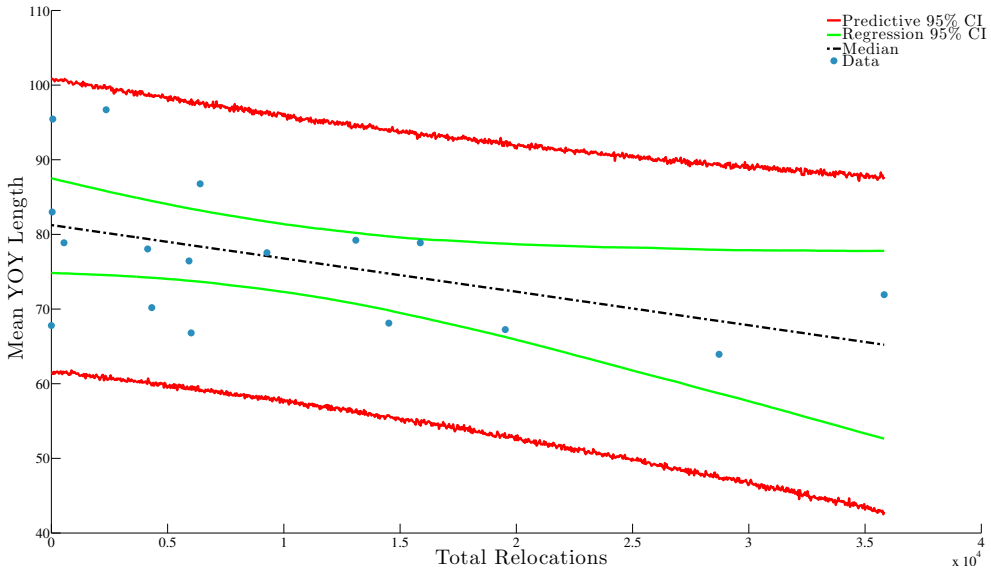

Figure 2.13: The relationship between the total number of in-stream relocations and mean YOY length. Each data point represents one year of data.

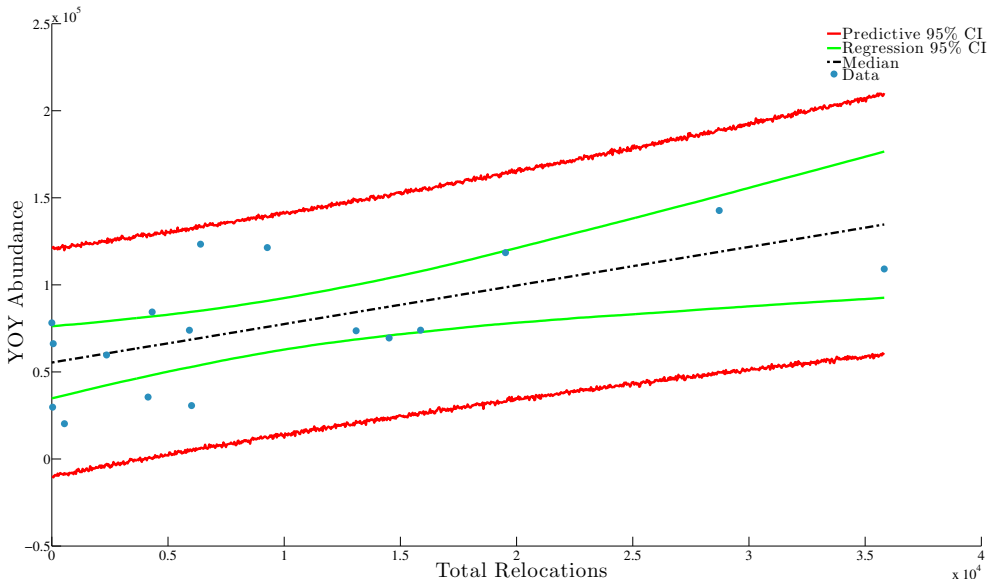

Figure 2.14: The relationship between the total number of in-stream relocations and total estimated YOY abundance. Each data point represents one year of data.

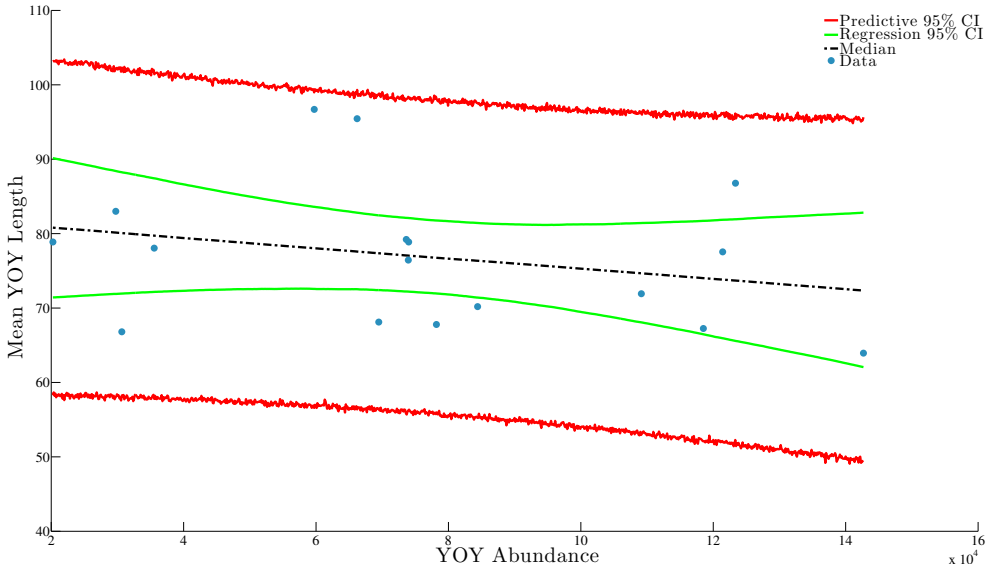

Figure 2.15: The relationship between the total total estimated YOY abundance and mean YOY length. Each data point represents one year of data.

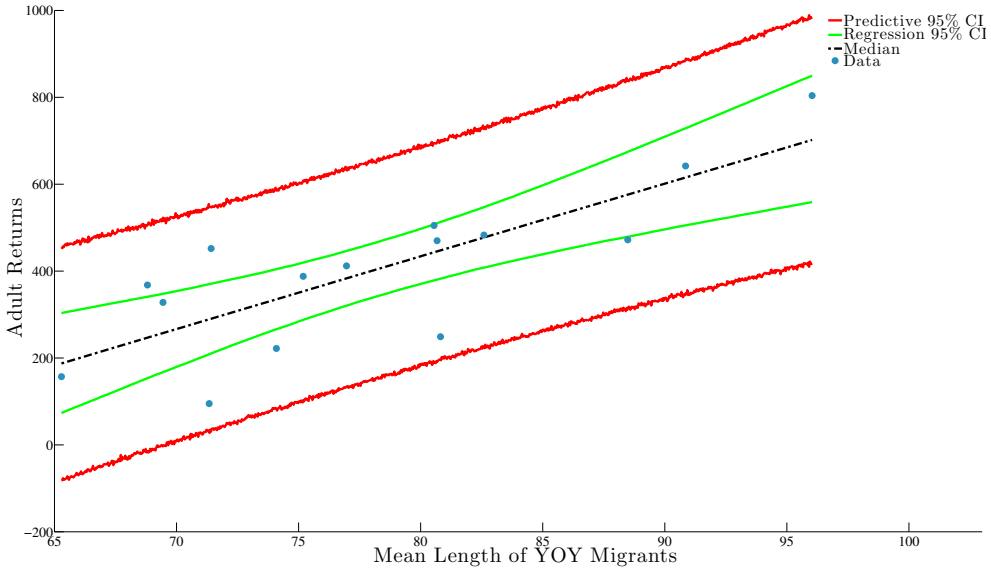

Figure 2.16: The relationship between weighted mean YOY migrant length (as calculated in Equation 2.10 based on the returning composition) and observed adult returns at San Clemente Dam.

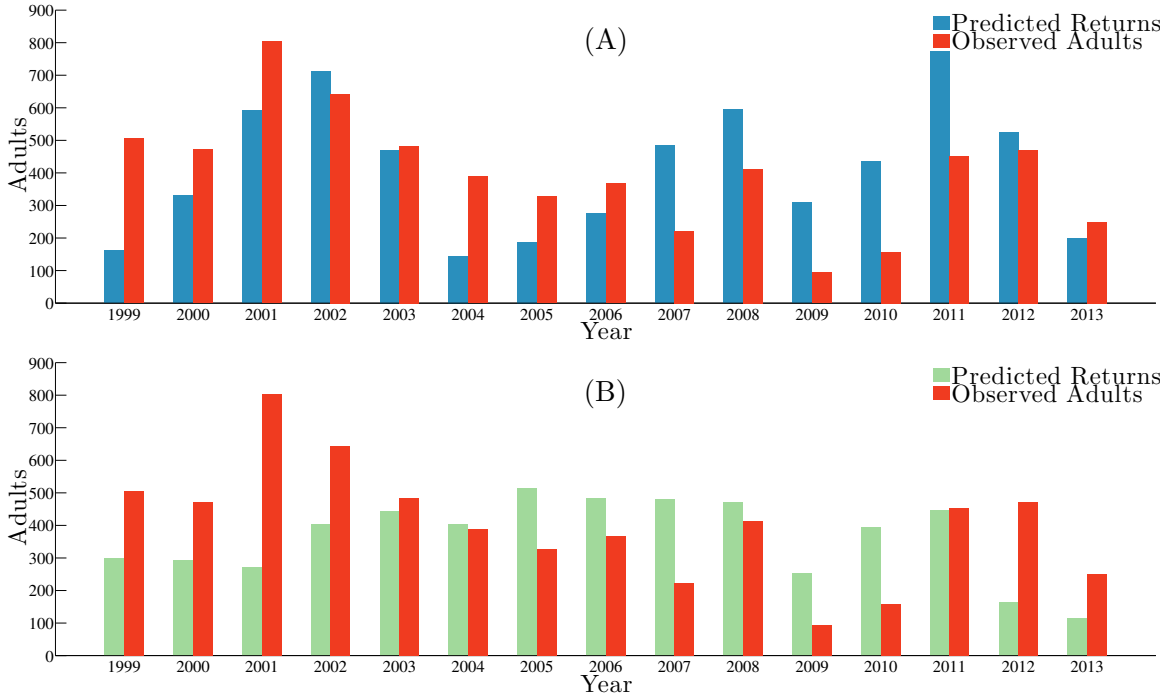

Figure 2.17: Predicted versus observed returning adults for the life history based model (A) and abundance based model (B).

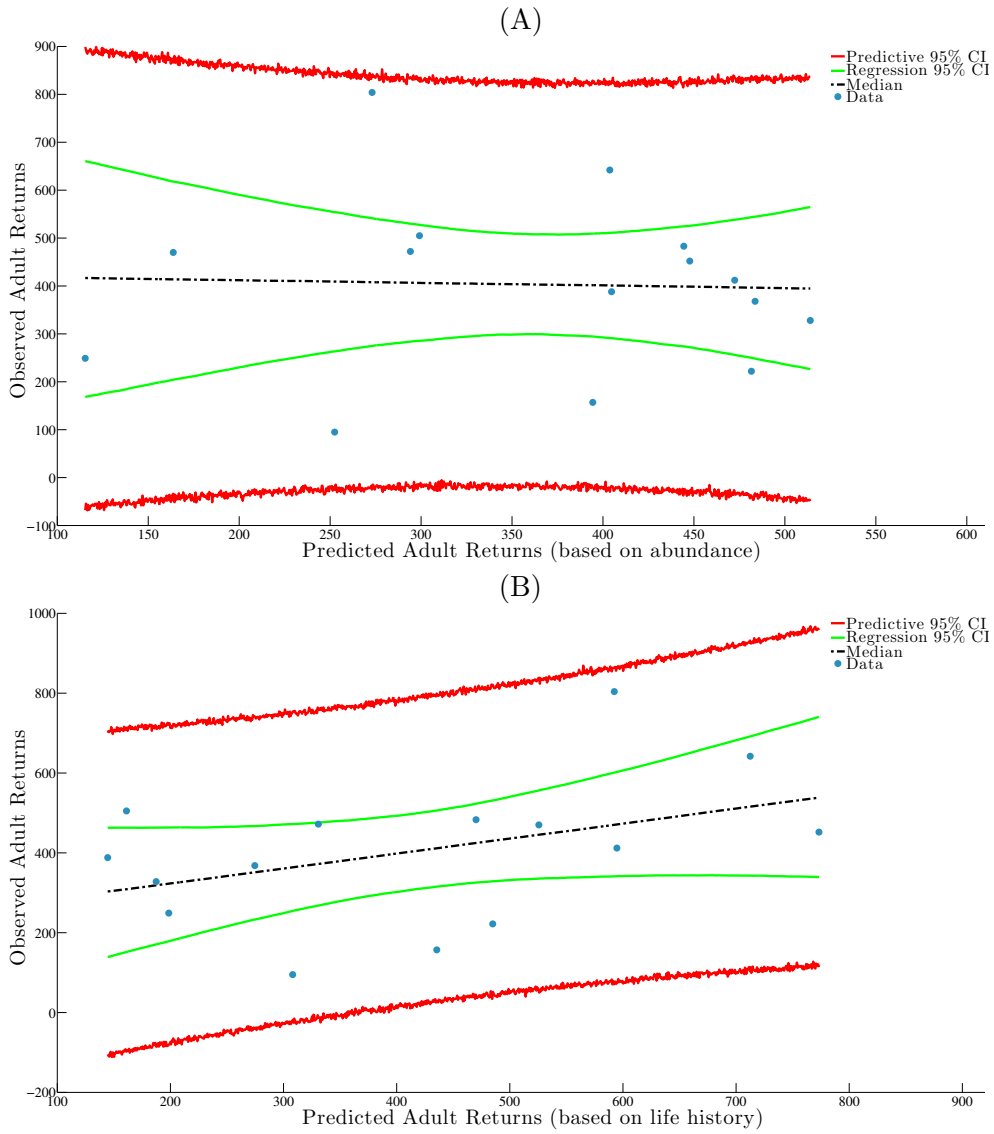

Figure 2.18: Predicted versus observed returning adults for the life history based model (A) and abundance based model (B) (Note different x axis).

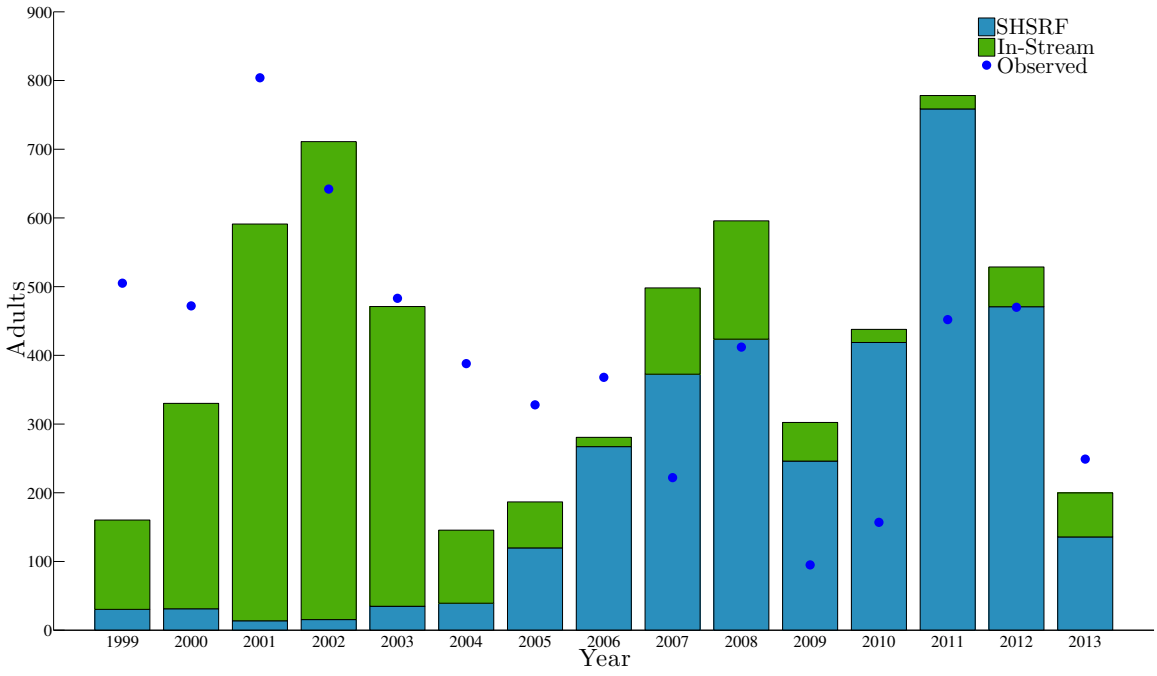

Figure 2.19: The predicted contributions from SHSRF (blue bar) and in-stream (green bar) individuals to the adult returns and observed adult returns (blue point).

(A)

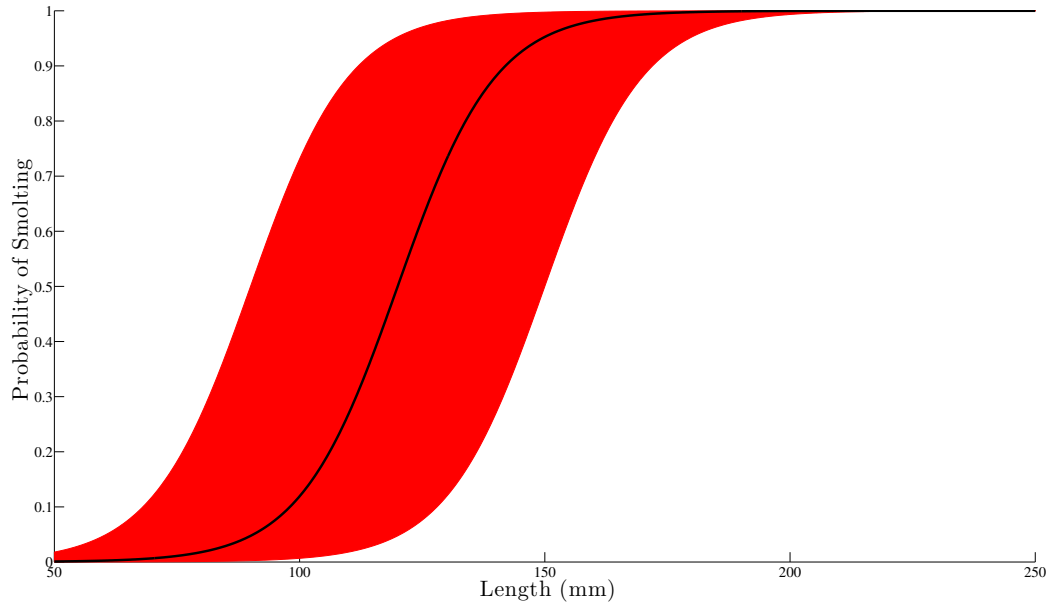

(B)

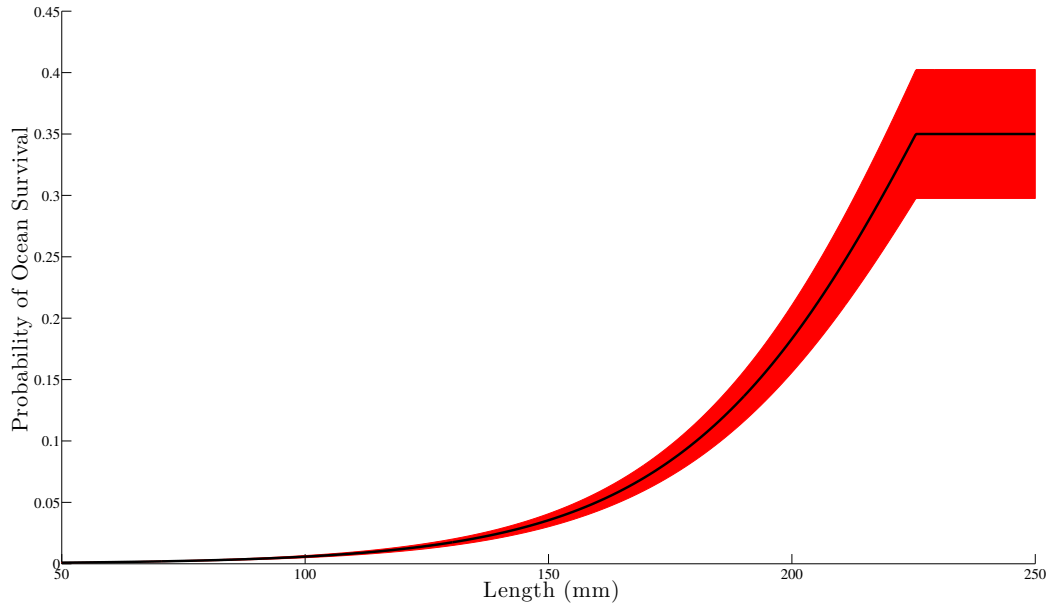

Figure 2.20: Curves demonstrating the range of values for smolting probability (A) and ocean survival (B) resulting from the sensitivity analysis. Black lines represent baseline value.

(A)

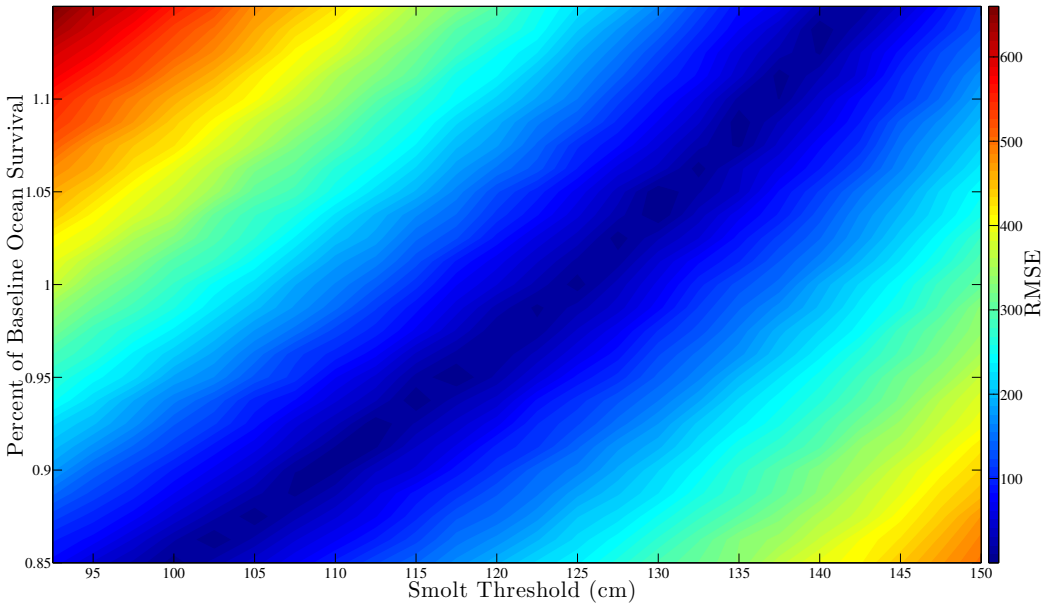

(B)

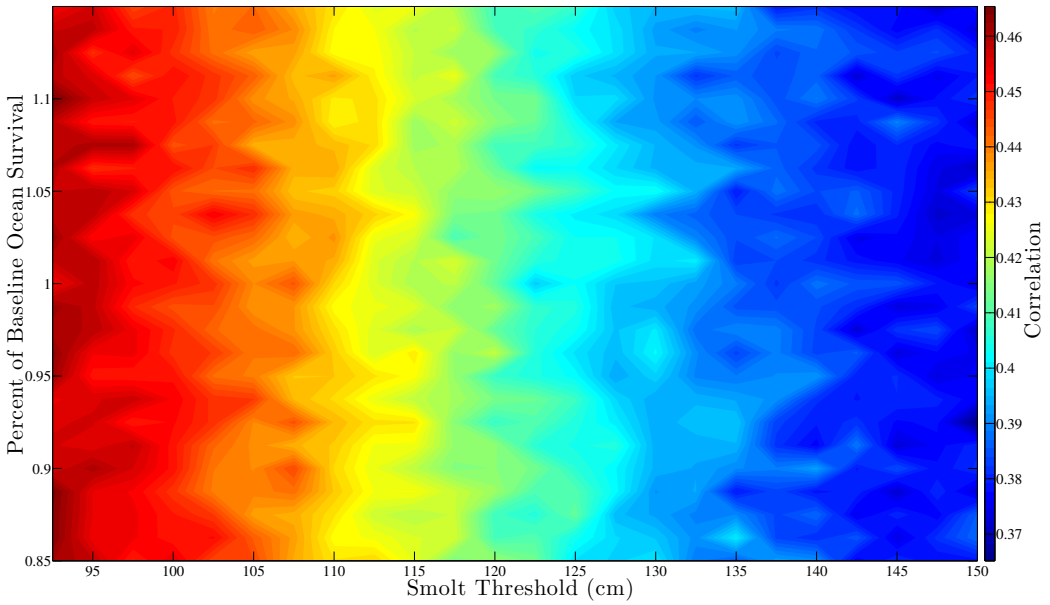

Figure 2.21: The RMSE (A) and correlation (B) between predicted and observed values as a function of both smolting threshold and ocean survival.

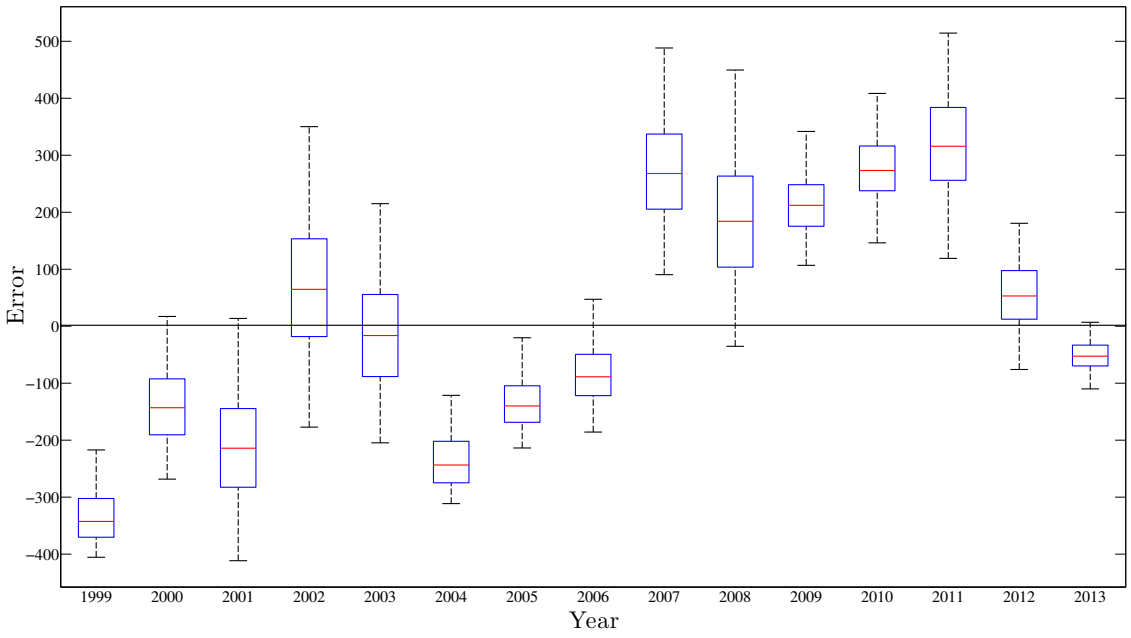

Figure 2.22: Absolute error between the number of predicted and observed adults across time for the different parameter values of explored in the sensitivity analysis.

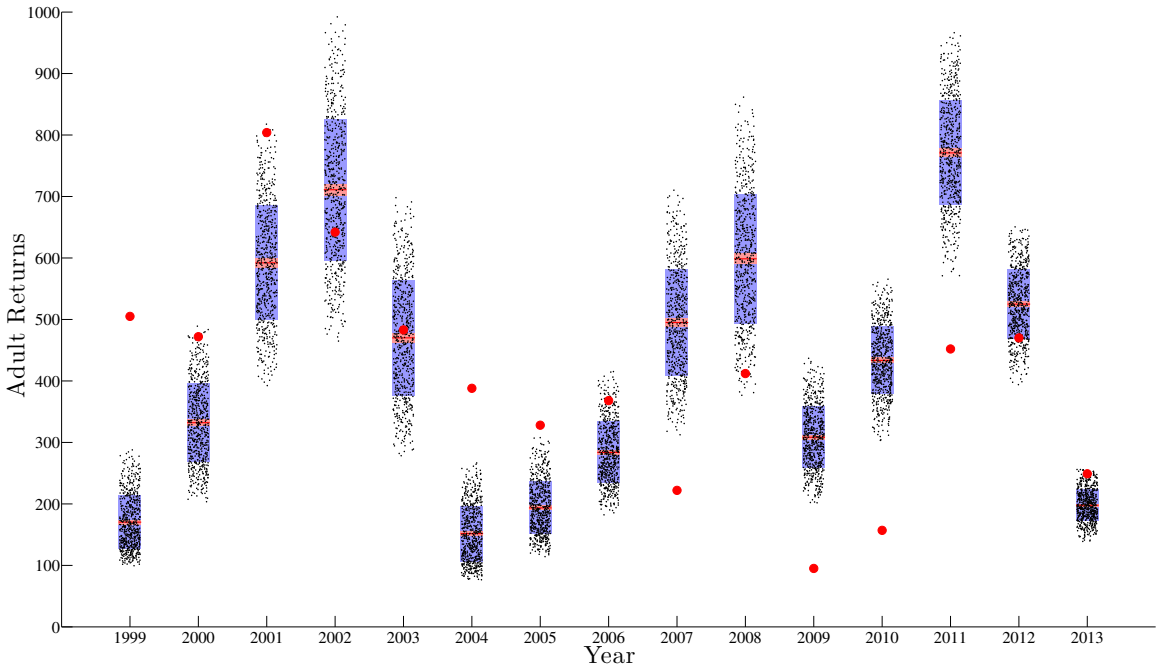

Figure 2.23: Time series of predictions based on the range of values explored through the sensitivity analysis for smolting threshold and ocean survival values and observed values of adult returns (red circles). Each point represents a parameter combination and red line represent mean value for all parameter combinations, red shaded region is the Standard Error of the Mean (SEM) and purple region is 1 standard deviation

Chapter 3

A Physiologically Structured Population Model for Steelhead*

3.1 Abstract

Steelhead trout (*Onchorhyncus mykiss*) show extensive variability in life histories. Thus, the majority of studies have focused on detailed bioenergetic and life history considerations while treating individuals as independent of their conspecifics. We present a Physiologically Structured Population Model (PSPM) that captures the vast variability in life history exhibited by steelhead populations by accounting for temperature-dependent growth, size-dependent mortality, and intraspecific competition. We demonstrate the power of our model through an exploration of the effects that size-dependent mortality and competition have on the individual life history attributes and population dynamics, parametrized with data from various studies in California. We also explore the effects that three different

*This chapter will be converted to a journal article by Lopez Arriaza, Mangel and de Roos entitled "A Physiologically Structured Population Model for Steelhead" for the journal *The American Naturalist*.

temperature regimes (historical, a constant increase or an increase in variability) have on population dynamics. We predict that under the historical temperature regime, increases in either the size asymmetry of competition or the dependence of size on mortality leads to delayed smolt timing. Due to size-dependent competition, increases in the dependence on size of mortality lead to longer mean lifespans and lower per-capita birth rates. Conversely, increases in mean asymptotic length due to increased size-dependent competition leads to higher per-capita birth rates in population. Although changes in temperature regimes do not result in consistent changes in the population dynamics, due to bioenergetic considerations, the constant increase scenario leads to higher population abundances, while the opposite is true for the scenario with increased variability. The results from the model suggest that although some general patterns occur across the parameter range, generalized statements about the effects of specific environmental changes should be made with caution.

3.2 Introduction

In general, modeling the dynamics of fish populations is of high interest due to their economic and ecological significance. Anadromous species, particularly those that take both migratory and resident forms, are of special importance due to both their role as keystone species in vertebrate communities and their susceptibility to climate change (Willson & Halupka, 1995). Since the predicted change in climate is expected to have major implications for habitat availability of anadromous species, it is important to have the proper tools to assess the consequences that these changes will have on species of concern (Reist et al., 2006; Crozier et al., 2008; Abdul-Aziz et al., 2011). However, the considerable variation in life

histories of some of these species poses new modeling challenges. In California, Steelhead trout (*Onchorhyncus mykiss*) are of particular interest. Four of the five Distinct Population Segments (DPSs), which are anadromous components of Evolutionarily Significant Units (ESUs) as defined by the Endangered Species Act (ESA), are listed as threatened and one is listed as endangered due to both natural and antrhopogenic factors (Waples, 1991).

California steelhead can either be anadromous (migrate from fresh water to the ocean and return to fresh water to spawn) or resident (complete their entire life cycle in fresh water), with both forms being functionally iteroparous. Like all salmonids, steelhead begin as eggs and develop into alevins, where they consume the egg yolk and begin to move up the gravel. Beginning in its first year of life, an individual makes the annual decision whether to smolt, mature in freshwater or remain in the river another year as an immature fish. The level of variation among life histories in salmonids, defined in terms of age at smolting, age at maturity, and single vs multiple spawning events, is extensive, with at least 32 possible trajectories (Figure 3.1) (Thorpe, 1998).

Although evidence exists for some genetic control of the life history of an individual, there is also considerable evidence of resident trout spawning anadromous offspring and anadromous trout spawning resident offspring (Pascual et al., 2001; Thrower et al., 2004; Olsen et al., 2006; Ciancio et al., 2008). Plasticity also occurs as a response to environmental conditions that an individual experiences; primarily an individual's body size and growth at a specific decision window (Mangel, 1994; Thorpe, 1998; Thorpe et al., 1998; Satterthwaite et al., 2010; Sloat et al., 2014b). Life-history variability within a population is thought to serve as a buffering mechanism against adverse environmental conditions, but

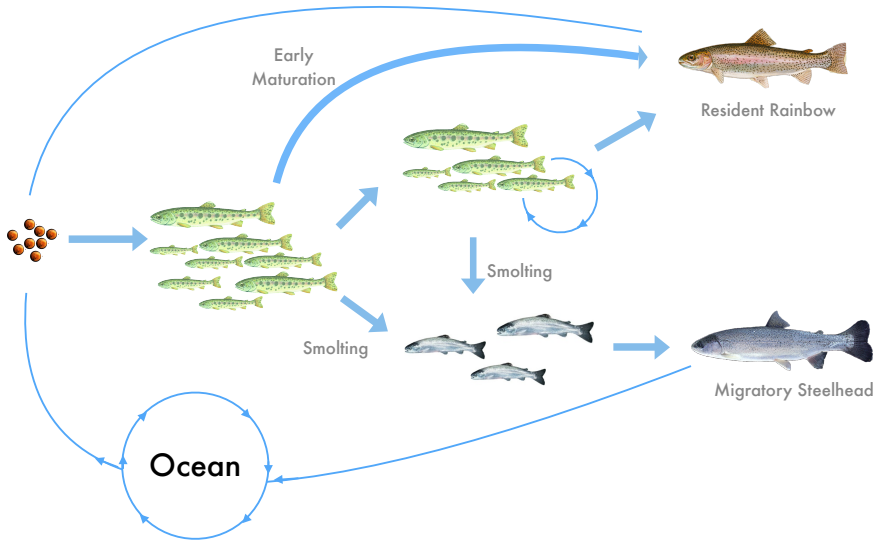

Figure 3.1: Simplified life history of steelhead trout demonstrating the complexity and variability in the life history of steelhead.

the extent of variation that is needed for the sustainability of a species is unknown (Quinn & Dittman, 1990; Moore et al., 2014). To date, the majority of efforts at restoring life-history variability and overall population levels have done little to return populations to historical levels (Boughton et al. 2007). Under the assumption that the life-history decision of an individual is driven by a combination of growth conditions and genetic cues, population structure (numbers, body size and growth rates) will be of particular importance to conserving life-history variation. This extensive variability creates a complex biological system and serves as an ideal system for modeling complex population dynamics.

In addition to the complexity posed by the life history variability, density depen-

dence among juveniles has the potential to completely alter the structure of a population (Nakano et al., 1991; Lorenzen, 1996; Vincenzi et al., 2008). This is especially true in environments in which individuals of multiple sizes are in direct competition for the same resource. This competition is often modeled as a symmetric process in which resources are reduced equally for every individual in the population (Lorenzen, 1996; Vincenzi et al., 2008). Although mathematically convenient, this approach often lacks the fidelity to nature to sufficiently capture the dynamics of the system because, in nature, this competition occurs asymmetrically and is often dominated by a size hierarchy, with larger individuals acquiring a larger portion of the resources. This competition for resources between individuals of different sizes may create bottleneck effects for the population at specific life-history stages and can therefore result in complex population dynamics (de Roos & Persson, 2013).

Physiologically Structured Population Models (PSPMs) provide a natural framework for accounting for these life-history complexities and population structure by explicitly and mechanistically characterizing the dynamics of a population in terms of the individual-level processes that describe its constituents and their interactions with the environment and each other. The wide range of applications as well as the development of mathematical tools for PSPMs has led to the growing paradigm of studying population and community dynamics in the context of the ontogenetic development of an individual (de Roos & Persson, 2013). Essential to the PSPM paradigm is the explicit mathematical description of the state of an individual (i-state) and the processes that characterize its life history (growth, survival, reproduction, and competition) and their interaction with the environmental state (e-state) that they experience (e.g. temperature and resource availability). It

is this clear mathematical description that allows the population level effects to emerge from processes that occur at the level of single individuals in the context of their environment. The mechanistic way in which PSPMs describe the life history of individuals by accounting for individual physiology, ontogentic development and the resultant population dynamics make them particularly well suited for studying individuals with very complex life histories in the context of intraspecific competition and environmental change.

In the following sections we describe in detail the development of a PSPM for steelhead trout. We begin with a comprehensive description of the within-year processes (individual growth, competition and mortality) and between-year processes (maturation and reproduction) that drive the population dynamics. We then present results on the effects that size-dependent mortality and size-dependent competition have on the population dynamics, population structure and life-history pathways of individuals. Finally, we explore the possible effects that expected climate change could have on the population dynamics predicted from the model by changing the temperature regime experienced by individuals. To illustrate, we parametrize our model using data for a population with the attributes representative of a Central California Coast population.

3.3 Conceptual Model

3.3.1 Model Formulation

With the aim of capturing the broad range of life-history pathways exhibited by steelhead, we model the entire life of the individual from birth to death. Since many processes determining the life history of an individual are highly correlated with an individ-

ual's mass, we characterize the i-state predominantly by irreversible and reversible mass. Irreversible mass, x, is composed of bones and organs that cannot be starved away and reversible mass, y, is composed of energy repositories such as fat, muscle, and gonads. We assume that non-starving juveniles and mature individuals maintain a constant ratio of reversible to irreversible mass denoted by q_j and q_m respectively. In addition to mass, we also characterize the i-state by body length, l (in cm), and age, a (in days). The development of individuals is also determined by the environment to which they are exposed. We therefore model the entire year and characterize the abiotic environment through time (in days) within the season beginning and ending at reproductive times ($t = 0$ and $t = 365$ respectively) and through the temperature at that given time, $T(t)$. The biotic environment is represented by competitive pressures imposed by an individual's conspecifics, which will be described below.

Two types of processes drive the ultimate life history of an individual; within-year processes that are described continuously (growth, intraspecific competition and survival) and between-year dynamics that are discrete events within the season (maturation, smolt transformation, migration and reproduction). In the following sections we describe the details of the within-year dynamics, between-year dynamics and the timing of the key events within the season.

Parameter	Definition	Baseline Value
μ_0	Background mortality	0.0045-0.008[f]
μ_1	Size-dependent mortality	0.0013-0.0[f]
μ_s	Starvation mortality	0.2[b]
α_l	Allometric constant in length-weight relationship	4.519[f]
β_l	Allometric exponent in length-weight relationship	0.322[f]
w_0	Weight of neonate individuals	0.15 grams[d,e]
Δ_{w_0}	Spread in weight of newborn individuals	0.01 grams[d,e]
w_m	Maturation weight	195 grams
$l_{\text{smolt}}(1)$	Critical length for smolting of year 1 individuals	12 cm[a,d]
$l_{\text{smolt}}(2)$	Critical length for smolting of year 2 individuals	13.5 cm[a,d]
$l_{\text{smolt}}(3)$	Critical length for smolting of year 3 individuals	15.5 cm[a,d]
σ_s	Spread in smolting probability	1.5 cm[a,d]
$l_m(0)$	Critical threshold for early maturation age 0	15.5 cm
$l_m(1)$	Critical threshold for early maturation age 1	16.5 cm
$l_m(2)$	Critical threshold for early maturation age 2	17.5 cm
c_1	Allometric constant in ingestion rate	0.09[c]
c_2	Allometric exponent in ingestion rate	0.7[c]
m_1	Allometric constant for metabolism	0.0169[c]
m_2	Allometric exponent for metabolism	0.783[c]
η_h	Half-saturation constant for access to resources	10^7
β	Exponent controlling size dependence strength in competition	0.0 - 0.1
q_j	Maximum juvenile irreversible to reversible mass ratio	0.74[b]
q_m	Maximum mature irreversible to reversible mass ratio	1.37[b]
q_s	Irreversible to reversible mass ratio threshold for starvation	0.2[b]

Table 3.1: Variable definitions, values, and citations for parameters. See Parameter Exploration for further details for parametrization and variants of values explored. Sources *a*: Beakes et al. (2010), *b*: Persson et al. (1998), *c*: Railsback & Rose (1999), *d*: Shapovalov & Taft (1954), *e*: Thrower et al. (2008), *f*: Independent Data

Within Year Dynamics (Continuous Dynamics)

Individual Growth

We model in-stream growth of an individual through a bionenergetically closed loop that balances the net mass intake, $E_g(x, y)$, of an individual as the difference of the total mass intake rate, $E(x, y)$, and the metabolic demand of the individual, $E_m(x, y)$:

$$E_g(x, y) = E(x, y) - E_m(x, y) \tag{3.1}$$

The total mass intake rate of an individual is determined by an allometric relationship to total mass scaled by a temperature dependent term, $\Phi_C(T)$, and a term accounting for competitive interactions between individuals, $A(t, l)$, which will be discussed in detail in the next section. We then set

$$E(x, y) = \Phi_C(T)A(t, l)c_1(x + y)^{c_2} \tag{3.2}$$

In a similar manner, the metabolic demands of an individual are determined by an allometric relationship to total mass and a different temperature dependent function.

$$E_m(x, y) = \Phi_M(T)m_1(x + y)^{m_2} \tag{3.3}$$

We follow the form developed by Thornton & Lessem (1978) to characterize the temperature dependence function for mass intake, Φ_C, and the relationship from Stewart et al. (1983) for metabolism, Φ_M; both of which have been reparametrized for steelhead (Hanson et al., 1997; Railsback & Rose, 1999). The net mass intake is then allocated towards the two different types of mass to maintain the reversible to irreversible mass ratio:

$$\kappa(x, y) = \begin{cases} \frac{1}{(1+q_j)q_j}\frac{y}{x} & \text{juvenille} \\ \frac{1}{(1+q_m)q_m}\frac{y}{x} & \text{mature} \end{cases} \tag{3.4}$$

Following this allocation rule, the rates of change of reversible and irreversible mass are:

$$\frac{dx}{da} = \begin{cases} \kappa(x,y)E_g(x,y) & E_g(x,y) > 0 \\ 0 & E_g(x,y) \leq 0 \end{cases} \tag{3.5}$$

$$\frac{dy}{da} = \begin{cases} (1-\kappa(x,y))E_g(x,y) & E_g(x,y) > 0 \\ E_g(x,y) & E_g(x,y) \leq 0 \end{cases} \tag{3.6}$$

In practice, individuals are often described by their length rather than mass. Instead of linking the length of an individual with total mass, $m = x + y$, which can fluctuate and could lead to a decreases in length, we assume that length is only related to irreversible mass and denote reference mass and length as:

$$m^* = (x + q_j x) \tag{3.7}$$

$$l = \alpha_l (m^*)^{\beta_l} \tag{3.8}$$

respectively. The reference mass is the mass that an individual would have if it were to maintain a stable juvenile reversible to irreversible mass ratio. Using this definition makes length independent of an individual's condition and also allows the possibility of modeling underweight individuals.

Competition

Competition often arises from the interactions of individuals attempting to access common resources (e.g. food, habitat). These interactions are often size-dependent (Metcalfe, 1986; Elliott, 2002; de Roos et al., 2003; Claessen et al., 2000). With this in mind,

we model the size-dependent interactions between individuals similarly to Le Bourlot et al. (2014) and denote the competitive ability of a focal individual of length, l, relative to a conspecific of length, λ, as:

$$C(l|\lambda) = \exp(\beta(\lambda - l)) \tag{3.9}$$

where the parameter, β determines the intensity of size-dependent competition that occurs. Two individuals are competitively equal when the competition function, $C(l|\lambda) = 1$. This occurs under two conditions: when $\beta = 0$ all individuals are always equally competitive; for all other values of β only individuals of the same size are equally competitive. In the latter case, as β increases, size dependence becomes more important, with larger individuals being more competitively dominant over smaller ones (Figure 3.2).

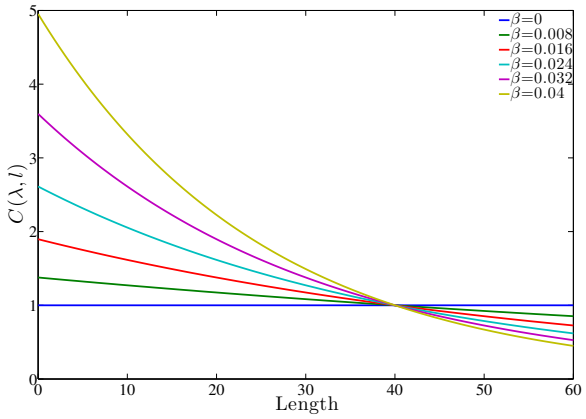

Figure 3.2: Competition described by the function $C(l|\lambda)$ as experienced by individual of length l competing with an individual of length $\lambda = 40$ cm for different values of β.

Based on the above definition of competitive ability, individuals of different lengths will experience their environment in different manners depending on the rest of the population; we describe this as the effective population density function, $\eta(t, l)$. At any time,

t, for an individual of length, l, within a population with a size distribution, $n(t, \lambda)$, that ranges from lengths l_b to l_M, we define the effective population density as:

$$\eta(t, l) = \int_{l_b}^{l_M} C(l|\lambda) n(t, \lambda) \lambda^2 d\lambda \tag{3.10}$$

This functional form can be thought of as summing the competitive effects that are imposed on an individual by the rest of the population. The λ^2 term within the integral accounts for the assumption that competitive interactions between individuals scales with body surface area. When $\beta = 0$ the effective population density becomes completely independent of the focal individual's length and is then identical for all individuals in the population.

We then describe how the effective population density that an individual experiences affects its access to the resources in the environment, $A(t, l)$,:

$$A(t, l) = \frac{\eta_H}{\eta_H + \eta(t, l)} \tag{3.11}$$

Here the half-saturation constant, η_H, scales the population density and describes the total amount of resources in the environment. We see that for larger values of effective population density, $\eta(l, t)$, an individual has lower access to resources. For the case in which $\beta = 0$ and all individuals are competitively equivalent, resulting in equal level of access to resources independent of length. Again, as β increases, larger individuals will have a lower effective population density, therefore having a higher access to the resources, with the inverse being true for smaller individuals.

Mortality

Within the stream, individuals face multiple sources of mortality. We account for all of these sources by modeling mortality as being composed of both size-dependent and

size-independent terms.

$$\mu(a) = \mu_0 + \mu_1 l(a)^{-1} + \mu_s(a) \tag{3.12}$$

where μ_0 accounts for the size independent (background) mortality and μ_1 accounts for the size dependence, which scales as the inverse of length (Lorenzen, 2000). Since we allow for the modeling of underweight individuals, we also account for mortality induced by starvation, μ_s, following de Roos & Persson (2001). An individual experiences mortality due to starvation when its reversible to irreversible mass ratio drops below the starvation condition, q_s.

$$\mu_s(a) = 0.2 \quad \text{if} \quad \frac{y}{x} \leq q_s \tag{3.13}$$

Given this definition for mortality, the survival of an individual to age a is given by

$$S(a) = \exp^{-\mu_0 a - \int_0^a \left\{\mu_1 l(a')^{-1} - \mu_s(a')\right\} da'} \tag{3.14}$$

Equation (3.14) shows that while instantaneous mortality only depends on an individual's size at a specific age, its survival is coupled to its growth trajectory through its entire life, leading to some non-intuitive results.

Although migrating individuals also experience size-dependent mortality in the ocean, the lack of knowledge about the oceanic phase of an individual's life history makes it difficult to model oceanic growth (McGurk, 1996; Kendall et al., 2015). We therefore model the size-dependent ocean survival of an emigrating individual as a logistic function of its smolting length, l_s (Satterthwaite et al., 2010).

$$\sigma(l_s) = 0.84 \times \frac{1}{1 + \exp(8.657 - 0.0369 l_s)} \tag{3.15}$$

Between Year Dynamics (Discrete Dynamics)

Event	Symbol	Nominal Value (day)
Time of reproduction	t_r	0
Time of emigration	t_e	90
Time of first maturation check	t_{m_1}	120
Time of second maturation check	t_{m_2}	275
Time of smolting decision	t_s	274

Table 3.2: Timing of the events of the discrete dynamics for the model

3.3.2 Maturation, Smolt Transformation and Reproduction

We consider five key events that drive the life history of an individual within the year: birth, early maturation, smolting, reproduction and death. To simplify the model, we assume there is no inter-annual or intraspecific variation in the timing of these events. In the model, the life of individuals, $a = 0$, begins at time $t = t_r = 0$ where we assume the birth and emergence of all individuals occurs simultaneously immediately after a spawning event. Following birth, an individual is faced with annual decisions for freshwater maturation, smolting and reproduction (Figure 3.3).

In general, the propensity of an individual to mature early is highly correlated with early growth, with fast-growing individuals maturing early (Thorpe et al., 1998; Thorpe, 1998; Sloat et al., 2014a). We model early maturity as a decision process depending on an individual's length at two time points in the year. At the time of the first early maturation decision, $t = t_{m_1}$, the individual is faced with the decision of allocating mass towards irreversible mass (gonads) in order to have the ability to reproduce during the following spawning event. If an individual's length is greater than the age-dependent early matu-

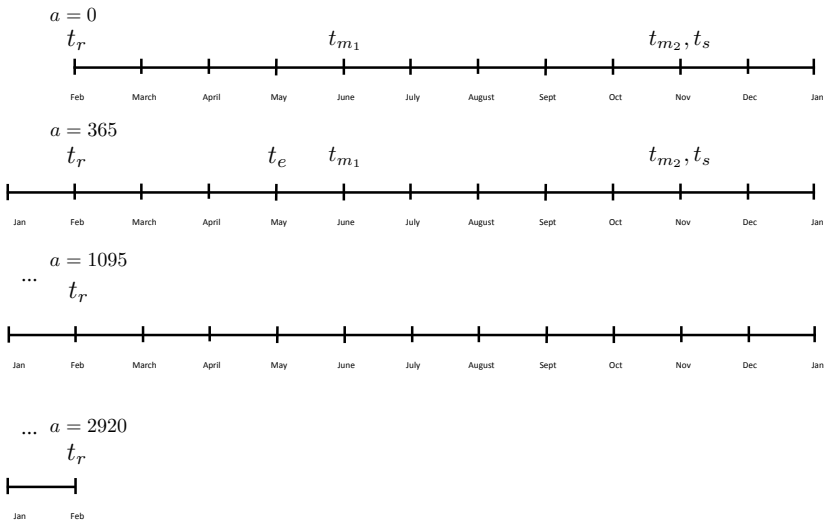

Figure 3.3: Timing of life history events within an individual's life as described in the conceptual model.

ration threshold length, $l_m(a)$, it begins allocating extra resources to irreversible mass. If an individual surpasses this threshold, then at a later time in the season, $t = t_{m_2}$, it must also assure that growth in the intermediate time has been adequate for successful reproduction. The precise mechanisms driving early maturation in steelhead are complex and not completely understood (see Kendall et al. (2015)), therefore, we set the threshold for the continuation of early maturation to be the occurrence of growth between $t = t_{m_1}$ and $t = t_{m_2}$:

$$m(a, t_{m_2}) > m(a - (t_{m_2} - t_{m_1}), t_{m_1}) \tag{3.16}$$

If this condition is satisfied an individual will continue allocating extra resources to irreversible mass (gonads) and spawn at the following reproductive event, t_r. If an individual's

summer growth has been insufficient to continue an early maturation track, it will stop allocating extra resources to irreversible mass and continue growing as a juvenile.

In addition to early maturation, the yearly decision of an individual to become an ocean-migrating smolt depends on its length at specific times. We model the probability that an individual smolts given it has length, l, and age, a, at the smolting decision, $t = t_s$ as:

$$P_s(l(t_s), a) = \frac{1}{1 + \exp\left(-\frac{l(t_s) - l_{\text{smolt}}(a)}{\sigma_s}\right)} \tag{3.17}$$

where $l_{\text{smolt}}(a)$ is the age specific length threshold at which point the probability of smolting is 0.5 and σ_s characterizes the dispersion around this threshold (Figure 3.4).

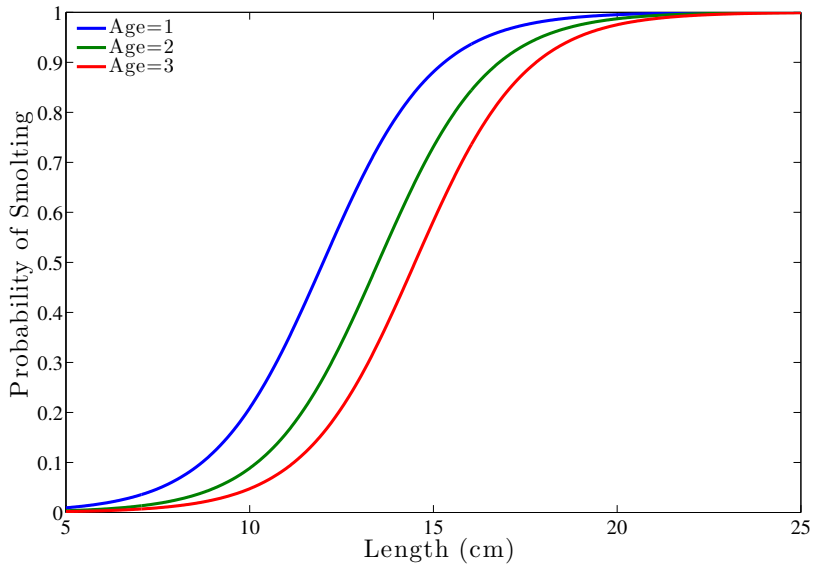

Figure 3.4: Age (in years) and length-dependent probability of an immature individual to smolt

An individual on the smolting life-history track will remain within the stream from time $t = t_s$ until it migrates at time $t = t_e$ in the next season. We assume that all

individuals who survive migration and the marine phase return within three years; with the return timing depending on the number of years spent in-stream based on empirical observations (Table 3.3) (Shapovalov & Taft, 1954). An individual who does not mature early or smolt prior to reaching an in-stream maturation size, w_m, follows a resident life history trajectory.

Table 3.3: The composition by percentage of the returning individuals given the number of years spent in stream. Returning compositions determined from data from Shapovalov & Taft (1954).

Years in Stream	Years in Ocean		
	1	2	3
1	53.26	45.65	0.019
2	52.74	46.90	0.36
3	70.47	29.529	0.001

Reproduction

Stream Maturing Individuals

At the time of reproduction, t_r, individuals who have reached maturity in-stream use all reversible mass that exceeds the standard reversible mass for juveniles $(y - q_j x)$ for the production of offspring. For simplicity we assume that there is no cost incurred for the production of an offspring. We further assume that the total mass $(\mathcal{W})$ allocated to the creation of offspring by the population is then distributed to create $(N = \frac{\mathcal{W}}{w_0})$ new individuals which are distributed to n_c+1 new cohorts. Since we have assumed that there is no cost of production for individuals, this yields cohorts with equal numbers of individuals $(\frac{N}{n_c+1})$. The masses of the offspring, w_i, within the cohorts are then evenly spaced around

w_0 with spacings Δ_{w_0} (Figure 3.5 , Table 3.1).

$$w_i = w_0 - \frac{1}{2}(n_c) \times \Delta w_0 + (i-1) \times \Delta w_0, \quad i = 1 \ldots n_c + 1 \tag{3.18}$$

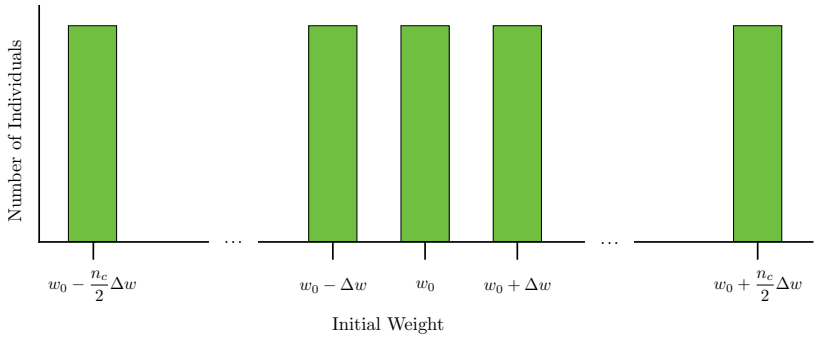

Figure 3.5: Distribution of weights for new born individuals.

Ocean Maturing Individuals

Due to the difficulty in tracking the exact bionenergetics of migrating individuals, we assume functional semelparity and model individual fecundity at spawning using a two-step process. With the knowledge that an individual's length at spawning is a very good predictor of fecundity and that the return length of an individual depends on its life history, we model the length at return, L_r for a migrating individual as linear regression on the number of stream, Y_r, and marine years, Y_m, that the individual experienced

$$L_r = \alpha_r + \beta_r Y_r + \beta_m Y_m \tag{3.19}$$

where α represents the baseline return length, β_r captures the dependence of return length on number of years spent within the stream and β_m captures the dependence of return length on the number of years spent in the ocean. Fitting Equation (3.19) to data from

Shapovalov & Taft (1954) allows us to derive quantitative estimates for the return length of an individual based on its life history (Figure 3.6 (A)).

Given an individual's return length, L_r, we model its fecundity by

$$F = \alpha_f L_r^{\beta_f} \tag{3.20}$$

with α_f=0.9471, $\beta_f = 2.1169$ estimated by Shapovalov & Taft (1954) (Figure 3.6 (B)).

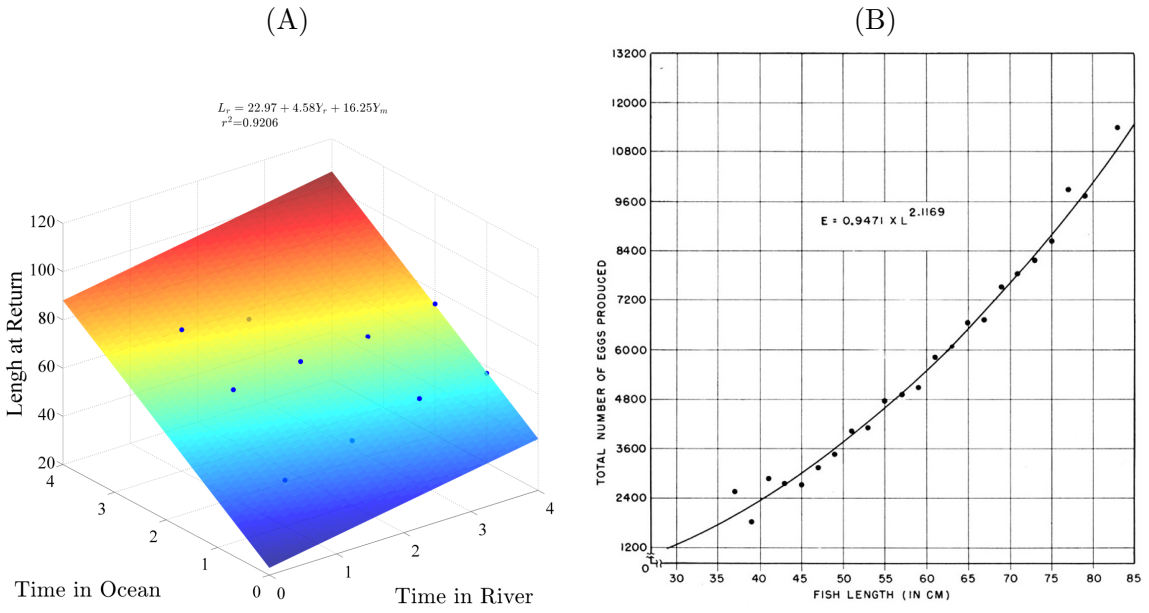

Figure 3.6: (A) Data (points) and linear regression fit (plane) for the length at return in centimeters for an individual who spent Y_r years in the stream and Y_m years in the marine environment. (B) Length-fecundity relationship from Shapovalov & Taft (1954) for Waddell steelhead.

3.4 Results

We present results parametrized with data from populations in both the Central California Coast and South-Central California Coast DPS's (Table 3.1). We limit the scope of our analysis to the effects that arise through the changes in size-dependent mortality, competitive effects and temperature regimes. We conducted numerical solutions for 500 years and analyzed the last 50 years of the numerical solutions to discard transient dynamics. We used the Escalator Boxcar Train (EBT) method (de Roos, 1988) as implemented in the EBTtool software for numerical solutions (https://staff.fnwi.uva.nl/a.m.deroos/EBT/).

3.4.1 Parameter exploration

We begin by studying how varying levels of competition and size-dependent mortality alter individual life history characteristics and the ultimate effects they have on population-level attributes. Exploring the entire parameter space (background mortality, μ_0, size-dependent mortality, μ_1 and competition, β) is beyond of the scope of this paper. Furthermore, many parameter combinations would not be biologically interesting.

To define the region of biological interest, we begin by ignoring density dependence (setting $A(t,l)$ constant) and consider the case in which starvation-induced mortality can be neglected ($\mu_s = 0$). Under these assumptions, for a given survival level, $\hat{S}$, and a reference growth trajectory to age, $\hat{a}$ ($\hat{x}(\hat{a})$), we develop a relationship between size-dependent and size-independent mortality based on Equation (3.14). That is, when mortality is completely size-independent, μ_1=0, the size-independent mortality term is

$$\mu_0 = \frac{-\log(\hat{S})}{\hat{a}} \tag{3.21}$$

Since survival is $\hat{S}$, we then have a linear relationship between size-dependent and size-independent mortality (Equation 3.14)

$$\mu_1 = -\frac{\mu_0 \hat{a} + \log(\hat{S})}{\int_0^{\hat{a}} l(s)^{-1} ds} \tag{3.22}$$

With this relationship, we can model growth trajectories for individuals as defined by Equations 3.5, and 3.6 and subsequently find pairs of size-dependent and -independent parameters constrained with a specific value of $\hat{S}$ at age $\hat{a}$. We set $\hat{S}$ at 1.8% from birth to the age of first emigration ($t = t_e, a = 455$), following Snover et al. (2006), whose survival estimates came from Shapovalov & Taft (1954). We could alternatively determine the combinations of μ_1 and μ_0 that yield a specific survival level by considering the growth of an individual from size at birth to a specific size (see Appendix B.1)

In addition to varying mortality rates, we explore a range of parameter values for β which result in different degrees of interference and exploitative competition.

3.4.2 Population Results: Baseline Temperature

The highly non-linear nature of the model results in highly variable population dynamics for different combinations of parameters explored (e.g. stable constant newborn production, oscillatory newborn production, and oscillatory newborn production with non-reproductive years (Figure 3.7)). The variability in the population dynamics makes precise inference on the effects from parameter changes difficult. In light of these complexities,

we treat simulation results of the model as *in-silica* experimental outputs and often compare summary statistics from each simulation for different parameter combinations. For the exploration of the effects that competition and size-dependent mortality induce in the population, we set the temperature regime experienced by individuals at the historic in-stream temperature profile for the Carmel River in California (Figure 3.8).

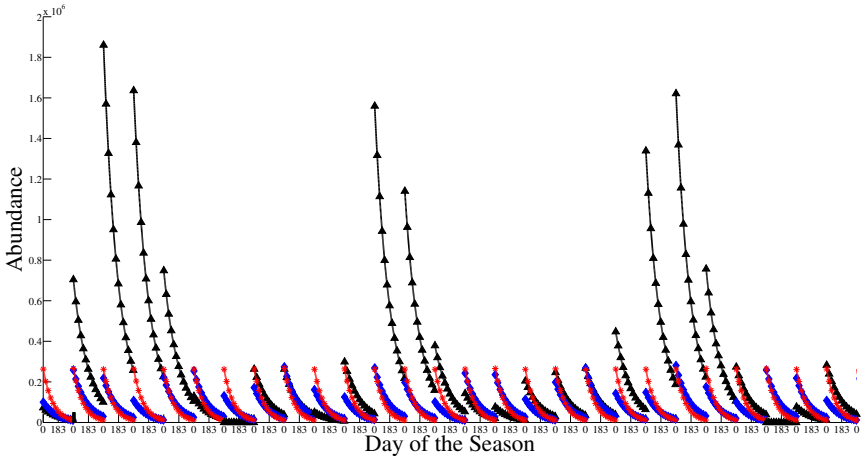

Figure 3.7: Sample dynamics of Young-Of-the Year (YOY) abundances for three different scenarios (low size dependent mortality, low competitive asymmetry (red); intermediate size dependent mortality, intermediate competitive asymmetry (blue); high size dependent mortality, high competitive asymmetry (black)).

As a verification of general patterns that occur in nature, in Figure 3.9 we show that, throughout the parameter range, increases in the total number of migrants leads to an increase in the total number of births due to the higher fecundity of ocean maturing individuals. Additionally, our model captures the range in length-at-age relationships that occur in nature with the largest individuals attaining growth that would only be exhibited in the marine environment and the mean length exhibited in our model matching those

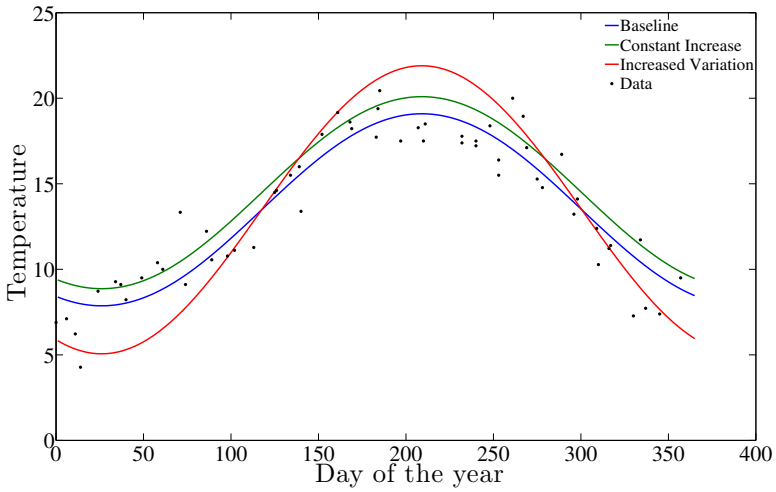

Figure 3.8: Temperature profiles for baseline temperature (blue) fit to Carmel River data (black), 1 °C constant increase (green) and increased variability (red).

found in the field (Figures 3.10 and 3.11) (Sogard et al., 2012).

3.4.3 Effects of migratory individuals

The presence of migratory individuals is not predicted to occur with every parameter combination, Namely, growing conditions must fall within the range that it is preferable for an individual to migrate rather than to select the residency life history path due to slow growth such that ocean mortality would be too great or rapid growth such that growth within the stream is sufficient for successful reproduction (Figure 3.12). In addition to determining the presence and absence of individuals, growth conditions also determine the age composition of the migrating individuals.

Due to the inclusion of density dependence in our model, migration has substantial effects on the individuals who remain in the stream. The reduction in the number of individuals from the in-stream environment eases some of the competitive interactions and

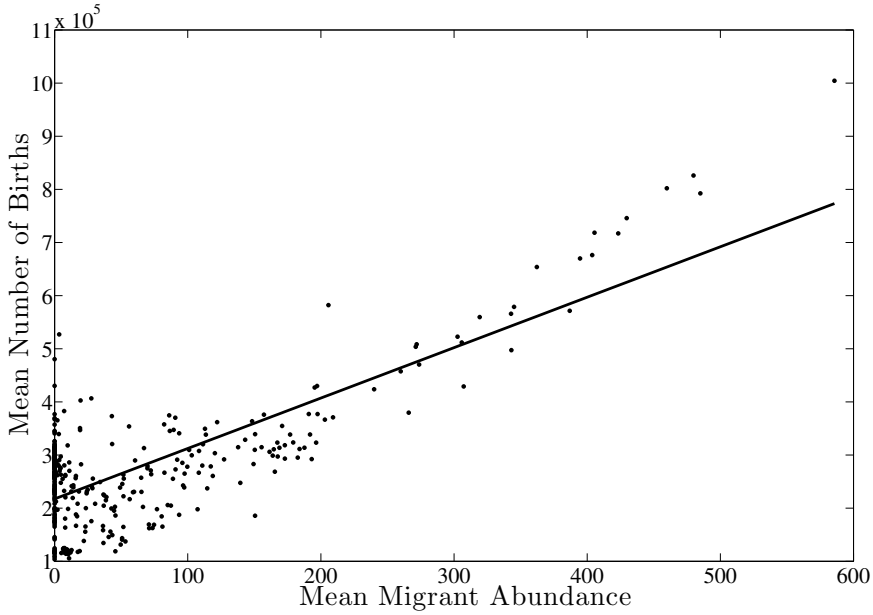

Figure 3.9: The relationship between mean number of migrants and mean number of births in the population throughout the parameter range. Each point represents the mean output from a single combination of values for mortality and competition parameters (3.1 for parameters explored)

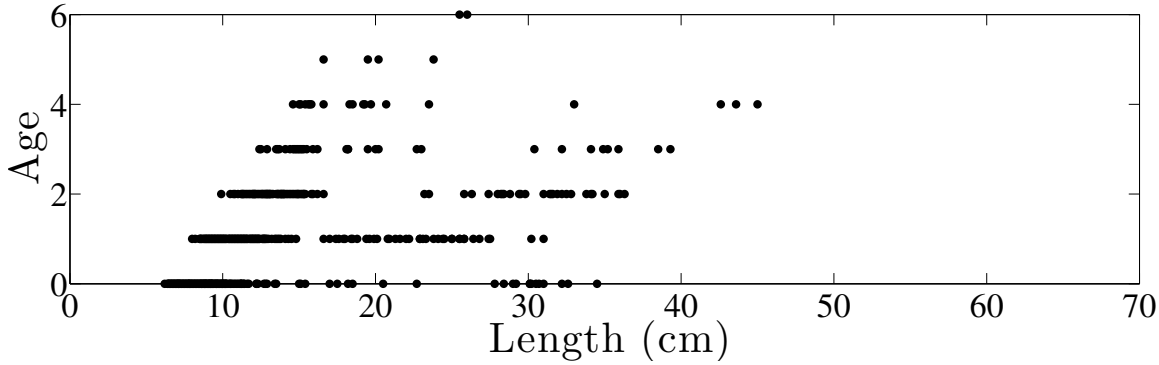

Figure 3.10: Mean length-at-age relationship for multiple watersheds in California found by Sogard et al. (2012)

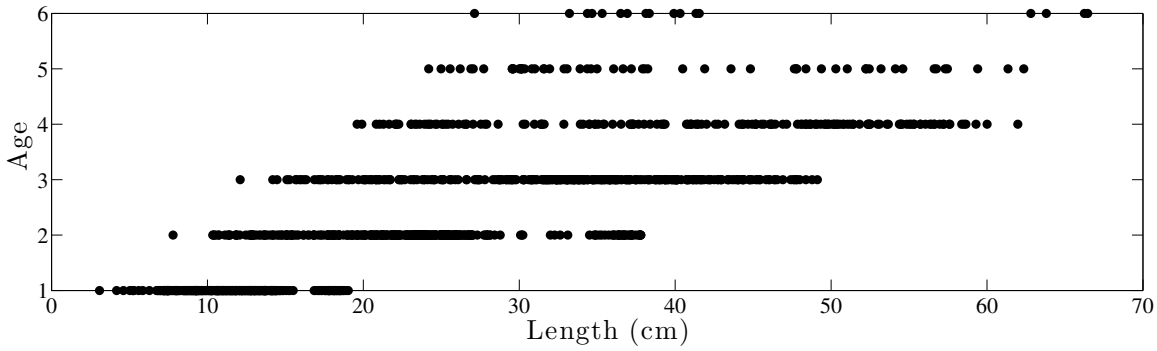

Figure 3.11: Mean length-at-age relationships for in-stream maturing individuals exhibited throughout all the parameter combinations explored in the model

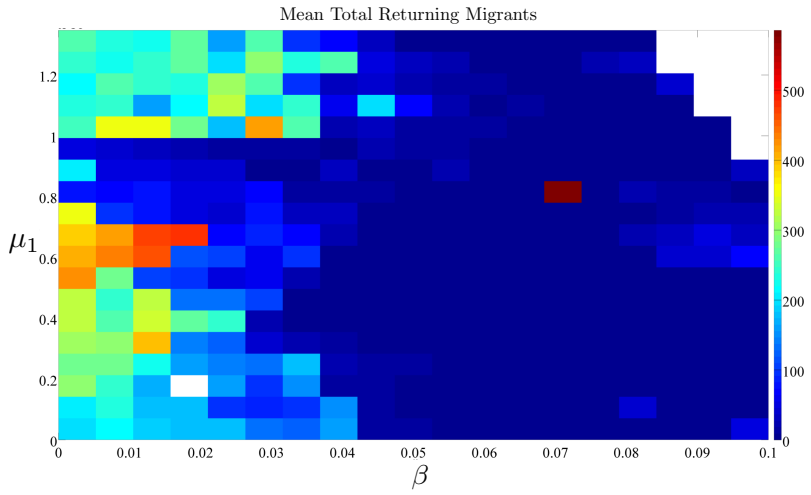

Figure 3.12: Mean total number of returning migrants as a function of the strength of size dependent mortality and asymmetric competition.

increases the accessibility to resources to all individuals who remain in the stream (Figure 3.13). Conversely, due to the high fecundity of ocean migrating individuals, at the time of reproduction the access to resources of individuals is reduced (Figure 3.13).

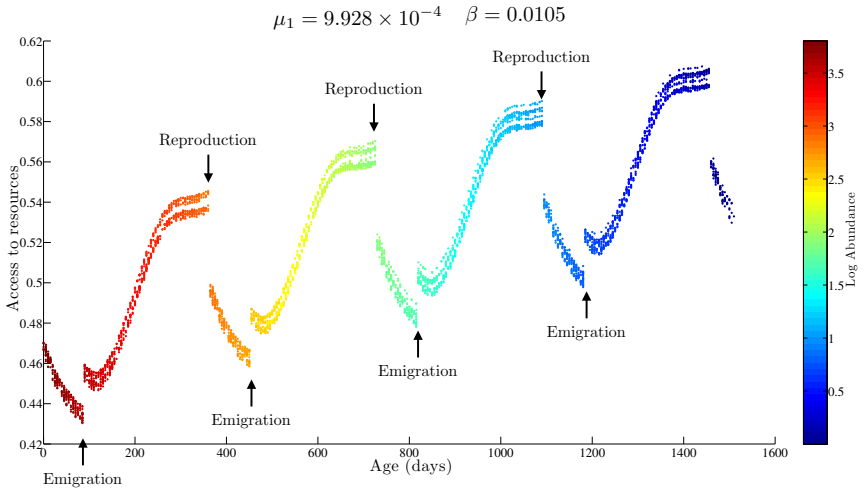

Figure 3.13: Sample of the effects of reproduction and emigration on the access of resources for individuals as a function of their age. Color represents log abundance of individuals present.

3.4.4 Effects of sources of mortality

As a proxy for per-capita birth rate, we normalized the mean number of births by the mean size of the population. Increasing the size-dependence of mortality leads to a decrease in the normalized mean number of births (Figure 3.15). In Figure 3.14, we show that increasing the size-dependence of mortality while holding overall mortality levels constant can lead to delayed smolting from age one to ages two and three. Both the reduction in normalized mean number of births and delayed smolting decisions are due to the fact that although the asymptotic lengths for all levels of size-dependent mortality (given β) are similar, the mean lifespan of an individual decreases as size-dependent mortality decreases (with overall mortality remaining equal). The shortened lifespan and increased growth rate leads to both higher number of individuals maturing early and contributing to

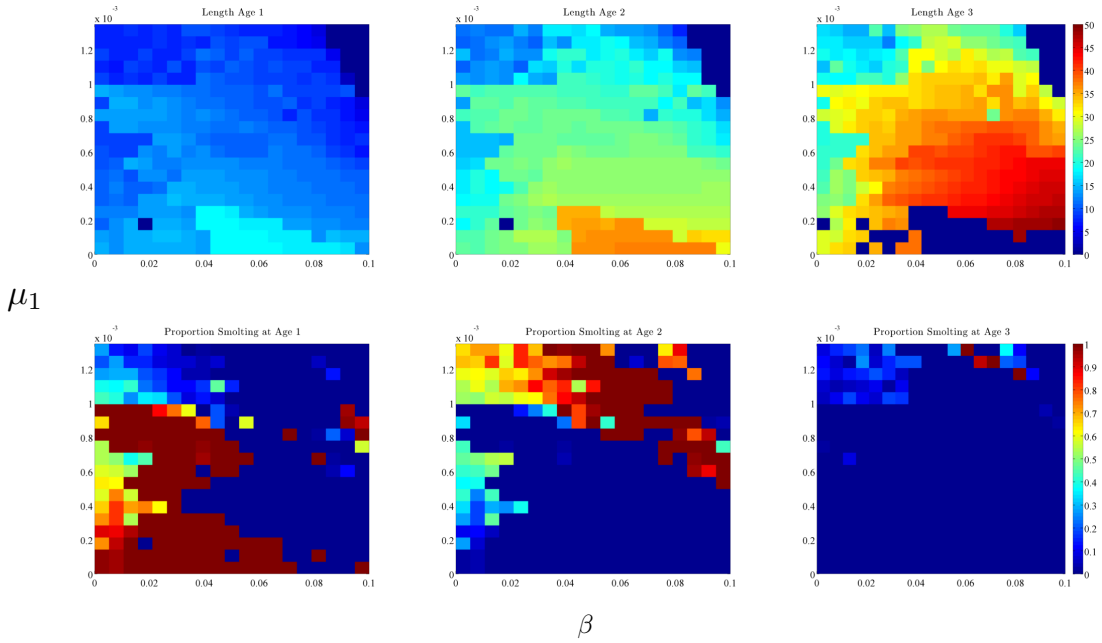

Figure 3.14: The mean age at length relationships (top row) and the proportion of individuals smolting from that age class (bottom row) throughout the parameter space (Note that not all parameter combinations result in migratory individuals)

the per-capita birth rate and later smolting individuals.

3.4.5 Effects of competition

In Figure 3.17b, we show sample dynamics for multiple combinations of size-dependent mortality and competition values to demonstrate the effect that increases in the competition parameter (β) has on the access the resources for individual with lengths l. For low values of size-dependent mortality, increasing competition results fast growing individuals and yields either age 1 smolting individuals or no migratory individuals. For intermediate and high levels of size-dependent mortality increases in competition result in

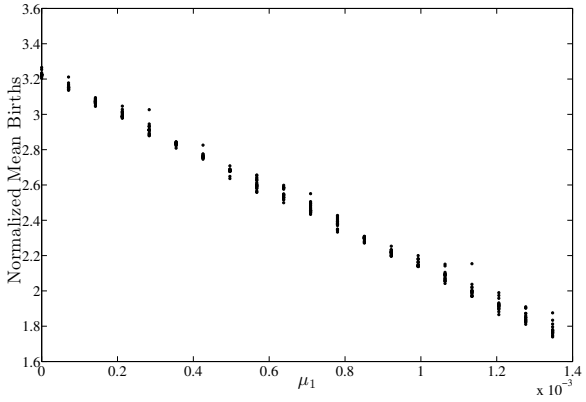

Figure 3.15: The relationship between the level of size-dependent mortality and the mean number of births (normalized by mean population abundance) for all values of size-dependent mortality.

delayed smolting from age 1 to ages 2 and 3 (Figure 3.14). Additionally, the relationship between asymmetric competition and the median number of births is complex with intermediate values generally yielding the lowest number of births (Figure 3.16). This effect is explained by two mechanisms: 1) low values of size dependent competition yield age 1 smolting individuals that are more numerous than age 2 or 3 smolting individuals and therefore larger adult returns and a larger number of newborns (Figure 3.12) in stream reproducing individuals are able to reach larger sizes due to their competitive advantage and reduction of competition with smolting individuals, thus having higher fecundity (Figure 3.17a).

3.4.6 Effects of climatic scenarios

We test the effects that changes in temperature regimes will have on both population dynamics and individual attributes by simulating populations under three different

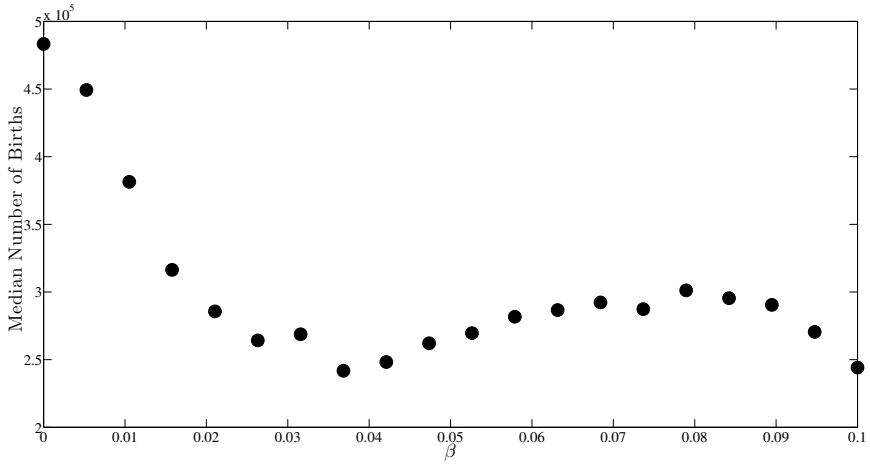

Figure 3.16: The median number of births as a function of the size dependent asymmetric competition.

temperature regimes and a subset of values for size-dependent mortality and competition (μ_1, β). We set the baseline scenario as the historical annual temperature profile of the Carmel River and then test two different in stream temperature scenarios: 1) a constant 1°C increase in the historical annual temperature regime and 2) a regime with the historical mean but increased variability in temperatures (Figure 3.8).

A change in temperature regimes can drastically alter the dynamics of the population for some parameter combinations, but may have little effect for others (Figure 3.18). Generally, the constant 1 °C increase scenario leads to higher mean number of migrating individuals which in turn leads to increased abundances; the opposite is true for the higher variability scenario (Figure 3.19). Although a large number of migrating individuals tends to lead to large population abundances, there are scenarios in which large population abundances are maintained through large numbers of resident individuals. The increase in abundance for the constant increase scenario is most likely attributed to the mean tempera-

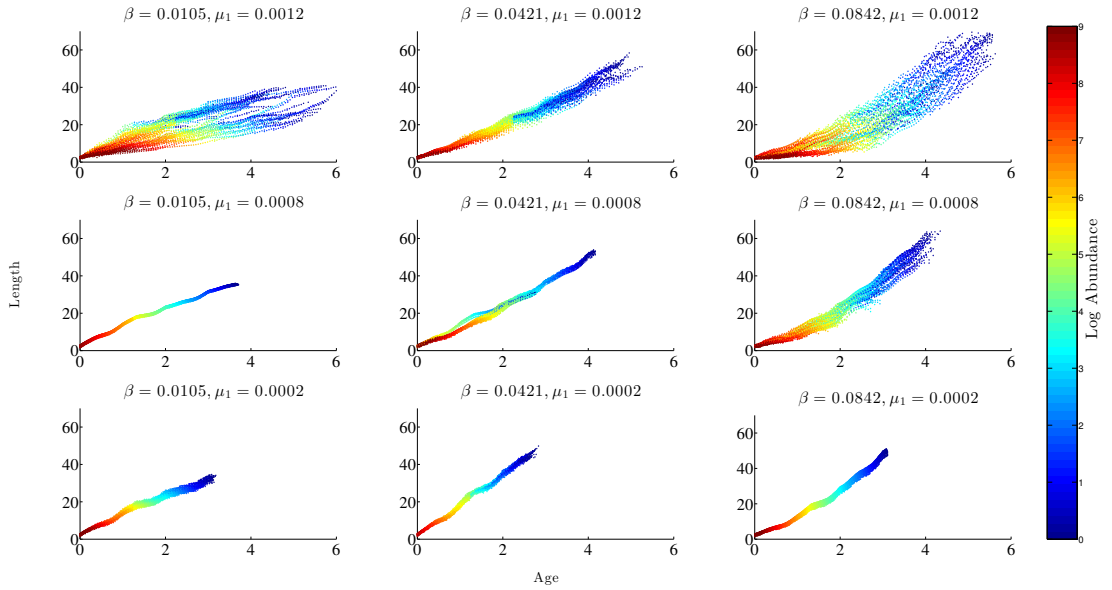

(a)

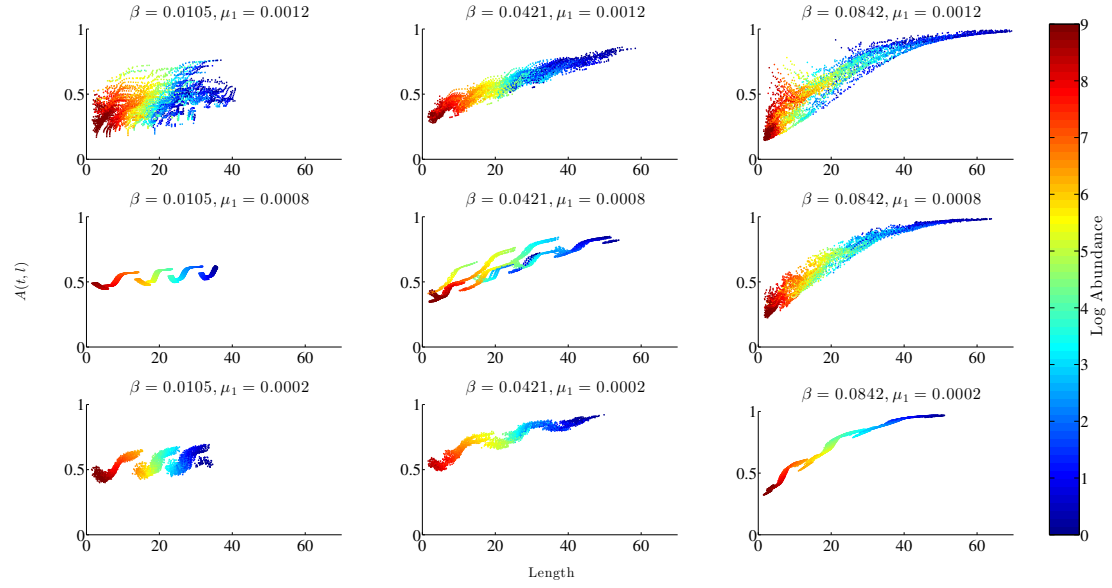

(b)

Figure 3.17: Sample dynamics for multiple parameter values for (a) length at age relationships and (b) length and access to resources. Each trajectory represents a cohort of multiple individuals whose log abundance is represented by the color.

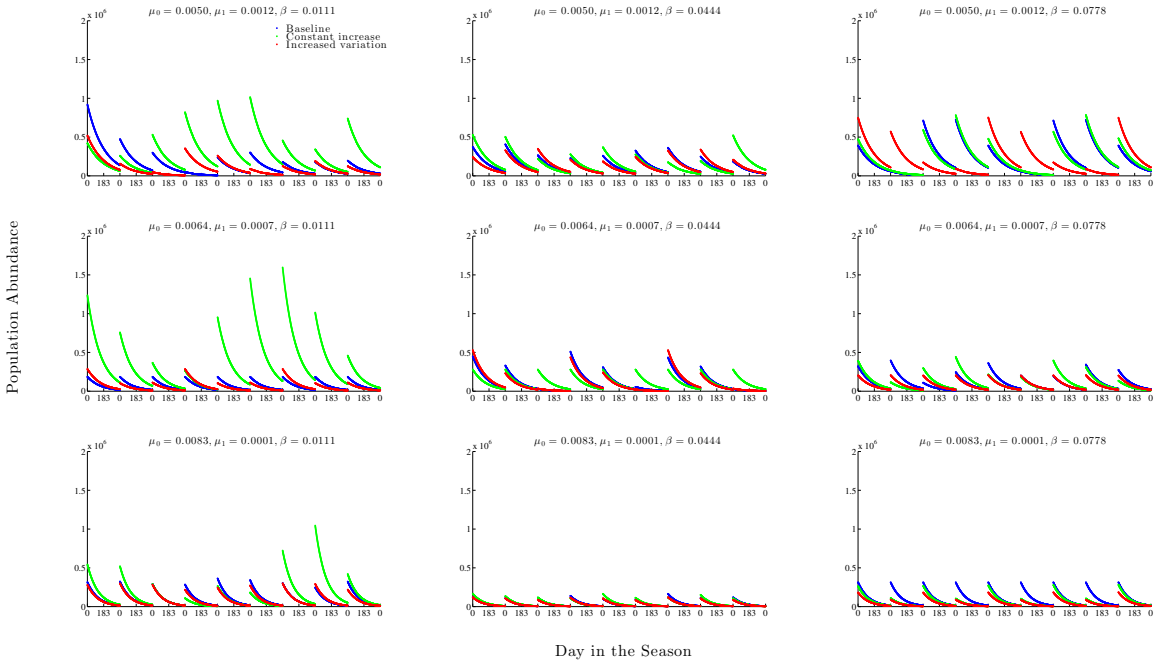

Figure 3.18: Sample dynamics of population abundance for the three temperature regimes (colors) and 9 combinations of mortality and competition parameters.

ture increase from 13.5 °C to 14.5 °C with the latter temperature being closer to the optimal temperature for growth for steelhead. (Myrick & Cech, 2004). Conversely, although the scenario with higher variability in yearly temperature maintains the same mean temperature (13.5 °C), it exposes individuals to temperatures that are less optimal for growth.

3.5 Discussion and Conclusions

Due to the importance of growth for steelhead life history choices, modeling studies have primarily focused on detailed descriptions of individual bioenergetics and the incorporation of threshold-based decisions for smolting and maturation while treating individuals as being independent of their conspecifics; with many of the current models focusing pri-

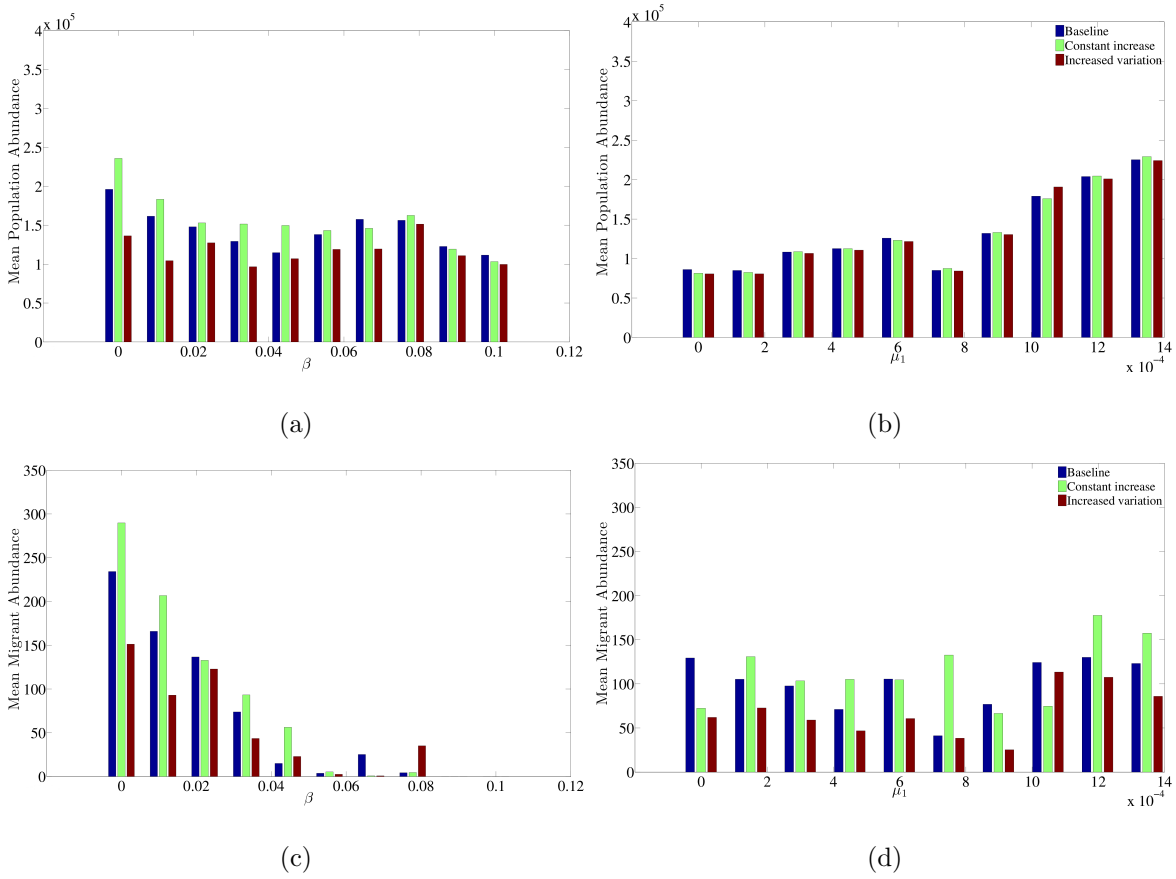

Figure 3.19: Mean population (a,b) and migrant abundances (c,d) as a function of competition (a,c) and size-dependent mortality (b,d) for the three different temperature regimes.

marily on the ability to describe ocean migrating individuals (e.g. Railsback & Rose (1999); Satterthwaite et al. (2009, 2010)). While these models have been able to accurately describe the dynamics and general patterns that are observed in populations, they do not incorporate intraspecific competition or model the entire life history of an individual and they often require an a priori specification of growth rates to match field observations specific to that population. Models that omit these mechanisms have provided important information on the general dynamics of the population but are unable to provide insight into the variability that is induced by size-dependent competitive effects that is indisputably present (Nakano et al., 1991; Elliott, 2002; Grant & Imre, 2005; Walters et al., 2013).

The primary aims of this study were to bypass these two common limitations by developing a model that accounts for the numerous history pathways that are available to steelhead and to explore the effects that competitive interactions between conspecifics has on these life-history choices, as well as ultimately on the dynamics of the population. With this aim, we modeled the asymmetric competitive interactions of individuals with different lengths with Equation 3.9 within the PSPM framework. Although the exact form used to describe the competition between two individuals was not derived from first principles, it resembles the one used by Le Bourlot et al. (2014), which resulted in dynamics that are similar to those arising from other intraspecific interactions. Our formulation of the interactions between individuals has the flexibility to model a gradient of competitive interactions ranging from scramble competition to interference competition. In the latter case, our formulation allows us to capture the competitive advantage that larger individuals have been shown to have in the access to resources; however, the precise strength of the asymmetry in

the interactions will certainly be both population- and habitat-dependent. Although different forms of the competition function would most likely yield qualitatively different results, our model analysis provides sensible results for the dynamics of steelhead populations as well as individual life histories. A sensitivity analysis could be done for different model implementations of the competition function but we limit our scope to that of Equation (3.9) and leave the analysis of alternate functions as an open avenue of exploration.

Although there are some general patterns that exhibit themselves throughout the parameter range, the results from our model suggest that the mechanisms influencing the population dynamics are complex and highly non-linear due to the feedbacks that are created by the interactions between individuals and the environment. These interdependencies make it increasingly difficult to make generalized statements about the effects of changes in environmental conditions without further consideration of specific cases. For example, in the different climatic scenarios it would not be unreasonable to expect some clear patterns due to different temperature regimes, however our model does not exhibit those characteristics. We attribute the lack of trends in the results for the different temperature scenarios to the complexity of our model; these results augment the lack of consensus of the effects of changes in temperature regimes will have on salmonid populations (Holtby, 1988; Schindler et al., 2005; Boughton et al., 2007; McCarthy et al., 2009; Crozier et al., 2010). Ultimately, the effects that different temperature regimes will have on the dynamics of a population will be highly dependent on the specific effects that it has on individual growth, which are likely to be population-dependent.

By exploring a range of combinations of size-dependent and independent mortality

levels, strengths of asymmetric competition and multiple temperature regimes, we have highlighted the ability of our model to capture the life history variability that exhibits itself throughout different populations. We also emphasize that the extent to which variability is observed within both the model and in nature depends considerably on the environmental conditions that individuals experience (Sogard et al., 2012).

As in many other studies on the population dynamics of steelhead, our model is limited by the lack of detailed knowledge available at the individual streams. For steelhead in particular, the precise mechanisms that drive the marine phase of individuals and the drivers of early maturation are poorly understood. In light of these limitations, our model can serve as a guide on the portions of steelhead life history which are most important to the population dynamics of steelhead. By highlighting the biological mechanisms that have the largest impact on the population dynamics, our model emphasizes the areas in which data collection and empirical data can be the most beneficial for both the understanding and management of steelhead. Perhaps with a more localized parametrization of the individual and the environment, the model developed here could be locally validated and serve as a useful resource management tool. Moreover, although the PSPM was described and developed with special reference to steelhead trout, this modeling approach can serve many other facultatively anadromous species.

3.6 Acknowledgments

This work was supported by funding from the Center for Stock Assessment Research (CSTAR), the National Science Foundation's GRFP and GROW programs and the

European Research Council under the European Union?s Seventh Framework Programme (FP/2007-2013) / ERC Grant Agreement No. 322814.

Chapter 4

A Bayesian Semi-Parametric Method for the Estimation of Individual Growth and Consumption*

4.1 Motivation and background

In the previous chapters, the growth of individuals has been described through the use of bioenergetic models whose functional forms have been assumed to be known with complete certainty. While this paradigm of modeling growth as a balance of the energy gained through consumption and metabolic costs is often able to capture the average growth patterns of individuals and provide insight into the dynamics of both individuals

*This chapter will be converted to a journal article by Lopez Arriaza, Munch, and Mangel entitled "A Bayesian Semi-Parametric Method for the Estimation of Individual Growth and Consumption" for the journal *Ecological Modeling*.

and populations, it cannot account for the uncertainty about the processes driving growth. Since the foundation of these types of models are the laws of thermodynamics, the cause of the discrepancies between the models and measured data are often to be assumed to be introduced by one or a combination of the following: 1) the model is incorrectly parametrized, 2) the input data used to drive the model are inaccurate, 3) the independent data being compared with the model results are wrong (Chipps & Wahl, 2008).

Even with the acknowledgment of these common problems, bioenergetic models have been increasingly applied in the study of various topics, ranging from the effects of climate change, effects of management strategies and the assessment of the health of populations, due in part to the *Fish Bioenergetics 3.0* software (commonly termed the Wisconsin bioenergetics model) (Boughton et al., 2007, 2015; Railsback & Rose, 1999; Satterthwaite et al., 2010; Hanson et al., 1997). However, these models are parameter intensive and precise parameter estimates are usually not available for the population of interest. The lack of parameter estimates often leads to parameter borrowing from other species, locations or life stages. Such parameter borrowing may lead to biased estimations of growth due to the genotypic and environmental differences between species and populations. Furthermore, even when parameter estimates are available for the species of interest, the parameters are usually estimated from laboratory experiments with limited validation on field data. The difficulty and large efforts required to accurately measure individual consumption in both field and laboratory settings poses a specific cause for concern for validation of these models and measurements are therefore limited in the literature. Additionally, the exact relationship between temperature and individual consumption is highly variable, with multiple

functional relationships available and commonly used (Ney, 1993).

In this chapter, I focus on the bioenergetics model commonly applied to for populations of steelhead in California. The specific model that I consider was developed for cold-water species and was subsequently adapted to California steelhead (Rand et al., 1993; Railsback & Rose, 1999; Satterthwaite et al., 2010). The change of weight, W, of an individual through time is:

$$\frac{dW}{dt} = f\, c\, \Phi_C\left(T(t)\right) W(t)^{0.86} - \alpha \Phi_M\left(T(t)\right) W(t) \tag{4.1}$$

In Equation (4.1), growth of an individual is a balance between anabolic factors $(f\, c\, \Phi_C(T(t))W(t)^{0.86})$ and catabolic costs $(\alpha \Phi_M W(t))$ at a specific time. Basal catabolism is a product of two terms: weight-specific catabolic costs, α, and the effect of temperature in catabolism, $\Phi_M\left(T(t)\right)$ (I use the particular form described by Brett (1952)). Anabolism is a product of four terms; relative energy density of food to fish tissue, f, the daily maximum weight of food that can be consumed by a 1g fish under optimal temperature conditions, c, the allometric relationship of consumption and fish weight, $W(t)^{0.86}$, and the functional relationship of maximum consumption and temperature, $\Phi_C(T(t))$. The functional form of temperature dependent maximum consumption, $\Phi_C(T(t))$, that is often used is that of Thornton and Lessem (1978) for cold-water species. This model formulation was first adapted to steelhead by Rand et al. (1993) and further parametrized for California steelhead by Railsback and Rose (1999), based on both experimental studies and reanalysis of historical data (Myrick & Cech, 2004; Van Winkle et al., 1998; From & Rasmussen, 1984). Due to the number of parameters that are involved, information for the estimation of these parameters is not population-specific and has also been borrowed across species.

Additionally, as a result of curve fitting the parameters for the temperature-consumption relationship do not follow the theoretical definitions which they were derived under (Railsback & Rose, 1999). There is a wide range of variability in the fidelity of these models to data from both laboratory experiments and field observations (Tyler & Bolduc, 2008), with the major point of contention being individual consumption. The aim of the current chapter is to forgo the assumption of a parametric relationship between temperature and consumption with unknown parameters and develop data-driven relationships. In order to do so, in section 4.2, I develop a state-space framework for the growth of individuals that models the temperature-consumption relationship through the use of non-parametric methods. The combination of the state-space framework and the non-parametric modeling allows us to account for multiple sources of uncertainty as well providing flexibility to learn from the data the relationship between temperature and consumption. As a validation and exploration of the limitations of the model, I apply my model to both simulated data (section 4.3.1) and data from growth experiments of steelhead (section 4.3.4). I conclude with results and discussion of their implications.

4.2 Model formulation

4.2.1 Re-Formulation of the Bioenergetics Model

The continuous-time bioenergetics model describing the growth of an individual in Equation 4.1 can be solved analytically by letting $v = W^{0.14}$, $\frac{dv}{dt} = 0.14\frac{W}{W^{0.86}}$ (for notational simplicity the explicit time dependence of weight is dropped). With this substitution

Equation 4.1 becomes

$$\frac{dv}{dt} + 0.14\alpha\Phi_M\left(T(t)\right)v = 0.14fc\,\Phi_C(T(t)) \tag{4.2}$$

Using the method of integrating factor I can arrive at an analytic solution for the transformed weight variable:

$$v(t) = e^{-0.14\alpha\int_{t_o}^{t}\Phi_M\left(T(\hat{t})\right)d\hat{t}}\int_{to}^{t}0.14fc\,\Phi_C\left(T(s)\right)e^{0.14\alpha\int_{s_o}^{s}\Phi_M\left(T(\hat{t})\right)d\hat{t}}ds \tag{4.3}$$

Which can then be written as a discrete time model

$$\begin{aligned} v(t) &= e^{-0.14\alpha\int_{t-1}^{t}\Phi_M\left(T(\hat{t})\right)d\hat{t}}v(t-1) \\ &+0.14fc\;e^{-0.14\alpha\int_{t_o}^{t}\Phi_M\left(T(\hat{t})\right)d\hat{t}}\int_{t-1}^{t}\Phi_C(T(s))e^{0.14\alpha\int_{s_o}^{s}\Phi_M\left(T(\hat{t})\right)d\hat{t}}ds \end{aligned} \tag{4.4}$$

For compactness I make the following definitions:

$$\delta = e^{-0.14\alpha\int_{t-1}^{t}e^{0.071T(\hat{t})}d\hat{t}} \tag{4.5}$$

$$g(t,s) = 0.14fe^{0.14\alpha\left(\int_{s_o}^{s}\Phi_M\left(T(\hat{t})\right)d\hat{t}-\int_{t_o}^{t}\Phi_M\left(T(\hat{t})\right)d\hat{t}\right)} \tag{4.6}$$

so that the discrete time model can be written as:

$$v_t = \delta_t v_{t-1} + \int_{t-1}^{t}c\Phi_C\left(T(s)\right)g(t,s)ds \tag{4.7}$$

Importantly, Equation (4.7) is the integral of consumption over the time interval from $t-1$ to t, which transforms the consumption process from the temperature domain to the time domain. This model formulation allows me to make inference on consumption based on (transformed) measurements of individual growth through time. Furthermore, the time-integration of consumption over specific time intervals will also provide a way to seamlessly incorporate temperature time-series data, which are often readily available and

particularly important to the growth of ectotherms, to make inferences for both consumption and growth for individuals based on the temperature regimes that were experienced during these periods.

4.2.2 Statistical Model

To make inferences about the consumption of individuals, I build a statistical Bayesian state-space model based on the deterministic discrete time model described by Equation 4.7. The top level of the state-space framework assumes that the transformed weight of multiple individuals is collected through time and that the measurements are subject to independent normal zero-mean error and following Sigourney et al. (2012), the measurement variance is fixed:

$$y_{i,t} = v_{i,t} + \epsilon_m \tag{4.8}$$

$$\epsilon_m \overset{iid}{\sim} N\left(0, \sigma_m^2\right) \tag{4.9}$$

I then assume that the growth of every individual is governed by the dynamics described by Equation 4.7 but is subject to normally distributed process stochasticity (*sensu* Hilborn & Mangel (1997)).

$$v_{i,t} = \delta_t v_{i,t-1} + \int_{t-1}^{t} c\Phi_C\left(T(s)\right) g(t,s) ds + \epsilon_p \tag{4.10}$$

$$\epsilon_p \overset{iid}{\sim} N\left(0, \sigma_p^2\right) \tag{4.11}$$

Since consumption is of particular interest, I assume that δ_t and $g(t,s)$ are deterministic and known. I place a uniform prior distribution on the initial size of an individual, $v_{i,0}$,

that asserts that the initial size of individuals is bounded but unknown and then adopt an inverse gamma prior distribution on the process stochasticity:

$$v_{i,0} \sim U(0, 500) \tag{4.12}$$

$$\sigma_p^2 \sim IG(10^{-2}, 10^{-2}) \tag{4.13}$$

The last term to account for in the discrete time model is the temperature-dependent consumption term. One of my primary aims is to avoid specifying a parametric form for this consumption term. To achieve this goal I place a Gaussian Process (GP) prior on $\Phi_C(T)$ in the temperature domain. The GP prior is completely specified by a mean function $m(T)$, which describes the average value of the prior at temperature, T, and a covariance function, $k(T, T')$, which describes the similarity of consumption values, $(\Phi_C(T), \Phi_C(T'))$ at different temperatures (T, T'). I use the Squared Exponential (SE) covariance function given by:

$$k(T, T') = \omega^2 \exp\left(-\frac{(T - T')^2}{l^2}\right) \tag{4.14}$$

In this representation of the SE covariance function, ω^2 defines the prior variance in consumption and l^2 represents the scale at which the correlation between points decays with temperature. To fully specify the GP prior I set $m(T) = 0$:

$$\Phi_C(T) \sim GP(0, k(T, T')) \tag{4.15}$$

$$k(T, T') = \omega^2 \exp\left(\frac{(T - T')^2}{l^2}\right) \tag{4.16}$$

Note that although the prior has been fully specified for consumption in the temperature domain, the data for each individual as well as the inference for all other parameters are time-dependent. The integral in Equation 4.7 transforms the GP prior to the time domain. Although integral transformations and products with deterministic functions are linear transformations and preserve the properties of GP priors, this transformation makes inference on the process in the temperature domain difficult and computationally costly because of the necessity to calculate the integral in Equation 4.7 at each Markov Chain Monte Carlo (MCMC) iteration. Thus, I choose to decompose the GP using an orthogonal eigenfunction expansion with basis functions $\{h_k(T), k = 1, 2, \ldots, \infty\}$:

$$\Phi_C(T) = \sum_{k=1}^{k=\infty} \mathcal{C}_k h_k(T) \tag{4.17}$$

$$\mathcal{C}_k \sim N(0, \lambda_k) \tag{4.18}$$

$$\int_{T_{\min}}^{T_{\max}} h_i(T) h_j(T) dT = \delta_{i,j} \tag{4.19}$$

$$\int_{T_{\min}}^{T_{\max}} k(T, T') h_k(T) dT = \lambda_k h_k(T') \tag{4.20}$$

Under this definition the model becomes

$$y_{i,t} = v_{i,t} + \epsilon_m \tag{4.21}$$

$$\epsilon_m \overset{iid}{\sim} N\left(0, \sigma^2\right) \tag{4.22}$$

$$v_{i,t} = \delta_t v_{t-1} + \sum_{k=1}^{k=\infty} \mathcal{C}_k \int_{t-1}^{t} h_k(T(s)) g(t,s) ds + \epsilon_p \tag{4.23}$$

$$\epsilon_p \overset{iid}{\sim} N\left(0, \sigma^2\right) \tag{4.24}$$

$$\mathcal{C}_k \sim N(0, \lambda_k) \tag{4.25}$$

$$\int_{T_{min}}^{T_{max}} k(T, T') h_k(T) dT = \lambda_k h_k(T) \tag{4.26}$$

Although a number of eigenfunctions are available, I choose to use a sine and cosine expansion for the GP:

$$\Phi_C(T) = \sum_{k=0}^{k=\infty} a_k \cos(kT) + b_k \sin(kT) \tag{4.27}$$

The relationship between a_k, b_k and the SE correlation function is known through Equation 4.20 which defines the eigenvalues $\{\lambda_k, k = 1, 2, \ldots, \infty\}$; the resulting integral involves error functions. I approximate the error function by allowing the lower and upper limits in Equation 4.20 to go to $\pm\infty$. Using this approximation, the eigenvalues of the expansion are defined as (see Appendix C.2 for detailed derivation)

$$\lambda_k \approx \exp\left(-\frac{1}{2} k^2 l^2\right) \sqrt{2\pi l^2} \tag{4.28}$$

With this eigenfunction decomposition of the Gaussian Process and approximation for the eigenvalues, the model can be redefined as

Observations

$$y_{i,t} = v_{i,t} + \epsilon_m \tag{4.29}$$

$$\epsilon_m \overset{iid}{\sim} N\left(0, \sigma_m^2\right) \tag{4.30}$$

Process

$$v_{i,t} = \delta_t v_{t-1} + \sum_{k=1}^{k=\infty} a_k \mathcal{I}_{\mathcal{C}}(k,t) + \sum_{k=1}^{k=\infty} b_k \mathcal{I}_{\mathcal{S}}(k,t) + \epsilon_p \tag{4.31}$$

$$\mathcal{I}_{\mathcal{C}}(k,t) = \int_{t-1}^{t} \cos(kT(s)) g(t,s) ds \tag{4.32}$$

$$\mathcal{I}_{\mathcal{S}}(k,t) = \int_{t-1}^{t} \sin(kT(s)) g(t,s) ds \tag{4.33}$$

$$\epsilon_p \overset{iid}{\sim} N\left(0, \sigma_p^2\right) \tag{4.34}$$

Priors

$$v_{i,0} \sim U(0, 500) \tag{4.35}$$

$$a_k \sim N\left(0, \lambda_k\right) \tag{4.36}$$

$$b_k \sim N\left(0, \lambda_k\right) \tag{4.37}$$

$$\lambda_k = \exp\left(-\frac{1}{2} k^2 l^2\right) \sqrt{2\pi l^2} \tag{4.38}$$

$$l^2 \sim \text{Gamma}(\alpha_l, \beta_l) \tag{4.39}$$

$$\sigma_p^2 \sim IG(10^{-2}, 10^{-2}) \tag{4.40}$$

Thus, the problem has been reduced to that of estimating the coefficients of the eigenfunction expansion. This alternate formulation of the GP conditionally linearizes the problem of estimating the parameters and makes inference on the consumption process Φ_C less complex. Additionally, using the eigenfunction expansion allows us to calculate

the integrals in Equations 4.32 and 4.33 only once. Under the newly respecified statistical model, all that is left is to place priors on the hyper parameters pertaining to the covariance function. Although the exact functional relationship between consumption and temperature is unknown, there is a vast amount of experimental data pertaining to the shape of the relationship between temperature and consumption that I can use to select the prior. Specifically, since consumption is unimodal, I am able to place an weakly informative prior on the length scale parameter, l^2.

To incorporate this knowledge into our prior, I utilize the results from Ylvisaker (1965) on the expected number of zero crossings (N) of a stationary GP (normalized and defined on the unit interval).

$$\text{Let: } \mathcal{G} \sim GP\left(0, C(\tau)\right) \tag{4.41}$$

where $\tau = t - t'$

$$\text{then: } E\{N\} = \frac{1}{\pi}\{-C''(\tau)\}^{\frac{1}{2}}\Big|_{\tau=0} \tag{4.42}$$

Although this result can't be utilized directly, it can be adapted to provide information about the number of minima/maxima in the unit interval. Let $\mathcal{D} = \frac{d\mathcal{G}}{dt}$; it follows from the linearity of the differential operator that:

$$\mathcal{D} \sim GP(0, C_{\mathcal{D}}(t, t')) \tag{4.43}$$

$$C_{\mathcal{D}}(t, t') = \frac{\partial^2 C(t, t')}{\partial t \partial t'} \tag{4.44}$$

From this result it can be seen that the expected number of minima/maxima of $\mathcal{G}$ (e.g. the

number of zero crossings of $\mathcal{D}$), $N_{\mathcal{D}}$, is given by:

$$E\{N_{\mathcal{D}}\} = \frac{1}{\pi}\{-C_D''(\tau)\}^{\frac{1}{2}}\Big|_{\tau=0} \tag{4.45}$$

$$= \frac{1}{\pi}\{C^{(4)}(\tau)\}^{\frac{1}{2}}\Big|_{\tau=0} \tag{4.46}$$

Using this result I am able to incorporate the knowledge that the temperature-consumption relationship is unimodal by setting an informative prior on the length-scale parameter such that $E\{N_{\mathcal{D}}\} = 1$. It is important to note that setting the prior for the length-scale parameter in this way only specifies the average number of minima and maxima that the prior will have and that this prior specification still yields multimodal realizations. With the model fully specified, I use a Metropolis-within-Gibbs MCMC algorithm to obtain posterior samples (see Appendix C.1 for derivation of full conditional distributions necessary for the MCMC inference).

4.3 Results

In the following section I perform extensive performance and validation by testing the model with simulated data under a temperature profile representative of a natural river system (the Carmel River), various amounts of simulated data and two different levels of error. I then apply the model to experimental data for steelhead trout. All posterior inference is done by implementing a Metropolis-within-Gibbs MCMC sampling approach with 50,000 iterations, a burn-in of 10,000 iterations, and the resulting chain is thinned to avoid autocorrelation by taking every 25th sample, resulting in an effective sample size 3,600.

4.3.1 Simulated Data

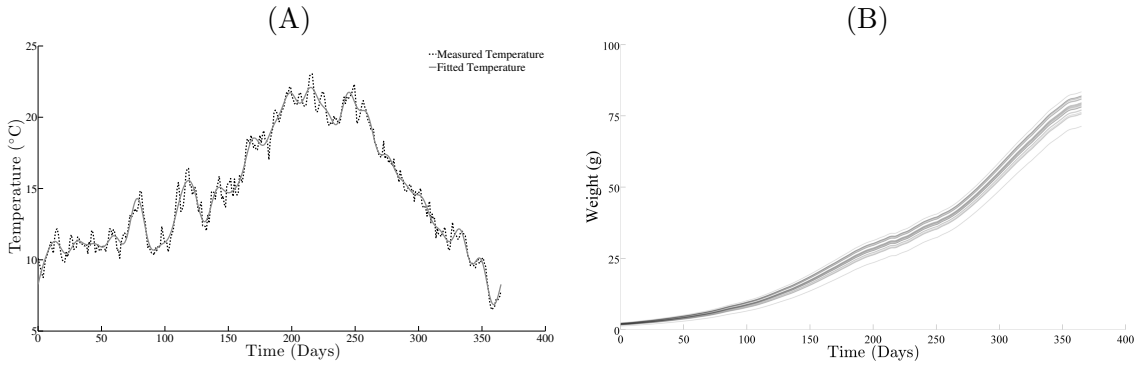

Figure 4.1: Temperature regime representative of the Carmel River (A) and deterministic growth trajectories for individuals with different initial sizes resulting from Equation 4.1 under this temperature profile. Divergence of the different trajectories is due to different initial weights.

The aim of testing our model with simulated data is to validate the model with a known consumption function and to check its performance under conditions with individual variation and measurement error. First, to test the ability of the model to recover the true consumption function and growth of individuals, I fit the model to simulated data from Equation 4.1 with no added error (observation or process). I then explore the performance of the model under conditions that represent natural systems by adding two levels of error (process stochasticity and measurement error). In both cases I simulate data by solving Equation 4.1 with a daily time-step for the duration of a year based on the measured temperature profile in Figure 4.1 (A). For the simulation with error, I introduce normally distributed process stochasticity at each time-step. After simulating the entire growth trajectory for all individuals I subsample a predetermined number of data points to constitute

our measurements and add independent normally distributed error for each individual at each measured time point. In this section, I consider 4 different scenarios of data availability, high and low temporal frequency (12 and 3 measurements respectively), high and low number of individuals (25 and 8 respectively) and each pairwise combination. Ultimately in order to perform inference I will be required to take the integral over the temperature profile. For computational purposes I approximate the temperature profile using a Fourier basis. Although this approximation of the temperature profile adds a small amount of error in our inference procedure, in practice, it is almost certain that the temperature that is actually experienced by individuals differs slightly from the temperature measured, and our approximation adds only a small additional error.

4.3.2 Noise-Free Synthetic Data

In the scenario where the data-generating model is exactly that of our statistical model and the measurements are made perfectly (Figure 4.2), the fit of the weights of individuals is quite good (Figure 4.3). In Figure 4.4, I show that as a function of time, I am able to capture the variable nature of consumption that is introduced due to the variable temperature.

In Figure 4.5, I show that I can accurately estimate the temperature-consumption relationship for the temperature ranges that were used to simulate the data. Different levels of data availability impact the certainty of the prediction of this relationship, with the number of data points having a larger impact than the number of individuals. For all of the scenarios, it is clear that the temperature regimes that were experienced for the longest duration (11 °C - 14 °C) have the least uncertainty associated with them. This can be

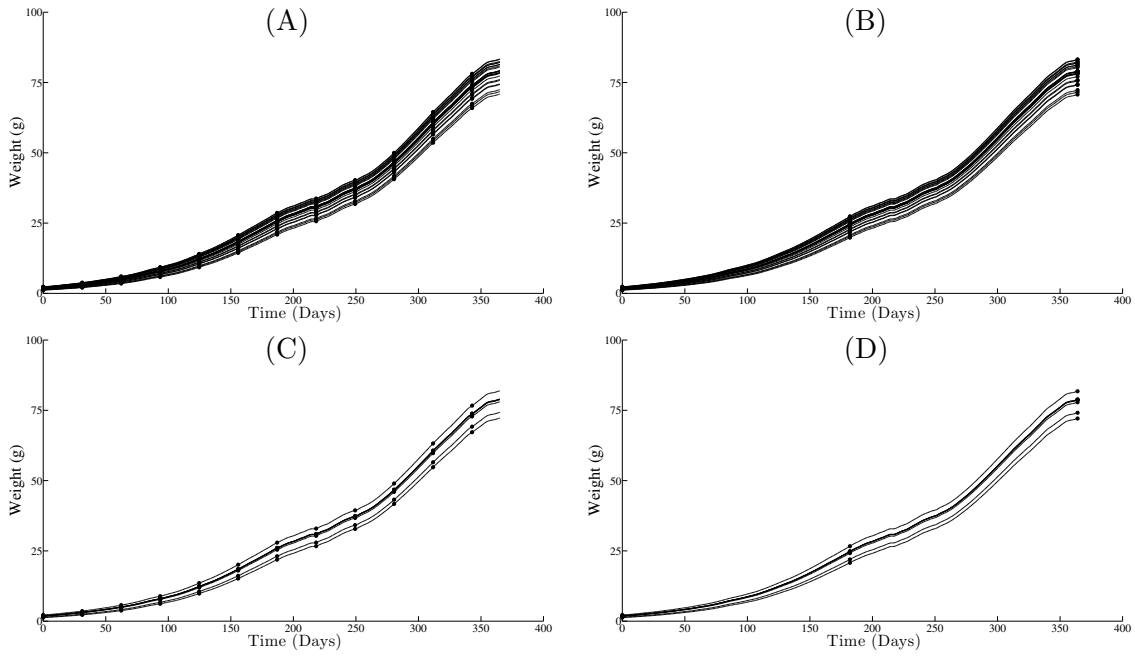

Figure 4.2: Simulated growth trajectories for noise-free synthetic data corresponding to the four different scenarios of data availability. Points represent measurement points and each line represents a different individual. Scenarios are A: 25 individuals, 12 samples, B: 25 individuals, 3 samples, C: 8 Individuals, 12 samples, D: 8 individuals, 3 samples.

seen by the much narrower 95 % C.I in Figure 4.5. While the model is able to accurately describe the relationship between consumption and temperature in the temperature ranges from which the data were simulated, outside of that range, the uncertainty increases and our ability to predict the relationship diminishes (Figure 4.6).

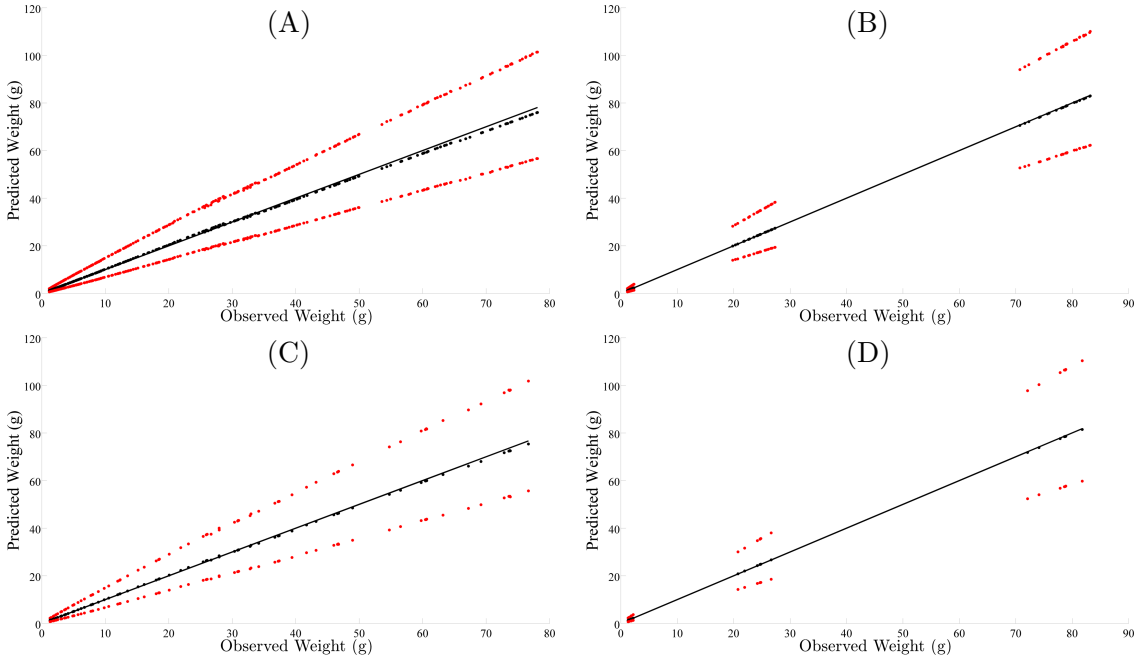

Figure 4.3: Simulated (noise-free) weights of individuals versus mean (black points) and 95 % C.I. (red) estimates for the different levels of data availability and the one-to-one line for reference.

4.3.3 Noisy Synthetic Data

The introduction of process stochasticity and measurement errors increases the uncertainty in the model. In Figure 4.7, I show that although I am doing a good job at estimating the mean weight of individuals, the variance and error in the prediction have increased

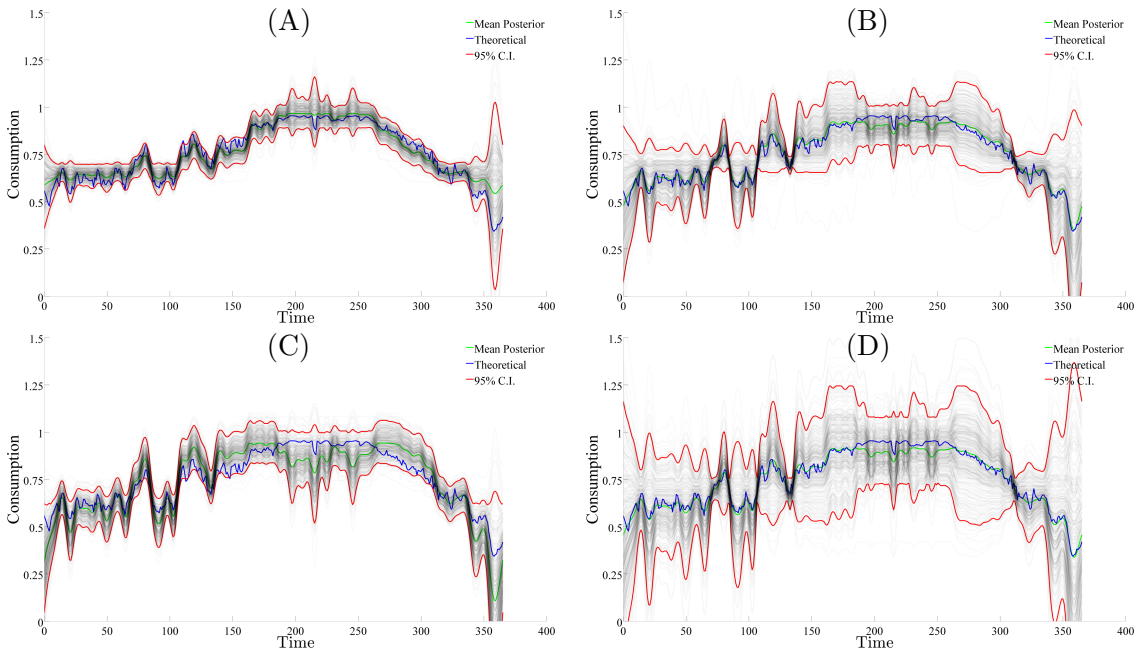

Figure 4.4: Posterior estimates of the consumption of individuals as a function of time for the four different levels of data availability based on noise-free synthetic data (A) 25 individuals 12 measurements B) 25 individuals 3 measurements C) 8 individuals 12 measurements D) 8 individuals 3 measurements).

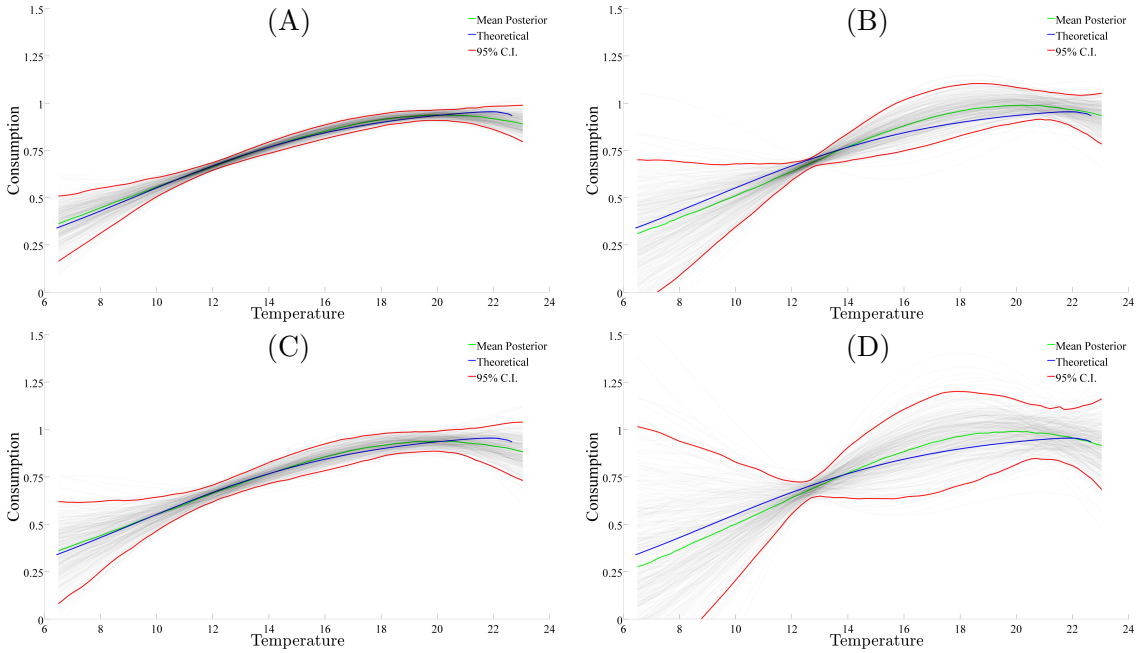

Figure 4.5: Posterior estimates of the consumption-temperature relationship for the temperature ranges used for the generation of synthetic data for the different levels of data availability based on noise-free synthetic data (A) 25 individuals 12 measurements B) 25 individuals 3 measurements C) 8 individuals 12 measurements D) 8 individuals 3 measurements). Magenta line represents the temperature-consumption relationship used to simulate the data.

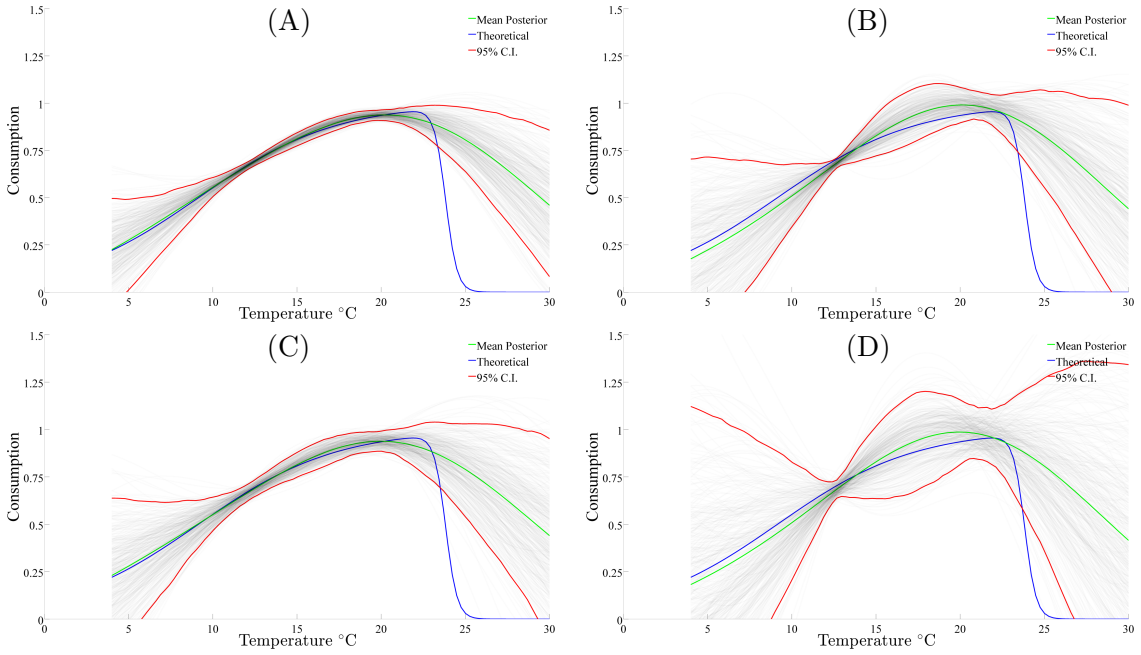

Figure 4.6: Mean (blue) and 95 % C.I. (red) posterior predictive estimates of the consumption-temperature relationship for temperature ranges commonly experienced by steelhead in natural systems based on inference for the different levels of data availability under noise-free synthetic data (A) 25 individuals 12 measurements B) 25 individuals 3 measurements C) 8 individuals 12 measurements D) 8 individuals 3 measurements). Green line represents the temperature-consumption relationship used to simulate the data.

and the 95% C.I. have also increased. For the ranges of temperature that are experienced the most, the model is still able to capture the general nature of the temperature-consumption relationship when compared to the true generating function (Figure 4.8). Outside of these regions, the estimate of the relationship is still reasonable but noticeably worse than in the noise-free example (Figure 4.9). Inference under the noisy data results in larger 95% C.I. under all 4 different levels of data availability, but the amount of uncertainty about our estimates is still predominantly driven by the number of measurements rather than the number of individuals. The model is also able to capture the consumption of individuals as a function of time and it does not appear that the smoothing of the temperature profile affects the models estimation (Figure 4.10).

4.3.4 Steelhead Growth Experiment Analysis

In this section I apply the model to the growth time series from a rearing experiment of California steelhead (see Beakes et al. (2010) for detailed experimental procedures). Here I focus on the time series of one of the experimental treatments (treatment 2) for individuals from two different origin populations: Scott Creek in the Central California Coast (CCC) and Coleman National Fish Hatchery from Northern California Central Valley (NCCV). Individuals were reared in two different years (2006 and 2007) with two different temperature regimes (Figure 4.11). While mortality during the experiment was low, I only consider individuals with complete measurement histories. I analyze the growth corresponding to the last 8 weight measurements (in grams) from the experiment. This results in 25 and 27 individuals in 2006 and 2007 respectively. As seen from the results in the simulated examples, this should be ample data to make inference on individual consumption.

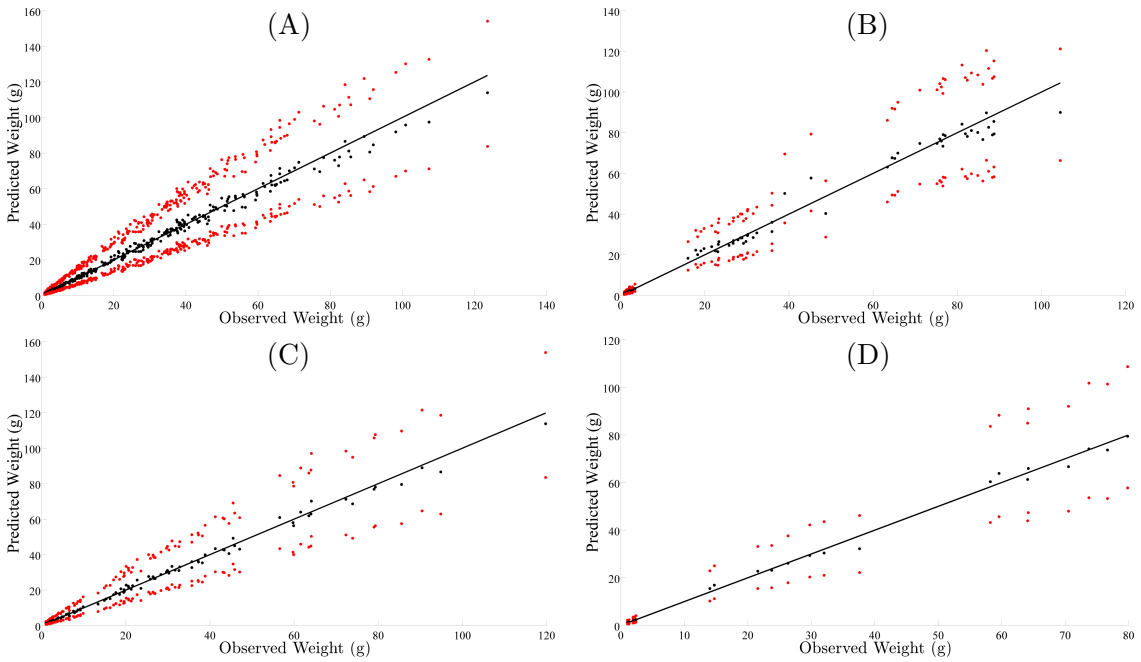

Figure 4.7: Simulated (noisy) weights of individuals versus mean (black points) and 95 % C.I. (red) estimates for the different levels of data availability (A) 25 individuals 12 measurements B) 25 individuals 3 measurements C) 8 individuals 12 measurements D) 8 individuals 3 measurements). The black line is the one-to-one line for reference.

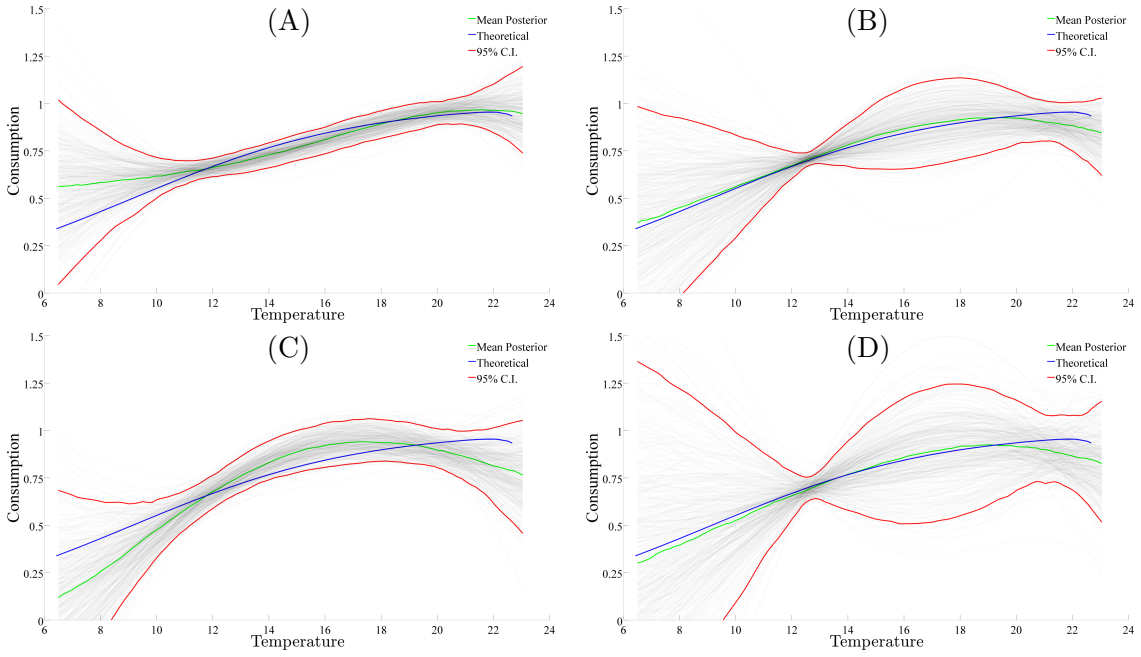

Figure 4.8: Posterior estimates of the consumption-temperature relationship for the temperature ranges used for the generation of synthetic data for the different levels of data availability based on noisy synthetic data (A) 25 individuals 12 measurements B) 25 individuals 3 measurements C) 8 individuals 12 measurements D) 8 individuals 3 measurements).

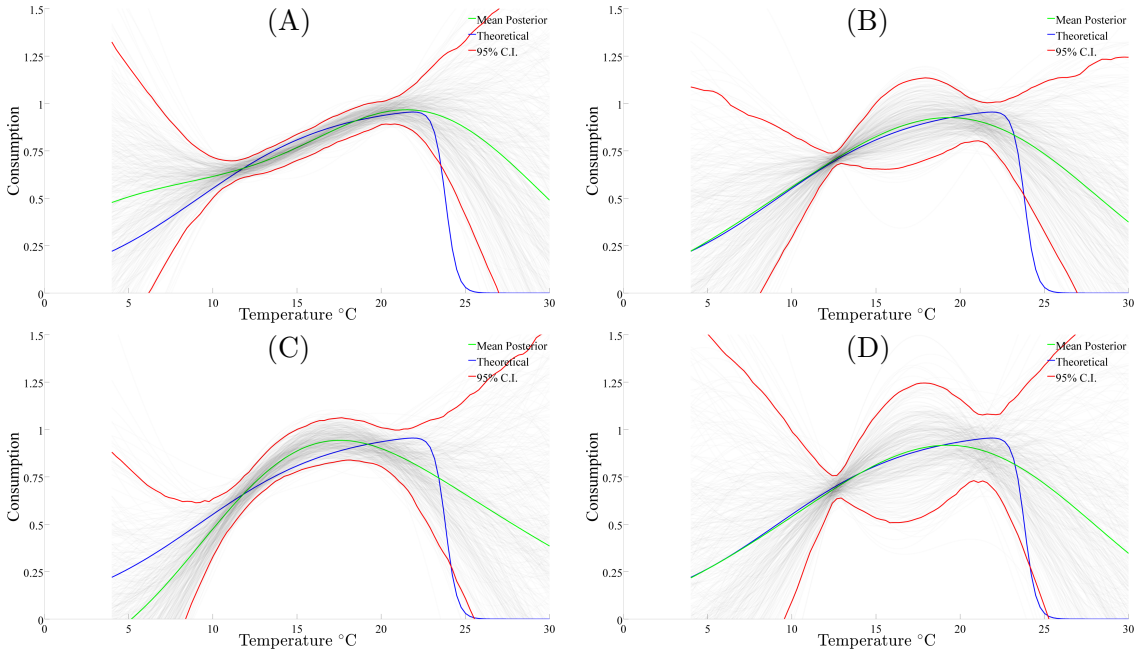

Figure 4.9: Posterior predictive estimates of the consumption-temperature relationship for temperature ranges commonly experienced by steelhead in natural systems based on inference for the different levels of data availability under noisy synthetic data (A) 25 individuals 12 measurements B) 25 individuals 3 measurements C) 8 individuals 12 measurements D) 8 individuals 3 measurements).

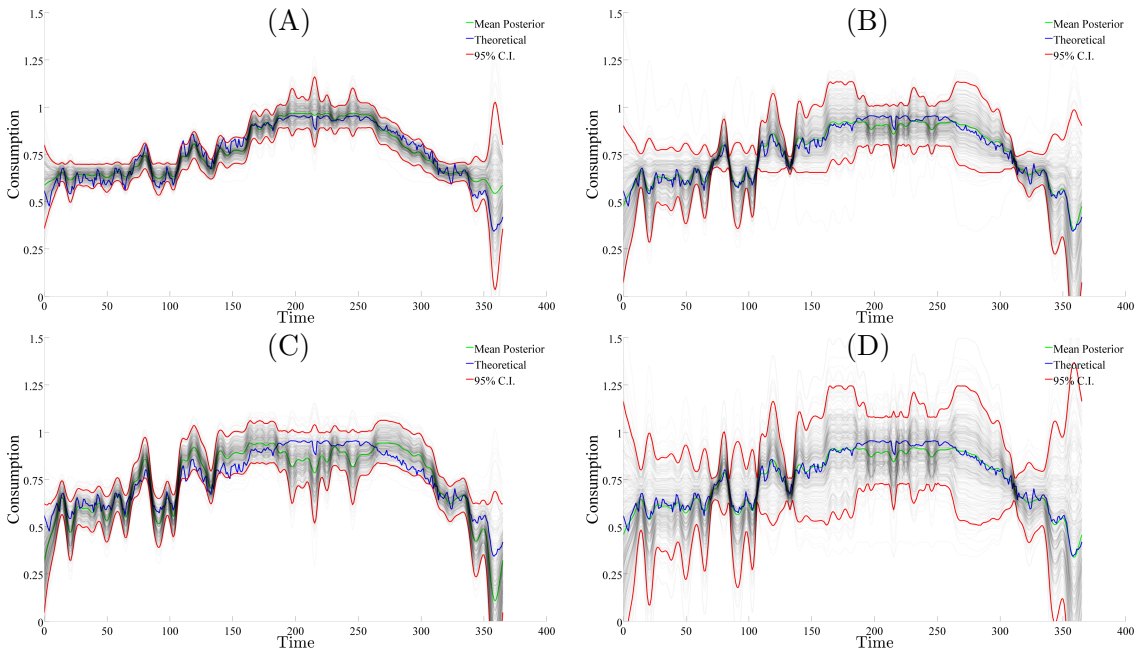

Figure 4.10: Posterior estimates of the consumption of individuals as a function of time for the four different levels of data availability based on noisy synthetic data (A) 25 individuals 12 measurements B) 25 individuals 3 measurements C) 8 individuals 12 measurements D) 8 individuals 3 measurements).

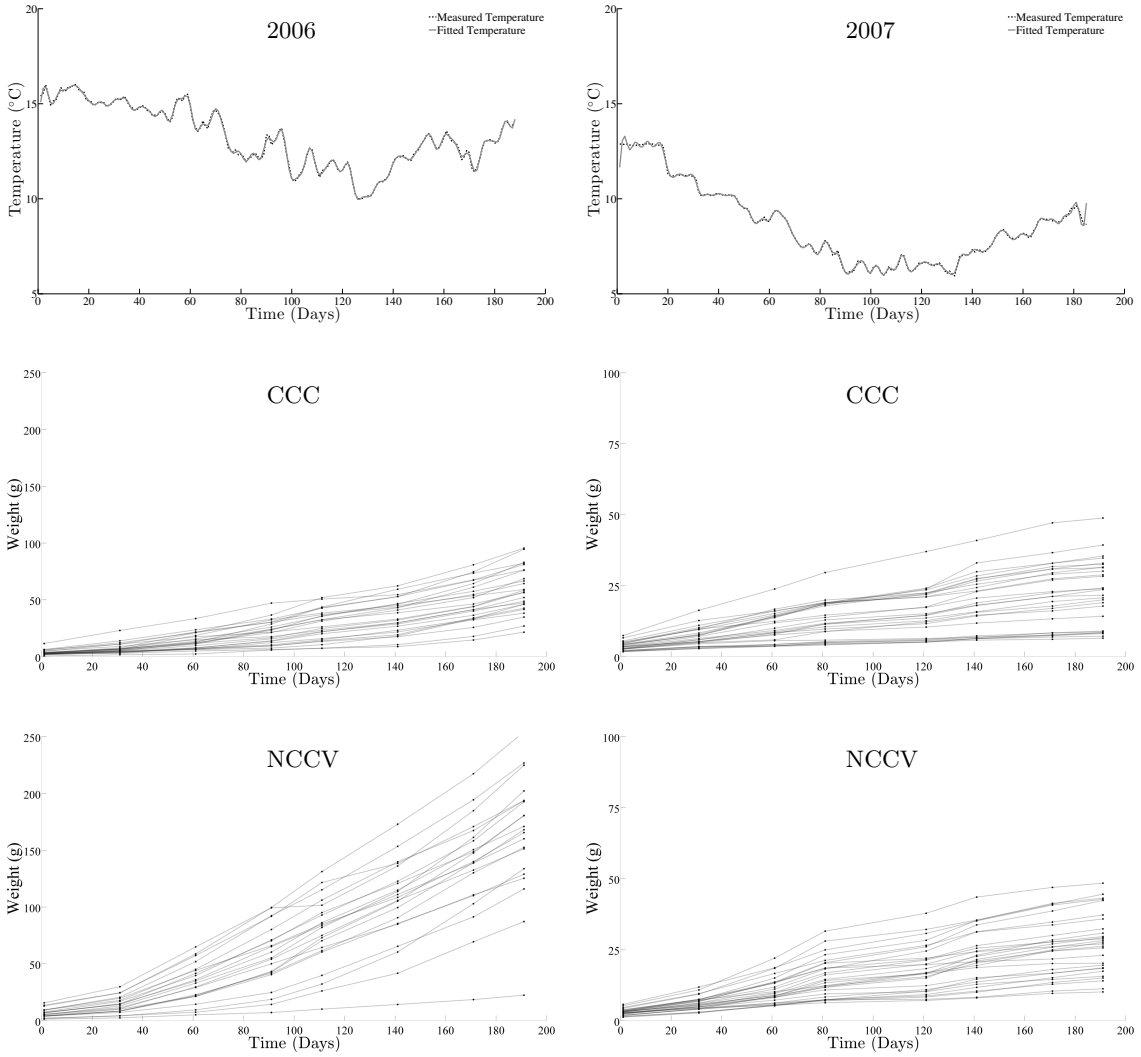

Figure 4.11: The temperature regimes (first row) and corresponding growth for the two different years (columns) for Scott Creek (CCC) (row 2) and Coleman Hatchery (NCCV) (row 3) in the experiments from Beakes et al. (2010).

The differences in growth between years can be attributed to the different temperature regimes. In both years the temperature regimes are relatively narrow with 2007 exhibiting a wider range of temperatures. In addition to the variability in growth exhibited between years, there are also clear differences in growth between the two strains (best seen in 2006). While this difference could possibly be attributed to the NCCV strains having adapted to experiencing warmer water regimes, therefore having an increased consumption level, the posterior estimates for the consumption-temperature relationship do not support this hypothesis (Figure 4.12). As opposed to the synthetic data examples, comparison between the posterior estimation of the temperature-relationship and a true consumption level is not straightforward. Instead here, I compare the posterior estimate of the model to a scaled version of the theoretical temperature-consumption function of Thornton & Lessem (1978). This allows me to compare the shapes of the relationship.

In general, for the temperature ranges that individuals experienced, the shape of the posterior estimate of the temperature-consumption relationship is in agreement with the theoretical relationship as described by Thornton & Lessem (1978) (Figure 4.12 green versus blue curve) . The temperature experienced by individuals is relatively constrained and lies on a fairly flat region of the theoretical curve. Additionally, the uncertainty related with the posterior estimate is relatively constrained in these temperature regions (Figure 4.12). The lack of knowledge about the temperature-consumption relationship outside of the temperature region is illustrated by the broad posterior predictive 95% C.I. associated with the temperature-consumption relationship for these temperatures (Figure 4.14). In addition to the relative agreement of the shape of the temperature-consumption relationship, the level

of mean level of consumption (c in Equation 4.1) is in relative agreement of those values found by Simon et al. (2013). The model is also able to accurately capture the growth (Figure 4.15).

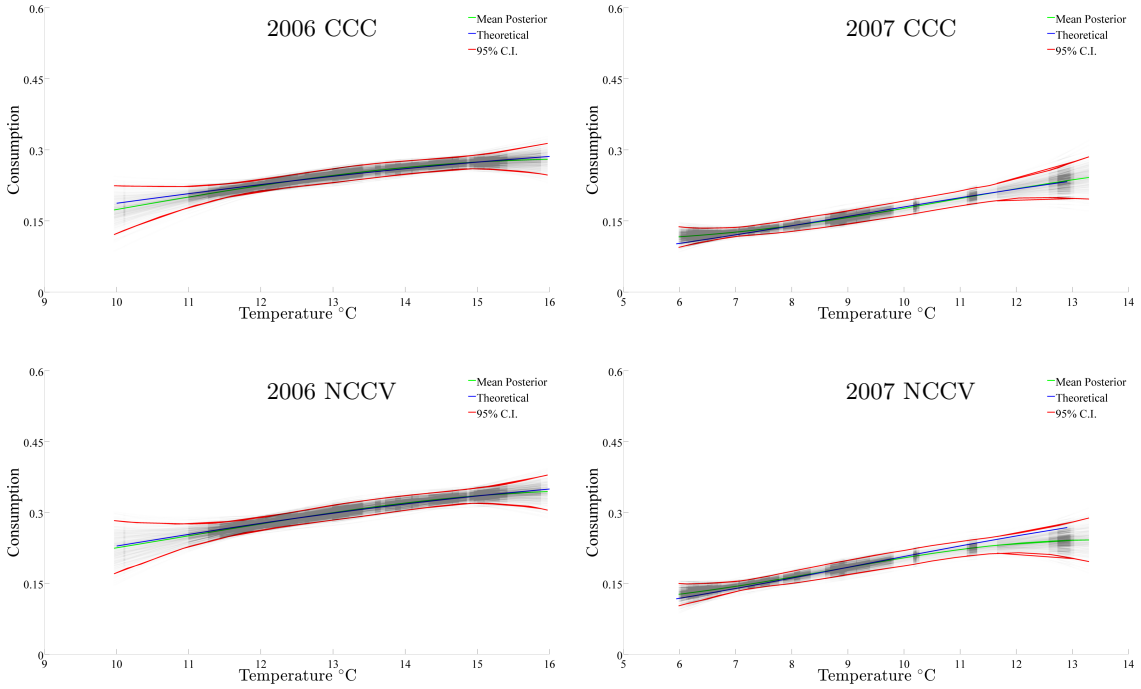

Figure 4.12: Posterior estimates of the consumption-temperature relationship for the temperature ranges that were experienced by the individuals in the four different experimental treatments.

4.4 Discusion and Conclusions

In this chapter I developed a method for modeling the growth of individuals using the framework of traditional bioenergetic models while avoiding many of the common pitfalls that come with these models. Primarily, the use of the BNP methodology within

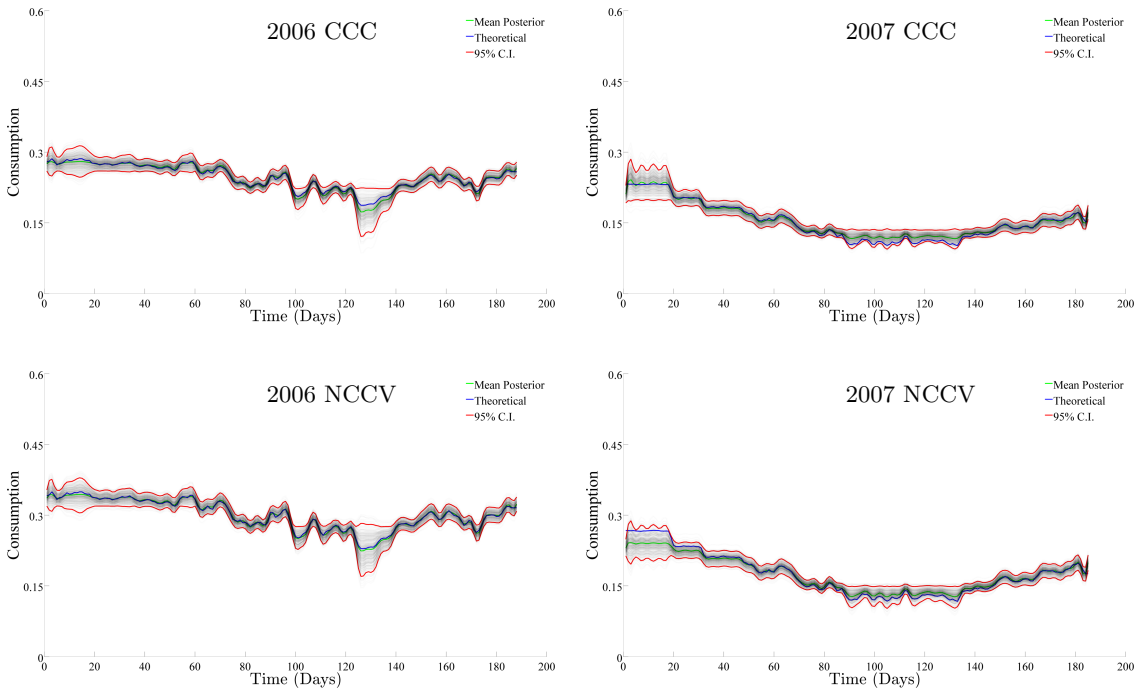

Figure 4.13: Posterior estimates of the consumption of individuals as a function of time for the four different experimental treatments.

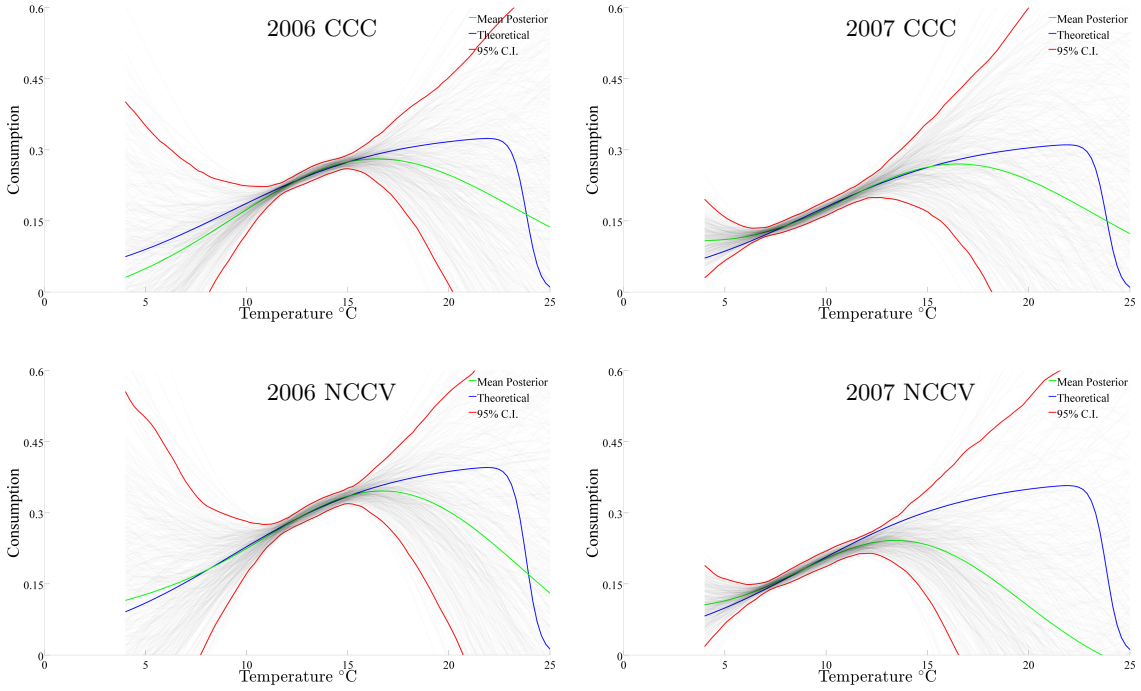

Figure 4.14: Posterior predictive estimates of the consumption-temperature relationship for temperature ranges commonly experienced by steelhead in natural systems based on inference from the four different experimental treatments.

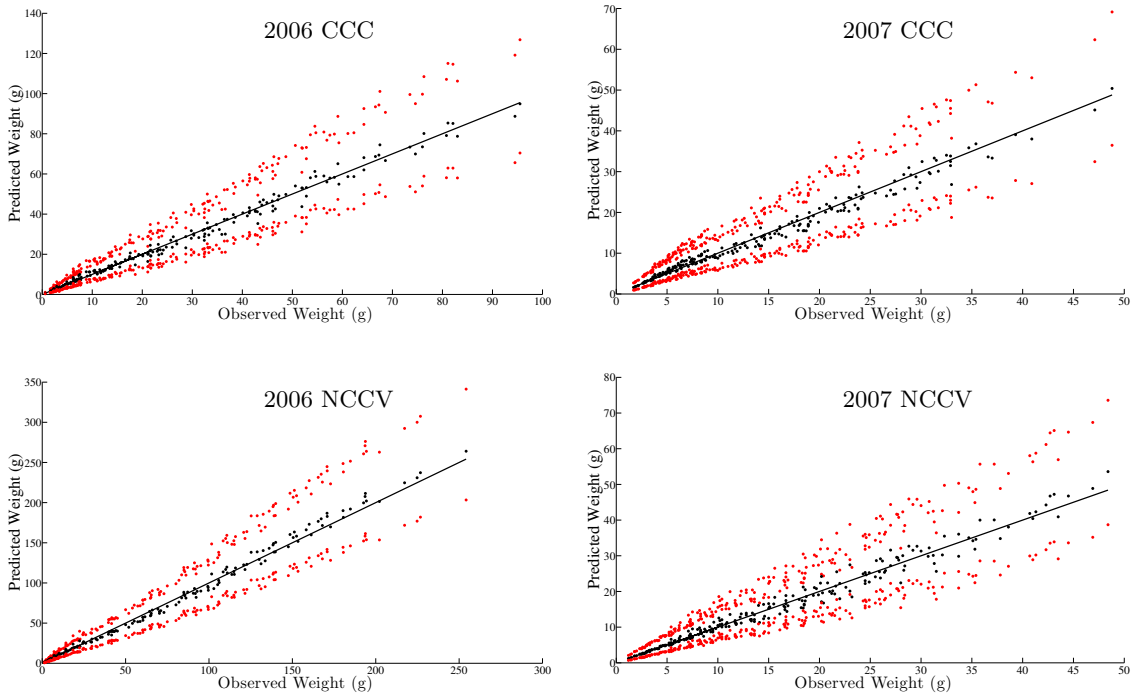

Figure 4.15: Posterior predictive estimates of the consumption-temperature relationship for temperature ranges commonly experienced by steelhead in natural systems based on inference from the four different experimental treatments.

a state-space framework allows the model to bypass the use of a specific functional form for the often contested relationship between temperature and consumption. This modeling approach allows us to account for the fact that different populations have likely developed different thermal preferences and tolerances based on their environment. In the model developed, I placed an GP prior on the temperature-consumption relationship and then used an eigenfunction approximation for it. Alternatively, the model could have been developed without the use of the GP framework from the beginning. Using the starting point of the GP framework allows for the seamless inclusion of a priori information on the decay rate of the coefficients. This approach allows us to incorporate the knowledge I have about the shape of the temperature-consumption relationship (being unimodal) through the use of weakly informative priors. One of the limitations of the modeling approach is that I assume all of the temporal variability in growth is due to temporal variability in temperature. Although in nature the temporal variability in growth is affected by a number of factors other than temperature (e.g. food availability, individual activity), the results from the experimental data provide promising results that the flexibility of the state-space framework will allow the error structure to capture the variability in growth due to different food rations in the experimental treatment.

The results from section 4.3.1 suggest that the modeling approach developed is robust to small amounts of data and relatively noisy data (both process stochasticity and measurement error). Additionally, the results from section 4.3.4 seem to support the use of the more traditional parametric approach to bioenergetic modeling based on the consumption-temperature relationship from Thornton & Lessem (1978), at least for the temperatures

that were considered in the experimental treatments. The results of the model also suggest that experimental work should be done on the growth of individuals near the theoretical peak of the temperature-consumption relationship (near 24°C). It would also be interesting to apply the model to an experimental treatment with a broad range of temperatures.

4.5 Acknowledgements

This work was supported by the NSF GRPF and the Center for Stock Assessment Research (CSTAR). Thank you for Prof. Kottas for the comments on this work.

Chapter 5

Conclusions

As I have highlighted in the work presented here, steelhead trout have arguably one of the most complex life histories of all Pacific salmonids. Due to this complexity, studies are often limited in their scope. I set out in this dissertation with the goal of shedding new light into both individual-level and population-wide attributes of steelhead trout through the employment of mathematical and statistical methods. Throughout the different chapters I employed a number of different tools and present knowledge about individual life history to understand the different patterns that are observed in nature.

In Chapter 2, I developed the framework to better explain the patterns that are observed in the steelhead population of the Carmel River. More specifically, I combined life history theory, historical data and mathematical models in order to improve predictions about the dynamics of the anadromous component of the steelhead population. While the model required many assumptions, I demonstrate that incorporating the current knowledge about the biology of steelhead increases the predictive power of the data and the model I

develop is better able to describe the patterns observed in nature. This work also highlights that having a smaller number of larger sized individuals may produce a larger number of returning adults and that a declining mean size in the Carmel River may be a large driver of the observed population decline. By looking at data from both wild individuals and individual that were partially reared in the Sleepy Hollow Steelhead Rearing Facility, I was able to determine that a possible switch from a period of predominant wild adult production to one in which adult production is primarily maintained through the SHSRF.

While in Chapter 2 I focus on the contribution to anadromous adults by YOY, in Chapter 3 I develop the modeling methodology to account for the entire life history of an individual. Although there is vast knowledge about the mechanisms driving the life history of individuals, many of the modeling studies have limited their focus on specific parts of the life history. By developing a Physiologically Structured Population Model (PSPM), I am able to account for many of the biological mechanisms driving the population dynamics of steelhead. The PSPM framework incorporates all of the important individual processes such as growth, survival, smolting, early maturation and reproduction in a mechanistic way. In addition to incorporating the full knowledge of these individual mechanisms, I am able to include variability in individual growth by incorporating a size-dependent competitive mechanism into the standard bioenergetic modeling. The flexibility of the PSPM framework is able to include the range of complexity present in steelhead life history and allows the resultant population dynamics to be driven by interactions between individuals and the environment. This way of modeling the steelhead populations yields complex population dynamics and the model is able to exhibit the range of dynamics that are observed in nature

based on different parameter combinations. In addition to the development of the model, I demonstrated the applicability of the model by investigating the effects that varying the temperature regime experienced by individuals has on population dynamics. This investigation highlighted the fact that all of the dynamics and interactions are highly non-linear and that predicting the effects of simple changes in temperature do not yield simple changes in the observed dynamics.

In Chapters 2 and 3, I modeled growth of individuals as a completely deterministic process governed by the thermodynamic considerations of bioenergetics. In addition to modeling growth as a known process, I also relied on the previously published parameters and temperature-consumption relationships available in the literature, which are sometimes contested. In Chapter 4, I develop the statistical methodology that allows me bypass the assumption about the temperature-consumption relationship and accounts for multiple sources of variability. This goal was accomplished with the development of a state-space model based on temporal measurements of individual growth and a Gaussian Process (GP) prior on the relationship between temperature and consumption. I demonstrate the effectiveness of the model under different levels of simulated data availability with varying amounts of measurement error and process stochasticity, in order to confidently apply it to real data. I then apply the model to data and demonstrate the ability even though some assumptions of the model are violated. In the temperature ranges explored, I show that the shape of the temperature-consumption relationship is in agreement with the function developed by Thornton & Lessem (1978) that is commonly used for steelhead.

In combination, the three chapters presented highlight a suite of methods that help

us better understand the dynamics that are observed in nature. I have also highlighted that by combining knowledge about individual life history in a mathematically mechanistic way one can better understand the dynamics of individual and populations . The development of methods that combine mathematical tools with biological knowledge are essential in predicting the effects that changes in temperature regimes, flow conditions and other habitat alterations will have in to both individuals and populations. In particular, temperature regimes are expected to be affected by climate change in the relatively near future. This expected change and the high dependence metabolic processes of ectotherms on water temperatures, modeling the bioenergetics of individuals as I have done in this work will be particularly important in accurately estimating the effects these changes will have. The methodologies developed here can also be helpful in informing management, policy and highlight the areas where knowledge gaps are present. Lastly, it is worth noting that while in this work I framed the development of the methodology with steelhead as the motivating factor and relied on assumptions were driven by steelhead biology, a large amount of this work can be abstracted and easily applied to other facultatively anadromous species.

Bibliography

Abdul-Aziz, O. I., Mantua, N. J., Myers, K. W. & Bradford, M. (2011). Potential climate change impacts on thermal habitats of Pacific salmon (*Oncorhynchus spp.*) in the North Pacific Ocean and adjacent seas. *Canadian Journal of Fisheries and Aquatic Sciences* **68**, 1660–1680. doi:10.1139/f2011-079.

Beakes, M. P., Satterthwaite, W. H., Collins, E. M., Swank, D. R., Merz, J. E., Titus, R. G., Sogard, S. M. & Mangel, M. (2010). Smolt transformation in two California steelhead populations: effects of temporal variability in growth. *Transactions of the American Fisheries Society* **139**, 1263–1275. doi:10.1577/T09-146.1.

Bond, M. H., Hayes, S. a., Hanson, C. V. & MacFarlane, R. B. (2008). Marine survival of steelhead (*Oncorhynchus mykiss*) enhanced by a seasonally closed estuary. *Canadian Journal of Fisheries and Aquatic Sciences* **65**, 2242–2252. doi:10.1139/F08-131.

Boughton, D. A., Adams, P. B., Anderson, E., Fusaro, C., Keller, E., Kelley, E., Lentsch, L. D., Nielsen, J. L., Perry, K., Regan, H. et al. (2006). Steelhead of the south-central/southern california coast: Population characterization for recovery

planning. Technical report, National Marine Fisheries Service, Southwest Fisheries Science Center.

Boughton, D. a., Gibson, M., Yedor, R. & Kelley, E. (2007). Stream temperature and the potential growth and survival of juvenile *Oncorhynchus mykiss* in a southern California creek. *Freshwater Biology* **52**, 1353–1364. doi:10.1111/j.1365-2427.2007.01772.x.

Boughton, D. a., Harrison, L. R., Pike, A. S., Arriaza, J. L. & Mangel, M. (2015). Thermal potential for steelhead life history expression in a Southern California alluvial river. *Transactions of the American Fisheries Society* **144**, 258–273. doi: 10.1080/00028487.2014.986338.

Brett, J. R. (1952). Temperature tolerance in young pacific salmon, genus *Oncorhynchus*. *Journal of the Fisheries Board of Canada* **9**, 265–323.

Carle, F. L. & Strub, M. R. (1978). A new method for estimating population size from removal data. *Biometrics* **34**, 621–630. doi:10.2307/2530381.

Chipps, S. R. & Wahl, D. H. (2008). Bioenergetics Modeling in the 21st Century: Reviewing New Insights and Revisiting Old Constraints. *Transactions of the American Fisheries Society* **137**, 298–313. doi:10.1577/T05-236.1.

Ciancio, J. E., Pascual, M. a., Botto, F., Amaya-Santi, M., O'Neal, S., Riva Rossi, C. & Iribarne, O. (2008). Stable isotope profiles of partially migratory salmonid populations in Atlantic rivers of Patagonia. *Journal of Fish Biology* **72**, 1708–1719. doi: 10.1111/j.1095-8649.2008.01846.x.

Claessen, D., de Roos, A. M. & Persson, L. (2000). Dwarfs and giants: cannibalism and competition in size-structured populations. *The American Naturalist* **155**, 219–237.

Crozier, L. G., Hendry, a. P., Lawson, P. W., Quinn, T. P., Mantua, N. J., Battin, J., Shaw, R. G. & Huey, R. B. (2008). Potential responses to climate change in organisms with complex life histories: evolution and plasticity in Pacific salmon. *Evolutionary Applications* **1**, 252–270. doi:10.1111/j.1752-4571.2008.00033.x.

Crozier, L. G., Zabel, R. W., Hockersmith, E. E. & Achord, S. (2010). Interacting effects of density and temperature on body size in multiple populations of Chinook salmon. *Journal of Animal Ecology* **79**, 342–349. doi:10.1111/j.1365-2656.2009.01641.x.

Doctor, K., Berejikian, B., Hard, J. J. & VanDoornik, D. (2014). Growth-mediated life history traits of steelhead reveal phenotypic divergence and plastic response to temperature. *Transactions of the American Fisheries Society* **143**, 317–333.

Elliott, J. (2002). Shadow competition in wild juvenile sea-trout. *Journal of Fish Biology* **61**, 1268–1281. doi:10.1006/jfbi.2002.2154.

From, J. & Rasmussen, G. (1984). A growth model, gastric evacuation, and body composition in rainbow trout, *Salmo gairdneri* richardson, 1836. *Dana* **3**, 139.

Garza, J. C. & Pearse, D. E. (2008). Population genetic structure of *Oncorhynchus mykiss* in the california central valley. *California Department of Fish and Game, Final Report for Contract PO485303, Santa Cruz* .

Grant, J. & Imre, I. (2005). Patterns of density-dependent growth in juvenile

stream-dwelling salmonids. *Journal of Fish Biology* **67**, 100–110. doi:10.1111/j.1095-8649.2005.00916.x.

Hanson, P. C., Johnson, T. B., Schindler, D. E. & Kitchell, J. F. (1997). Fish Bioenergetics 3.0 software for Windows.

Hilborn, R. & Mangel, M. (1997). *The ecological detective: confronting models with data*, volume 28. Princeton University Press.

Holtby, L. B. (1988). Effects of logging on stream temperatures in carnation creek british columbia, and associated impacts on the coho salmon (*Oncorhynchus kisutch*). *Canadian Journal of Fisheries and Aquatic Sciences* **45**, 502–515. doi:10.1139/f88-060.

Kendall, N. W., Mcmillan, J. R., Sloat, M. R., Buehrens, T. W., Quinn, T. P., Pess, G. R., Kuzishchin, K. V., Mcclure, M. M. & Zabel, R. W. (2015). Anadromy and residency in steelhead and rainbow trout (*Oncorhynchus mykiss*): a review of the processes and patterns. *Canadian Journal of Fisheries and Aquatic Sciences* **342**, 319–342.

King, J. T. (2010). Ten-Year Summary of the Monterey Peninsula Water Management District's Bioassessment Program on the Carmel River. Technical Report November, Bioassessment Services.

Le Bourlot, V., Tully, T. & Claessen, D. (2014). Interference versus Exploitative Competition in the Regulation of Size-Structured Populations. *The American naturalist* **184**, 609–23. doi:10.1086/678083.

Lorenzen, K. (1996). A simple von Bertalanffy model for density-dependent growth in extensive aquaculture, with an application to common carp (*Cyprinus carpio*). *Aquaculture* **146**, 191–205. doi:10.1016/0044-8486(95)01229-X.

Lorenzen, K. (2000). Allometry of natural mortality as a basis for assessing optimal release size in fish-stocking programmes. *Canadian Journal of Fisheries and Aquatic Sciences* **57**, 2374–2381. doi:10.1139/f00-215.

Mangel, M. (1994). Life History Variation and Salmonid Conservation. *Conservation Biology* **8**, 879–880.

Mangel, M. & Munch, S. B. (2005). A life-history perspective on short-and long-term consequences of compensatory growth. *The American Naturalist* **166**, 155–176.

McCarthy, S. G., Duda, J. J., Emlen, J. M., Hodgson, G. R. & Beauchamp, D. a. (2009). Linking Habitat Quality with Trophic Performance of Steelhead along Forest Gradients in the South Fork Trinity River Watershed, California. *Transactions of the American Fisheries Society* **138**, 506–521. doi:10.1577/T08-053.1.

McGurk, M. (1996). Allometry of marine mortality of Pacific salmon. *Oceanographic Literature Review* pp. 77–88.

Metcalfe, N. (1986). Intraspecific variation in competitive ability and food intake in salmonids: consequences for energy budgets and growth rates. *Journal of Fish Biology* .

Moore, J. W., Yeakel, J. D., Peard, D., Lough, J. & Beere, M. (2014). Life-history diversity and its importance to population stability and persistence of a migratory

fish: steelhead in two large north american watersheds. *J Anim Ecol* doi:10.1111/1365-2656.12212.

Myrick, C. & Cech, J. J. (2004). Temperature effects on juvenile anadromous salmonids in California's central valley: what don't we know? *Reviews in Fish Biology and Fisheries* pp. 113–123.

Nakano, S., Kachi, T. & Nagoshi, M. (1991). Individual growth variation of red-spotted masu salmon, *Oncorhynchus masou rhodurus*, in a mountain stream. *Japanese Journal of Ichthyology* **38**.

Ney, J. J. (1993). Bioenergetics modeling today: growing pains on the cutting edge. *Transactions of the American Fisheries Society* **122**, 736–748.

Olsen, J. B., Wuttig, K., Fleming, D., Kretschmer, E. J. & Wenburg, J. K. (2006). Evidence of partial anadromy and resident-form dispersal bias on a fine scale in populations of *Oncorhynchus mykiss*. *Conservation Genetics* **7**, 613–619. doi: 10.1007/s10592-005-9099-0.

Pascual, M., Bentzen, P., Rossi, C. R., Mackey, G. & Kinnison, M. T. (2001). First Documented Case of Anadromy in a Population of Introduced Rainbow Trout in Patagonia , Argentina. *Transactions of the American Fisheries Society* **1**, 53–67.

Pavlov, D., Savvaitova, K., Kuzishchin, K., Gruzdeva, M., Mal'Tsev, A. Y. & Stanford, J. (2008). Diversity of life strategies and population structure of kamchatka mykiss *Parasalmo mykiss* in the ecosystems of small salmon rivers of various types. *Journal of Ichthyology* **48**, 37–44.

Pearse, D. E., Hayes, S. a., Bond, M. H., Hanson, C. V., Anderson, E. C., MacFarlane, R. B. & Garza, J. C. (2009). Over the falls? Rapid evolution of ecotypic differentiation in steelhead/rainbow trout (*Oncorhynchus mykiss*). *Journal of Heredity* **100**, 515–525. doi:10.1093/jhered/esp040.

Persson, L., Leonardsson, K., de Roos, a. M., Gyllenberg, M. & Christensen, B. (1998). Ontogenetic scaling of foraging rates and the dynamics of a size-structured consumer-resource model. *Theoretical population biology* **54**, 270–93. doi: 10.1006/tpbi.1998.1380.

Quinn, T. P. (2005). *The Behavior and Ecology of Pacific Salmon and Trout*. University of Washington Press.

Quinn, T. P. & Dittman, a. H. (1990). Pacific salmon migrations and homing: mechanisms and adaptive significance. *Trends in ecology & evolution* **5**, 174–7. doi: 10.1016/0169-5347(90)90205-R.

Quinn, T. P., Seamons, T. R., Vøllestad, L. A. & Duffy, E. (2011). Effects of growth and reproductive history on the egg size–fecundity trade-off in steelhead. *Transactions of the American Fisheries Society* **140**, 45–51.

Railsback, S. & Rose, K. (1999). Bioenergetics Modeling of Stream Trout Growth : Temperature and Food Consumption Effects. *Transactions of the American Fisheries Society* pp. 37–41.

Rand, P. S., Stewart, D. J., Seelbach, P. W., Jones, M. L. & Wedge, L. R. (1993).

Modeling Steelhead Population Energetics in Lakes Michigan and Ontario. *Transactions of the American Fisheries Society* pp. 37–41.

Reist, J. D., Wrona, F. J., Prowse, T. D., Power, M., Dempson, J. B., King, J. R. & Beamish, R. J. (2006). An Overview of Effects of Climate Change on Selected Arctic Freshwater and Anadromous Fishes. *AMBIO: A Journal of the Human Environment* **35**, 381–387. doi:10.1579/0044-7447(2006)35[381:AOOEOC]2.0.CO;2.

de Roos, a. M. (1988). Numerical methods for structured population models: The Escalator Boxcar Train. *Numerical Methods for Partial Differential Equations* **4**, 173–195. doi:10.1002/num.1690040303.

de Roos, A. M. (1997). A gentle introduction to physiologically structured population models. In *Structured-Population Models in Marine, Terrestrial, and Freshwater Systems*, Eds. S. Tuljapurkar & H. Caswell, volume 18 of *Population and Community Biology Series*, pp. 119–204. Springer US. doi:10.1007/978-1-4615-5973-3_5.

de Roos, A. M. & Persson, L. (2001). Physiologically structured models - from versatile technique to ecological theory. *Oikos* **94**, 51–71. doi:doi:10.1034/j.1600-0706.2001.11313.x.

de Roos, A. M. & Persson, L. (2013). *Population and Community Ecology of Ontogenetic Development*. Princeton University Press. doi:10.2307/j.ctt1r2g73.

de Roos, A. M., Persson, L. & McCauley, E. (2003). The influence of size-dependent life-history traits on the structure and dynamics of populations and communities. *Ecology Letters* **6**, 473–487. doi:10.1046/j.1461-0248.2003.00458.x.

Satterthwaite, W. H., Beakes, M. P., Collins, E. M., Swank, D. R., Merz, J. E., Titus, R. G., Sogard, S. M. & Mangel, M. (2009). Steelhead Life History on California's Central Coast: Insights from a State-Dependent Model. *Transactions of the American Fisheries Society* **138**, 532–548. doi:10.1577/T08-164.1.

Satterthwaite, W. H., Beakes, M. P., Collins, E. M., Swank, D. R., Merz, J. E., Titus, R. G., Sogard, S. M. & Mangel, M. (2010). State-dependent life history models in a changing (and regulated) environment: steelhead in the California Central Valley. *Evolutionary Applications* **3**, 221–243. doi:10.1111/j.1752-4571.2009.00103.x.

Schindler, D. E., Rogers, D. E., Scheuerell, M. D. & Abrey, C. A. (2005). Effects of changing climate on zooplankton and juvenile sockeye salmon growth in southwestern alaska. *Ecology* **86**, 198–209.

Seber, G. A. F. & Le Cren, E. (1967). Estimating Population Parameters from Catches Large Relative to the Population. *Journal of Animal Ecology* **36**, 631–643.

Shapovalov, L. (1967). Biology and Management of Steelhead Trout in California. Technical Report 98, California Department of Fish and Game.

Shapovalov, L. & Taft, A. C. (1954). The Life Histories of the Steelhead Rainbow Trout (*Salmo gairdneri gairdneri*) and Silver Salmon (*Oncorhynchus kisutch*) with special reference to Wadell Creek, California. *State of California, Department of Fish and Game* .

Sigourney, D. B., Munch, S. B. & Letcher, B. H. (2012). Combining a Bayesian nonparametric method with a hierarchical framework to estimate individ-

ual and temporal variation in growth. *Ecological Modelling* **247**, 125–134. doi: 10.1016/j.ecolmodel.2012.08.009.

Simon, C. A., Satterthwaite, W. H., Beakes, M. P., Swank, D. R., Merz, J. E., Titus, R. G., Susan, M. & Mangel, M. (2013). Individual and Population Level Variation in Growth Parameters for Steelhead Trout *Oncorhynchus mykiss* in Central California. Technical report, University of California, Santa Cruz, Santa Cruz.

Sloat, M., Fraser, D., Dunham, J., Falke, J., Jordan, C., McMillan, J. & Ohms, H. (2014a). Ecological and evolutionary patterns of freshwater maturation in pacific and atlantic salmonines. *Reviews in Fish Biology and Fisheries* **24**, 689–707. doi:10.1007/s11160-014-9344-z.

Sloat, M. R., Reeves, G. H. & Jonsson, B. (2014b). Individual condition, standard metabolic rate, and rearing temperature influence steelhead and rainbow trout (*Oncorhynchus mykiss*) life histories. *Canadian Journal of Fisheries and Aquatic Sciences* **71**, 491–501.

Snider, B. & Titus, R. G. (2000). Lower American River emigrations survey, October 1996-September 1997. Technical Report December, California Department of Fish And Game.

Snider, W. M. (1983). Reconnaissance of the Steelhead Resource of the Carmel River Drainage, Monterey County. *Department of Fish and Game* .

Snover, M. L., Watters, G. M. & Mangel, M. (2006). Top-down and bottom-up

control of life-history strategies in coho salmon (*Oncorhynchus kisutch*). *The American naturalist* **167**, E140–57. doi:10.1086/502804.

Sogard, S. M., Merz, J. E., Satterthwaite, W. H., Beakes, M. P., Swank, D. R., Collins, E. M., Titus, R. G. & Mangel, M. (2012). Contrasts in Habitat Characteristics and Life History Patterns of *Oncorhynchus mykiss* in California's Central Coast and Central Valley. *Transactions of the American Fisheries Society* **141**, 747–760. doi: 10.1080/00028487.2012.675902.

Stewart, D., Weininger, D., Rottiers, D. V. & Edsall, T. A. (1983). An energetics model for lake trout, *Salvelinus namaycush*: application to the Lake Michigan population. *Canadian Journal of Fisheries and Aquatic Sciences* .

Thornton, K. & Lessem, A. (1978). A Temperature Algorithm for Modifying Biological Rates. *Transactions of the American Fisheries Society* **107**, 284–287.

Thorpe, J. (1998). Salmonid Life-History Evolution As A Constraint On Marine Stock Enhancement. *Bulletin of Marine Science* **62**, 465–475.

Thorpe, J. E., Mangel, M., Metcalfe, N. B. & Huntingford, F. A. (1998). Modelling the proximate basis of salmonid life-history variation, with application to atlantic salmon, *Salmo salar L. Evolutionary Ecology* **12**, 581–599.

Thrower, F., Guthrie, I., Charles, Nielsen, J. & Joyce, J. (2004). A comparison of genetic variation between an anadromous steelhead, *Oncorhynchus mykiss*, population and seven derived populations sequestered in freshwater for 70 years. *Environmental Biology of Fishes* **69**, 111–125. doi:10.1023/B:EBFI.0000022880.52256.92.

Thrower, F. P., Joyce, J. E., Celewycz, A. G. & Malecha, P. W. (2008). The potential importance of reservoirs in the western United States for the recovery of endangered populations of anadromous steelhead. *American Fisheries Society* .

Tyler, J. a. & Bolduc, M. B. (2008). Individual Variation in Bioenergetic Rates of Young-of-Year Rainbow Trout. *Transactions of the American Fisheries Society* **137**, 314–323. doi:10.1577/T05-238.1.

Van Winkle, W., Jager, H., Railsback, S., Holcomb, B., Studley, T. & Baldrige, J. (1998). Individual-based model of sympatric populations of brown and rainbow trout for instream flow assessment: model description and calibration. *Ecological Modelling* **110**, 175–207.

Vincenzi, S., Crivelli, A. J., Jesensek, D. & De Leo, G. a. (2008). The role of density-dependent individual growth in the persistence of freshwater salmonid populations. *Oecologia* **156**, 523–34. doi:10.1007/s00442-008-1012-3.

Walters, A. W., Copeland, T. & Venditti, D. a. (2013). The density dilemma: Limitations on juvenile production in threatened salmon populations. *Ecology of Freshwater Fish* **22**, 508–519. doi:10.1111/eff.12046.

Waples, R. (1991). Pacific Salmon, *Oncorhynchus spp.*, and the Definition of "Species" Under the Endangered Species Act. *Marine Fisheries Review* **53**, 11–22.

Willson, M. F. & Halupka, K. C. (1995). Anadromous Fish as Keystone Species in Vertebrate Communities. *Conservation Biology* **9**, 489–497. doi:10.1046/j.1523-1739.1995.09030489.x.

Ylvisaker, N. D. (1965). The expected number of zeros of a stationary gaussian process. *The Annals of Mathematical Statistics* pp. 1043–1046.

Appendix A

Chapter 2

A.1 Abundance Estimates

Using depletion electrofishing data, I am able to estimate the total abundance of a given sampling site in a given year. The depletion electrofishing data were collected by isolating a section of the river with the use of nets to impede any migration in or out of the selected reach. The isolated reach was then electrofished and individuals removed until the pre-specified number of passes have been completed. With data of the number of individuals removed during each pass, I am able to estimate the total population abundance present prior to any removals. A rough approach to estimate the initial population abundance is a regression estimation on the cumulative catch

$$\text{Cumulative Catch} = \text{Catch } \times \beta + \epsilon \tag{A.1}$$

Using this approach, the slope coefficient β for the catch in each subsequent pass is estimated and then total abundance can be estimated when the catch reaches zero.

Many different approaches have been developed to bypass the multiple assumptions that are required for this estimate to be valid. While these different approaches improve the total abundance estimate, they often come with their own assumptions and require specific sampling methodologies and different levels of data availability. Instead of using one of these more sophisticated methods, I employ two different commonly used methods depending on the number of depletion passes performed. For the case in which three or more passes were performed, I use the Bayesian estimator developed by Carle & Strub (1978). Briefly, this methodology assumes that the likelihood of catching C_i individuals in a given pass given an initial population size N_0 is given by a multinomial distribution

$$L(C|N_0, p) = \frac{N_0! p^T q^{KN_0 - X - T}}{(N-T)! \prod_i C_i!} \tag{A.2}$$

Here C is the vector containing the number of individuals captured in successive catches, K is the total number of removal attempts, $T = \sum_i C_i$ is the total number of individuals captured and $X = \sum_i (K-i)C_i$. Additionally individuals assumed to have equal probability of capture $q = 1 - p$, where p is the probability of escape. Following Carle & Strub (1978), I place a beta prior ($p \sim \text{Beta}(\alpha, \beta)$) on the escape probability and then integrate out nuisance parameters. This results in a closed form estimate for the probability density of the total initial abundance

$$p(N|C) \propto \frac{N!(\alpha+\beta-1)!(T+\alpha-1)!(KN-X-T+\beta-1)!}{\prod_i C_i!(N-T)!(\alpha-1)!(\beta-1)!(KN-X+\alpha+\beta-1)!} \tag{A.3}$$

Here I use the uniform prior ($\alpha, \beta = 1$) and use the maximum estimate from Carle & Strub (1978) as the abundance estimate.

In the cases where only two depletion passes were performed I use the abundance estimate from Seber & Le Cren (1967). The likelihood for the number of individuals caught

during two subsequent passes is given by

$$p(C_1, C_2) = \frac{N_0!}{C_1!C_2!(N_0 - C_1 - C_2)!} p^{C_1}(qp)^{C_2}(q^2)^{N_0 - C_1 - C_2} \tag{A.4}$$

Under this likelihood, I use the expected value for abundance

$$\hat{N_0} = \frac{C_1^2}{C_1 - C_2} \tag{A.5}$$

A.2 Cohort Fitting

In order to determine the full contribution that YOY individuals are expected to provide to the number of returning adults I must identify the different size classes present at any given site in any given year. Since I know that reproduction of different individuals doesn't occur continuously, I assume that length distributions of each age class within the population can be approximated by a normal distribution. With this assumption, the total length-frequency distribution of the population at the jth site in year t can be modeled as a mixture of K normal distributions $\alpha_k N(\mu_k, \sigma_k)$with different weights ($\alpha_k$), means ($\mu_k$) and variances ($\mu_k$) and K representing the total number of age classes present.

$$\mathbf{l}_{t,j} \sim \sum_{k=1}^{k=K} \alpha_k N(\mu_k, \sigma_k) \tag{A.6}$$

For a given K, I find maximum likelihood estimates for $\alpha_k, \mu_k, \sigma_k^2$ and corresponding Bayesian Information Criteria (BIC) value using Matlab's Expectation Maximization (EM) algorithm. I fit the four models with $K = 1 \ldots 4$ and select the model with the lowest BIC as the best model. Using this model, I can then sample the individuals which were not measured but were estimated to be present at the site during that sampling event (as described in A.1). After sampling the lengths for the individuals that were not captured

during the sampling events, I assign each individual to a specific age class based on the probability that an individual came from the kth normal distribution.

A.3 Bayesian Linear Regression

In section 2.4 I utilize Bayesian linear regression with standard diffuse priors (uniform distributions on β and $\log(\sigma^2)$) to analyze the relationships between different measured variables

$$y = c + x\beta + \epsilon_i \tag{A.7}$$

$$\epsilon_i \sim N(0, \sigma^2) \tag{A.8}$$

$$p(\beta, \sigma^2) \propto \frac{1}{\sigma^2} \tag{A.9}$$

Here y and x are the response and predictor variables respectively; c and β describe the mean value of the response and the linear relationship of the response and the predictor respectively. Under this model definition MCMC inference is straight forward with all full conditionals for the parameters resulting in closed form solutions.

Appendix B

Chapter 3

B.1 Calculating baseline mortality levels

In section3.4.1 we determine the baseline mortality levels following Snover et al. (2006) based on a predefined growth trajectory to the time of emigration for individuals. More specifically, we chose a representative growth trajectory for an individual and determined the combinations of, μ_0 and μ_1 would yield a survival level of 1.8% to outmigration (a=455). Here we chose a growth trajectory that would lead to a size of 10.5 cm by age 1 and a size of 12.8 cm by outmigration (Figure B.1).

Alternatively, we can determine the survival for an individual based on the growth ($g(x)$) from size at birth x_b up to a give size x (de Roos, 1997)

$$S = \exp\left(-\int_{x_b}^{x} \frac{\mu(s)}{g(s)} ds\right) \tag{B.1}$$

We make the simplifying conditions that we can neglect density dependence ($A(t,l) = constant$) and that growing conditions are sufficient such that individuals don't experi-

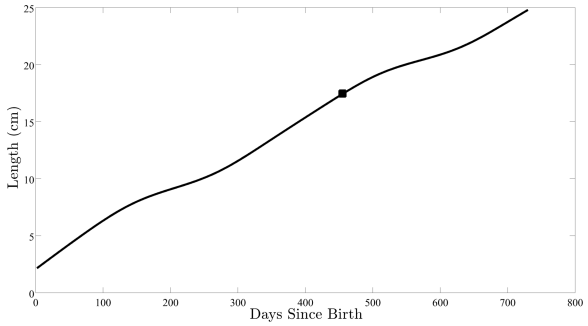

Figure B.1: Growth trajectory used for the estimation of μ_1 and μ_0. Marker on the growth trajectory represents day of out migration (a=455).

ence starvation mortality ($\mu_s = 0$). Under these simplifying assumptions, the growth and mortality of a juvenile can be written as:

$$g(x) = \kappa(x, q_j x) E_g(x + q_j x) \tag{B.2}$$

$$= \frac{E_g(x + q_j x)}{(1 + q_j)} \tag{B.3}$$

$$\mu(x) = \mu_0 + \frac{\mu_1}{\alpha_l \left(x + q_j x\right)^{\beta_l}} \tag{B.4}$$

respectively. Now, rather than specifying a specific growth trajectory, we can determine combinations of μ_0 and μ_0 that result in a specific survival level, $\hat{S}$, to size x as:

$$\int_{x_b}^{x} \frac{\left(\mu_0 + \frac{\mu_1}{\alpha_l (s + q_j s)^{\beta_l}}\right)(1 + q_j)}{E_g(s + q_j s)} ds = -ln(\hat{S}) \tag{B.5}$$

B.2 Individual Level Dynamics

In Figures B.2, B.3, B.4, we demonstrate the individual level dynamics for six different parameter combinations (Figure B.2 (a) high size-dependent mortality, no asymmetric competition, Figure B.2 (b) low size-dependent mortality, no asymmetric competition, Figure B.3 (a) high size-dependent mortality, high asymmetric competition, Figure B.3 (b)

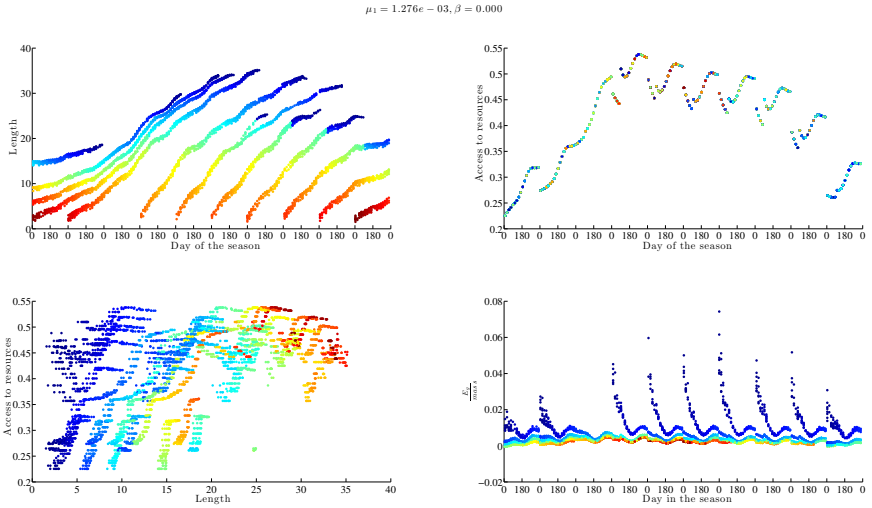
$\mu_1 = 1.276e-03, \beta = 0.000$
Length
Day of the season
Access to resources
Day of the season
Access to resources
Length
$\frac{E_i}{max_i}$
Day in the season

(a)

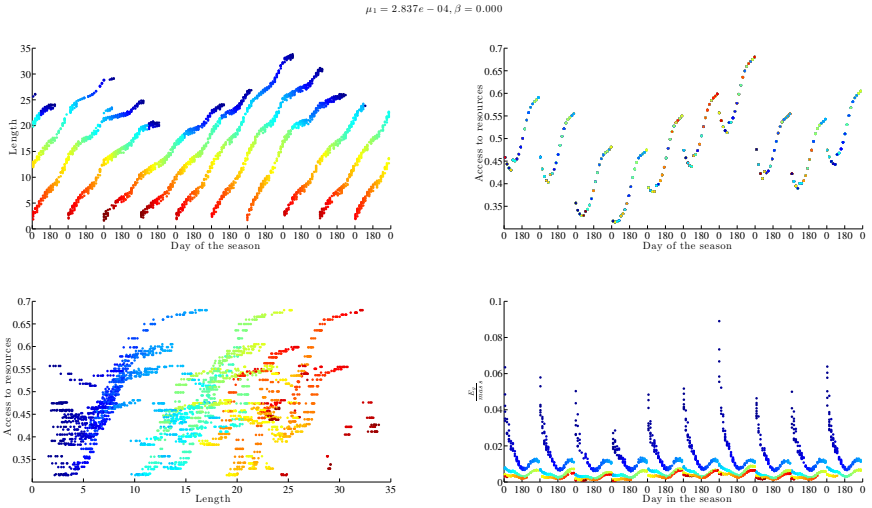
$\mu_1 = 2.837e-04, \beta = 0.000$
Length
Day of the season
Access to resources
Day of the season
Access to resources
Length
$\frac{\Delta_i}{max_i}$
Day in the season

(b)

Figure B.2

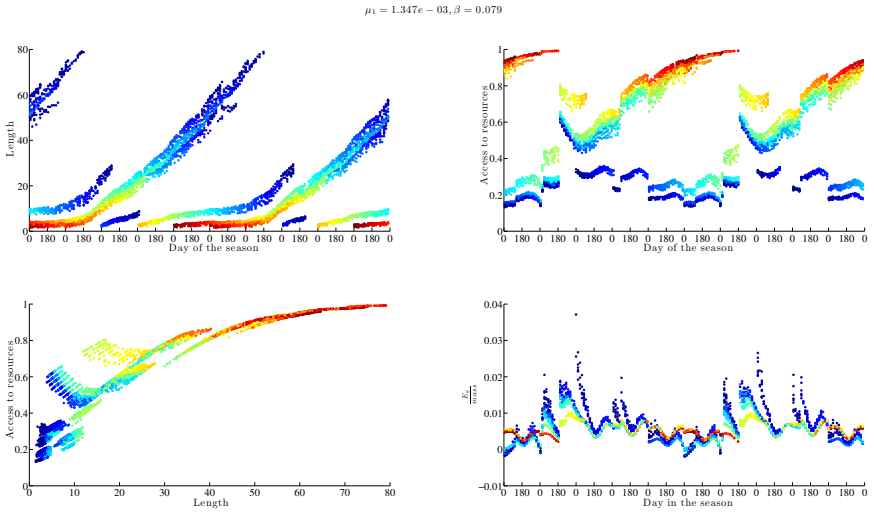
$\mu_1 = 1.347e-03, \beta = 0.079$
Length
Day of the season
Access to resources
Day of the season
Access to resources
Length
$\frac{E_c}{mass}$
Day in the season

(a)

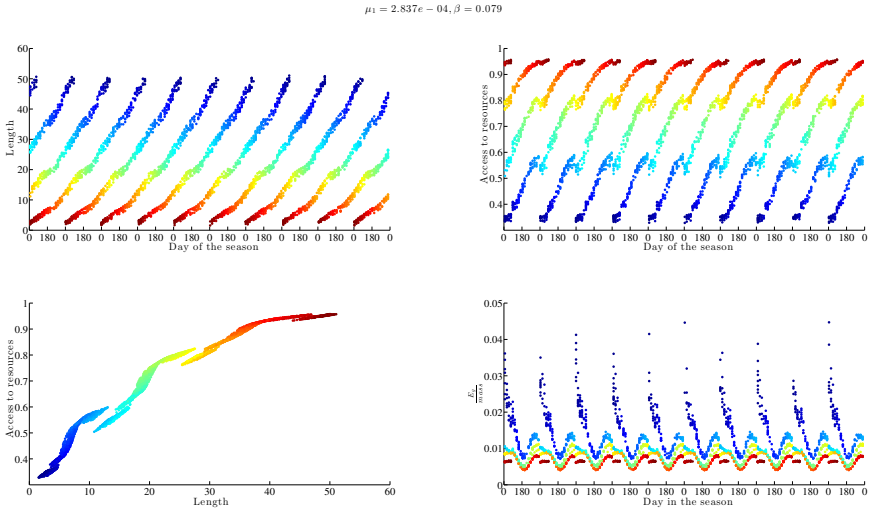
$\mu_1 = 2.837e-04, \beta = 0.079$
Length
Day of the season
Access to resources
Day of the season
Access to resources
Length
$\frac{E_c}{mass}$
Day in the season

(b)

Figure B.3

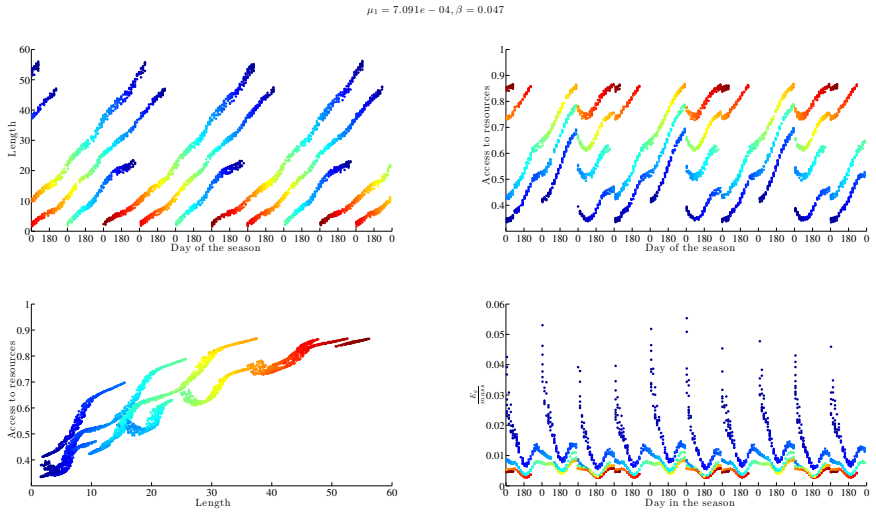
$\mu_1 = 7.091e-04, \beta = 0.047$
Length
Day of the season
Access to resources
Day of the season
Access to resources
Length
$\frac{dL}{dt}$
Day in the season

(a)

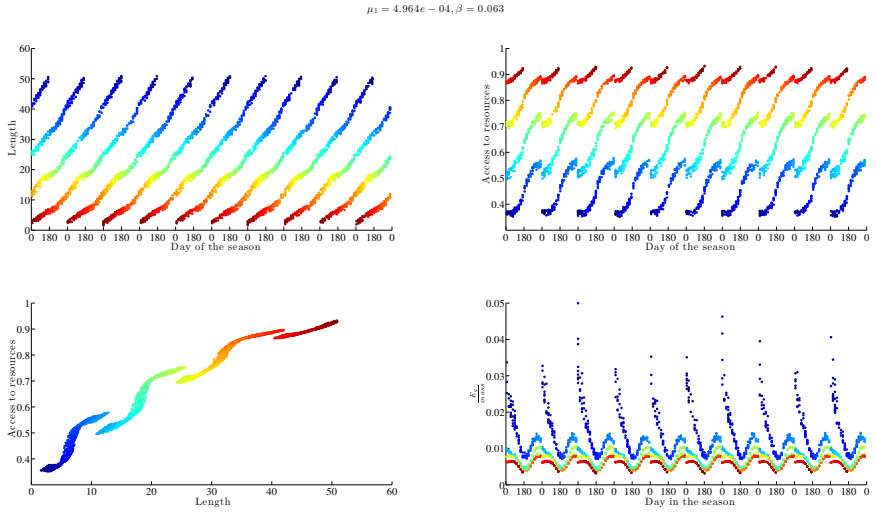
$\mu_1 = 4.964e-04, \beta = 0.063$
Length
Day of the season
Access to resources
Day of the season
Access to resources
Length
$\frac{dL}{dt}$
Day in the season

(b)

Figure B.4

low size-dependent mortality, high asymmetric competition, Figure B.3 (a) intermediate size-dependent mortality, Figure B.3 (b) intermediate asymmetric competition).

In the case with high size-dependent mortality and no asymmetric competition Figure B.2 (a), we get a buildup of multiple cohorts of individuals and a subsequent relaxation which leads to oscillating levels of asymptotic lengths. Even with relaxed size-dependent mortality Figure B.3 (a), the buildup and relaxation occurs, but to a lesser extent. In the scenario with high levels of asymmetric competition and high size-dependent mortality, we have an oscillatory pattern in the length of individuals with three different trajectories available. Individuals that are born when the population abundance is high experience very high competition and therefore are stunted and have very short lifespans due to the lack of ability to grow. The subsequent cohort born is exposed to a lower population abundance, competition and is able to live substantially longer and reach a larger size, lastly the population born during low population abundance is the most numerous and experiences much lower competition than the other two. This results in extremely high growth rates, longevity and asymptotic size. When there is high asymmetric competition but low size-dependent mortality (high size-independent mortality) no oscillation happens because large individuals do not have a mortality advantage over small individuals which relaxes competition for smaller individuals. The relaxation caused by background mortality results in drastically different minimum access to resources for individuals between the two scenarios with high asymmetric competition are $A(t,l) = 0.35$ and $A(t,l) = 0.175$. Although for all the scenarios a reproductive event reduces the access to resources, the level at which it affects different year cohorts is driven by the size asymmetry of competition.

Appendix C

Chapter 4

C.1 Derivation of Conditional Posteriors

In this appendix I present the derivation of the full conditional distributions necessary for the implementation of the Metropolis-within-Gibbs algorithm utilized for results in section 4.3. Recalling the full statistical model for developed in section 4.2.2

Observations

$$y_{i,t} = v_{i,t} + \epsilon_m \tag{C.1}$$

$$\epsilon_m \overset{iid}{\sim} N\left(0, \sigma_m^2\right) \tag{C.2}$$

Process

$$v_{i,t} = \delta_t v_{i,t-1} + \sum_{k=0}^{k=\infty} \left\{a_k \mathcal{I}_{\mathcal{C}}(k,t) + b_k \mathcal{I}_{\mathcal{S}}(k,t)\right\} + \epsilon_p \tag{C.3}$$

$$\mathcal{I}_{\mathcal{C}}(k,t) = \int_{t-1}^{t} \cos(kT(s)) g(t,s) ds \tag{C.4}$$

$$\mathcal{I}_{\mathcal{S}}(k,t) = \int_{t-1}^{t} \sin(kT(s)) g(t,s) ds \tag{C.5}$$

$$\epsilon_p \overset{iid}{\sim} N\left(0, \sigma_p^2\right) \tag{C.6}$$

Prior

$$a_k \sim N(0, \lambda_k(\omega^2, l^2)) \tag{C.7}$$

$$b_k \sim N(0, \lambda_k(\omega^2, l^2)) \tag{C.8}$$

$$\lambda_k = \omega^2 \exp\left(-\frac{k^2 l^2}{2}\right) \sqrt{2\pi l^2} \tag{C.9}$$

$$l^2 \sim \text{Gamma}(\alpha_l, \beta_l) \tag{C.10}$$

$$\sigma_p^2 \sim IG(1,1) \tag{C.11}$$

$$v_{i,0} \sim U(0, 500) \tag{C.12}$$

the full posterior distribution for the unknown parameters given the priors can be written as

$$p(\vec{a},\vec{b},\vec{v},\sigma_p^2,l|\vec{y}) \propto \prod_{i=1}^{i=N}\prod_{t=0}^{t=T}\exp(-\frac{(y_{i,t}-v_{i,t})^2}{2\sigma_m^2})\times \tag{C.13}$$

$$\prod_{i=1}^{i=N}\prod_{t=0}^{t=T}(\sigma_p^2)^{-\frac{1}{2}}\exp\left(-\frac{1}{2\sigma_p^2}\left(v_{i,t}-\left(\delta_t v_{i,t-1}+\sum_{k=0}^{k=\infty}\{a_k\mathcal{I}_{\mathcal{C}}(k,t)+b_k\mathcal{I}_{\mathcal{S}}(k,t)\}\right)\right)^2\right)\times \tag{C.14}$$

$$\prod_{k=0}^{k=K}(\lambda_k)^{-\frac{1}{2}}\exp\left(-\frac{a_k^2}{2\lambda_k}\right)\times\prod_{k=0}^{k=K}(\lambda_k)^{-\frac{1}{2}}\exp\left(-\frac{b_k^2}{2\lambda_k}\right)\times \tag{C.15}$$

$$p(l^2)p(\sigma_p^2)\prod_{i=1}^{i=N}p(v_{i,0}) \tag{C.16}$$

I can then derive full posterior marginals to do MCMC sampling.

$$p(\sigma_p^2|a_j,\vec{b},\vec{v},l,\vec{y}) \sim \Gamma^{-1}(\alpha_p+\frac{NT}{2},$$
$$\sum_{i=1}^{N}\sum_{t=0}^{T}\frac{1}{2}\left(v_{i,t}-\left(\delta_t v_{i,t-1}+\sum_{k=0}^{k=\infty}\{a_k\mathcal{I}_{\mathcal{C}}(k,t)+b_k\mathcal{I}_{\mathcal{S}}(k,t)\}\right)\right) \tag{C.17}$$

$$p(\vec{v}|a_j,\vec{b},\vec{v},\sigma_p^2,l,\vec{y}) \sim \Gamma^{-1}(\alpha_p+\frac{NT}{2},$$
$$\sum_{i=1}^{N}\sum_{t=0}^{T}\frac{1}{2}\left(v_{i,t}-\left(\delta_t v_{i,t-1}+\sum_{k=0}^{k=\infty}\{a_k\mathcal{I}_{\mathcal{C}}(k,t)+b_k\mathcal{I}_{\mathcal{S}}(k,t)\}\right)\right) \tag{C.18}$$

$$p(a_j|\vec{b},\vec{v},\sigma_p^2,l,\vec{y}) \propto$$

$$\prod_{i=1}^{i=N}\prod_{t=0}^{t=T}\exp\left(-\frac{1}{2\sigma_p^2}\left(v_{i,t}-\left(\delta_t v_{i,t-1}+\sum_{k=0}^{k=\infty}\left\{a_k\mathcal{I}_{\mathcal{C}}(k,t)+b_k\mathcal{I}_{\mathcal{S}}(k,t)\right\}\right)\right)^2\right)\times$$

$$(\lambda_j)^{-\frac{1}{2}}\exp\left(-\frac{a_j^2}{2\lambda_j}\right) \tag{C.19}$$

$$\propto$$

$$\prod_{i=1}^{i=N}\prod_{t=0}^{t=T}\exp\left(-\frac{1}{2\sigma_p^2}\left(v_{i,t}-\left(\delta_t v_{i,t-1}+\sum_{\substack{k=0\\k\neq j}}^{k=\infty}\left\{a_k\mathcal{I}_{\mathcal{C}}(k,t)+b_k\mathcal{I}_{\mathcal{S}}(k,t)\right\}\right)-a_j\mathcal{IC}(j,t)\right)^2\right)\times$$

$$(\lambda_j)^{-\frac{1}{2}}\exp\left(-\frac{a_j^2}{2\lambda_j}\right) \tag{C.20}$$

$$\propto$$

$$\prod_{i=1}^{i=N}\prod_{t=0}^{t=T}\exp\left(-\frac{\mathcal{IC}(j,t)^2}{2\sigma_p^2}\left(\frac{v_{i,t}-\left(\delta_t v_{i,t-1}+\sum_{\substack{k=0\\k\neq j}}^{k=\infty}\left\{a_k\mathcal{I}_{\mathcal{C}}(k,t)+b_k\mathcal{I}_{\mathcal{S}}(k,t)\right\}\right)}{\mathcal{IC}(j,t)}-a_j\right)^2\right)\times$$

$$(\lambda_j)^{-\frac{1}{2}}\exp\left(-\frac{a_j^2}{2\lambda_j}\right) \tag{C.21}$$

If I then define

$$\tau_t^2=\frac{\sigma_p^2}{\mathcal{IC}(j,t)^2} \tag{C.22}$$

$$\xi_{i,t}=\frac{v_{i,t}-\left(\delta_t v_{i,t-1}+\sum_{\substack{k=0\\k\neq j}}^{k=\infty}\left\{a_k\mathcal{I}_{\mathcal{C}}(k,t)+b_k\mathcal{I}_{\mathcal{S}}(k,t)\right\}\right)}{\mathcal{IC}(j,t)} \tag{C.23}$$

Then

$$\propto$$

$$\prod_{i=1}^{i=N}\prod_{t=0}^{t=T}\exp\left(-\frac{1}{2\tau_t^2}\left(\xi_{i,t}-a_j\right)^2\right)\times\exp\left(-\frac{a_j^2}{2\lambda_j}\right) \tag{C.24}$$

$$=\prod_{i=1}^{i=N}\prod_{t=0}^{t=T}\exp\left(-\frac{1}{2\tau_t^2}\left(\xi_{i,t}-a_j\right)^2-\frac{a_j^2}{2\lambda_j}\right) \tag{C.25}$$

$$=\exp\left(\sum_{i=1}^{i=N}\sum_{t=1}^{t=T}-\frac{1}{2\tau_t^2}\left(\xi_{i,t}-a_j\right)^2-\frac{a_j^2}{2\lambda_j}\right) \tag{C.26}$$

$$=\exp\left(\sum_{i=1}^{i=N}\sum_{t=1}^{t=T}-\frac{1}{2\tau_t^2}\left(\xi_{i,t}^2-2a_j\xi_{i,t}+a_j^2\right)-\frac{a_j^2}{2\lambda_j}\right) \tag{C.27}$$

$$=\exp\left(-\sum_{i=1}^{i=N}\sum_{t=1}^{t=T}\frac{\xi_{i,t}^2}{2\tau_t^2}+2a_j\sum_{i=1}^{i=N}\sum_{t=1}^{t=T}\frac{\xi_{i,t}}{2\tau_t^2}-a_j^2\left(\sum_{i=1}^{t=N}\sum_{t=1}^{t=T}\frac{1}{2\tau_t^2}+\frac{1}{2\lambda_j}\right)\right) \tag{C.28}$$

$$\propto$$

$$\exp\left(2a_j\sum_{i=1}^{i=N}\sum_{t=1}^{t=T}\frac{\xi_{i,t}}{2\tau_t^2}-a_j^2\left(\sum_{i=1}^{i=N}\sum_{t=1}^{t=T}\frac{1}{2\tau_t^2}+\frac{1}{2\lambda_j}\right)\right) \tag{C.29}$$

$$=\exp\left(-\frac{1}{2}\left(\sum_{i=1}^{i=N}\sum_{t=1}^{t=T}\frac{1}{\tau_t^2}+\frac{1}{\lambda_j}\right)\left(a_j-\left(\sum_{i=1}^{i=N}\sum_{t=1}^{t=T}\frac{\xi_{i,t}}{1\tau_t^2}\right)\left(\sum_{i=1}^{i=N}\sum_{t=1}^{t=T}\frac{1}{\tau_t^2}+\frac{1}{\lambda_j}\right)^{-1}\right)^2\right) \tag{C.30}$$

$$a_j\sim N\left(\left(\sum_{i=1}^{i=N}\sum_{t=1}^{t=T}\frac{\xi_{i,t}}{\tau_t^2}\right)\left(\sum_{i=1}^{i=N}\sum_{t=1}^{t=T}\frac{1}{\tau_t^2}+\frac{1}{\lambda_j}\right)^{-1},\left(\sum_{i=1}^{i=N}\sum_{t=1}^{t=T}\frac{1}{\tau_t^2}+\frac{1}{\lambda_j}\right)^{-1}\right) \tag{C.31}$$

The derivation for the full conditional for b_j is identical to that of a_j.

C.2 Approximation for Eigenvalues of Squared Exponential Covariance Kernel

In Chapter 4, I rely on the approximation of the eigenvalues corresponding to the eigenproblem

$$\int_{T_{\min}}^{T_{\max}} k(T,T')h_k(T)dT = h_k(T')\lambda_k \tag{C.32}$$

In the approximation that I utilize, I allow the bounds $T_{\min}$ and $T_{\max}$ to to go $-\infty$ and ∞ respectively. In this appendix I first provide a bound for the error that results from this approximation and then show the derivation of the solution to this eigenvalue problem.

C.2.1 Bounding the Error

$$E = \int_{-\infty}^{\infty} \exp\left(-\frac{T-T'}{2l^2}\right)\cos(kT)dT - \int_{T_{\min}}^{T_{\max}} \exp\left(-\frac{T-T'}{2l^2}\right)\cos(kT)dT \tag{C.33}$$

$$= \int_{-\infty}^{T_{\min}} \exp\left(-\frac{T-T'}{2l^2}\right)\cos(kT)dT + \int_{T_{\max}}^{\infty} \exp\left(-\frac{T-T'}{2l^2}\right)\cos(kT)dT \tag{C.34}$$

$$|E| = \left|\int_{-\infty}^{T_{\min}} \exp\left(-\frac{T-T'}{2l^2}\right)\cos(kT)dT + \int_{T_{\max}}^{\infty} \exp\left(-\frac{T-T'}{2l^2}\right)\cos(kT)dT\right| \tag{C.35}$$

$$\leq \left|\int_{-\infty}^{T_{\min}} \exp\left(-\frac{T-T'}{2l^2}\right)\cos(kT)dT\right| + \left|\int_{T_{\max}}^{\infty} \exp\left(-\frac{T-T'}{2l^2}\right)\cos(kT)dT\right| \tag{C.36}$$

$$\leq \int_{-\infty}^{T_{\min}} \left|\exp\left(-\frac{T-T'}{2l^2}\right)\right| |\cos(kT)|\, dT + \int_{T_{\max}}^{\infty} \left|\exp\left(-\frac{T-T'}{2l^2}\right)\right| |\cos(kT)|\, dT \tag{C.37}$$

$$= \int_{-\infty}^{T_{\min}} \left|\exp\left(-\frac{T-T'}{2l^2}\right)\right| dT + \int_{T_{\max}}^{\infty} \left|\exp\left(-\frac{T-T'}{2l^2}\right)\right| dT \tag{C.38}$$

$$= \int_{-\infty}^{T_{\min}} \exp\left(-\frac{T-T'}{2l^2}\right) dT + \int_{T_{\max}}^{\infty} \exp\left(-\frac{T-T'}{2l^2}\right) dT \tag{C.39}$$

$$\text{let } u = \frac{T-T'}{l}, \text{ then } du = \frac{dT}{l} \tag{C.40}$$

$$= l\left[\int_{-\infty}^{u_{\min}} \exp\left(-\frac{u^2}{2}\right) du + \int_{u_{\max}}^{\infty} \exp\left(-\frac{u^2}{2}\right) du\right] \tag{C.41}$$

$$= l\left[\int_{-\infty}^{u_{\min}} -\frac{1}{u}\frac{d}{du}\left\{\exp\left(-\frac{u^2}{2}\right)\right\} du + \int_{u_{\max}}^{\infty} -\frac{1}{u}\frac{d}{du}\left\{\exp\left(-\frac{u^2}{2}\right)\right\}\right] du \tag{C.42}$$

$$= l\left[-\frac{1}{u}\exp\left(-\frac{u^2}{2}\right)\Big|_{-\infty}^{u_{min}} - \int_{-\infty}^{u_{\min}} \frac{1}{u^2}\exp\left(-\frac{u^2}{2}\right) du + -\frac{1}{u}\exp\left(-\frac{u^2}{2}\right)\Big|_{u_{\min}}^{\infty} - \int_{u_{\max}}^{\infty} \frac{1}{u^2}\exp\left(-\frac{u^2}{2}\right) du\right] \tag{C.43}$$

$$= l\left[-\frac{1}{u_{\min}}\exp\left(-\frac{u_{\min}^2}{2}\right) - \int_{-\infty}^{u_{\min}} \frac{1}{u^2}\exp\left(-\frac{u^2}{2}\right) du + \frac{1}{u_{\max}}\exp\left(-\frac{u_{\max}^2}{2}\right) - \int_{u_{\max}}^{\infty} \frac{1}{u^2}\exp\left(-\frac{u^2}{2}\right) du\right] \tag{C.44}$$

$$= l\left[-\frac{l}{T_{\min}-T'}\exp\left(-\frac{(T_{\min}-T')^2}{2l^2}\right) - \int_{-\infty}^{u_{\min}} \frac{1}{u^2}\exp\left(-\frac{u^2}{2}\right) du + \frac{l}{T_{\max}-T'}\exp\left(-\frac{(T_{\max}-T')^2}{2l^2}\right) - \int_{u_{\max}}^{\infty} \frac{1}{u^2}\exp\left(-\frac{u^2}{2}\right) du\right] \tag{C.45}$$

The leading term of the error

$$\frac{l^2}{T_{\max}-T'}\exp\left(-\frac{(T_{\max}-T')^2}{2l^2}\right)-\frac{l^2}{T_{\min}-T'}\exp\left(-\frac{(T_{\min}-T')^2}{2l^2}\right) \tag{C.46}$$

C.2.2 Approximation of the Eigenvalues

$$\lambda_k\cos(kT')=\int_{-\infty}^{\infty}e^{-\frac{(T-T')^2}{2l^2}}\cos(kT)dT \tag{C.47}$$

$$=\int_{-\infty}^{\infty}e^{-\frac{(T-T')^2}{2l^2}}\left(\frac{e^{ikT}+e^{-ikT}}{2}\right)dT \tag{C.48}$$

$$=\frac{1}{2}\left[\int_{-\infty}^{\infty}e^{-\frac{(T-T')^2}{2l^2}}e^{ikT}dT+\int_{-\infty}^{\infty}e^{-\frac{(T-T')^2}{2l^2}}e^{-ikT}dT\right] \tag{C.49}$$

$$=\frac{1}{2}\left[\int_{-\infty}^{\infty}e^{-\frac{1}{2l^2}((T-T')^2-2ikTl^2)}dT+\int_{-\infty}^{\infty}e^{-\frac{1}{2l^2}((T-T')^2+2ikTl^2)}dT\right] \tag{C.50}$$

$$=\frac{1}{2}\left[\int_{-\infty}^{\infty}e^{-\frac{1}{2l^2}(T^2-2TT'+T'^2-2ikTl^2}dT+\int_{-\infty}^{\infty}e^{-\frac{1}{2l^2}(T^2-2TT'+T'^2+2ikTl^2)}dT\right] \tag{C.51}$$

$$=\frac{1}{2}\left[\int_{-\infty}^{\infty}e^{-\frac{1}{2l^2}(T^2-2T(T'+ikTl^2)+T'^2)}dT+\int_{-\infty}^{\infty}e^{-\frac{1}{2l^2}(T^2-2T(T'-ikTl^2)+T'^2)}dT\right] \tag{C.52}$$

$$=\frac{1}{2}\left[\int_{-\infty}^{\infty}e^{-\frac{1}{2l^2}((T-(T'+ikTl^2))^2-(T'+ikTl^2)^2+T'^2)}dT\right.$$
$$\left.+\int_{-\infty}^{\infty}e^{-\frac{1}{2l^2}((T-(T'+ikTl^2))^2-(T'-ikTl^2)^2+T'^2)}dT\right] \tag{C.53}$$

$$=\frac{1}{2}e^{-\frac{1}{2l^2}T'^2}\left[\int_{-\infty}^{\infty}e^{-\frac{1}{2l^2}(T-(T'+ikl^2))^2}e^{\frac{1}{2l^2}(T'+ikl^2)^2}dT\right.$$
$$\left.+\int_{-\infty}^{\infty}e^{-\frac{1}{2l^2}(T-(T'-ikl^2))^2}e^{\frac{1}{2l^2}(T'-ikl^2)^2}dT\right] \tag{C.54}$$

$$=\frac{1}{2}e^{-\frac{1}{2l^2}T'^2}\left[e^{\frac{1}{2l^2}(T'+ikl^2)^2}\int_{-\infty}^{\infty}e^{-\frac{1}{2l^2}(T-(T'+ikl^2))^2}dT\right.$$
$$\left.+e^{\frac{1}{2l^2}(T'-ikl^2)^2}\int_{-\infty}^{\infty}e^{-\frac{1}{2l^2}(T-(T'-ikl^2))^2}dT\right] \tag{C.55}$$

$$= \frac{1}{2} e^{-\frac{1}{2l^2}T'^2} \left[e^{\frac{1}{2l^2}(T'+ikl^2)^2} \sqrt{(2\pi l^2)} + e^{\frac{1}{2l^2}(T'-ikl^2)^2} \sqrt{(2\pi l^2)} \right] \tag{C.56}$$

$$= \frac{1}{2} e^{-\frac{1}{2l^2}T'^2} \sqrt{(2\pi l^2)} \left[e^{\frac{1}{2l^2}(T'+ikl^2)^2} + e^{\frac{1}{2l^2}(T'-ikl^2)^2} \right] \tag{C.57}$$

$$= \frac{1}{2} e^{-\frac{1}{2l^2}T'^2} \sqrt{2\pi l^2} \left[e^{\frac{1}{2l^2}(T'^2+2T'ikl^2+(ikl^2)^2)} + e^{\frac{1}{2l^2}(T'^2-2T'ikl^2+(ikl^2)^2)} \right] \tag{C.58}$$

$$= \frac{1}{2} e^{-\frac{1}{2l^2}T'^2} \sqrt{2\pi l^2)} \left[e^{\frac{1}{2l^2}(T'^2+2T'ikl^2-k^2(l^2)^2)} + e^{\frac{1}{2l^2}(T'^2-2T'ikl^2-k^2(l^2)^2)} \right] \tag{C.59}$$

$$= \frac{1}{2} e^{-\frac{1}{2l^2}T'^2} \sqrt{2\pi l^2)} \left[e^{\frac{1}{2l^2}(T'^2-k^2(l^2)^2)} \left(e^{ikT'} + e^{-ikT'} \right) \right] \tag{C.60}$$

$$= e^{-\frac{1}{2l^2}T'^2} \sqrt{2\pi l^2} \left[e^{\frac{1}{2l^2}(T'^2-k^2(l^2)^2)} \left(\frac{e^{ikT'} + e^{-ikT'}}{2} \right) \right] \tag{C.61}$$

$$= e^{-\frac{1}{2l^2}T'^2} \sqrt{2\pi l^2} e^{\frac{1}{2l^2}(T'^2-k^2(l^2)^2)} \cos(kT') \tag{C.62}$$

$$= e^{-\frac{k^2 l^2}{2}} \sqrt{2\pi l^2} \cos(kT') \tag{C.63}$$

The integration procedure follows nearly identically for the coefficients associated with sine eigenfunctions and yields the identical coefficients.

C.3 Inclusion of Time Varying Food Levels

In Chapter 4, I analyzed data from the experiment on steelhead trout performed by Beakes et al. (2010). During that analysis, I neglected to account for the knowledge that there was time varying feeding treatments during the experiment. Beakes et al. (2010) report the ration volume fed to the different treatments as a percentage of total biomass of individuals in the two different feeding treatments (low and high). I attempt to incorporate this knowledge and perform inference with the model by scaling the consumption function, Φ_C, by these percentages during the respective feeding treatment times. The the treatment called for high and low feeding treatments over the last 8 measurement times as follows

From the analysis of the model that includes time varying feeding treatments, the

Measurement	2006	2007
1	3	2
2	2	1
3	2	1
4	3	3
5	3	3
6	3	3
7	3	3
8	3	3

Table C.1: Feeding regimes for treatment 2 as a percentage of biomass as reported in **?**. Values correspond to feeding level during period prior to measurement

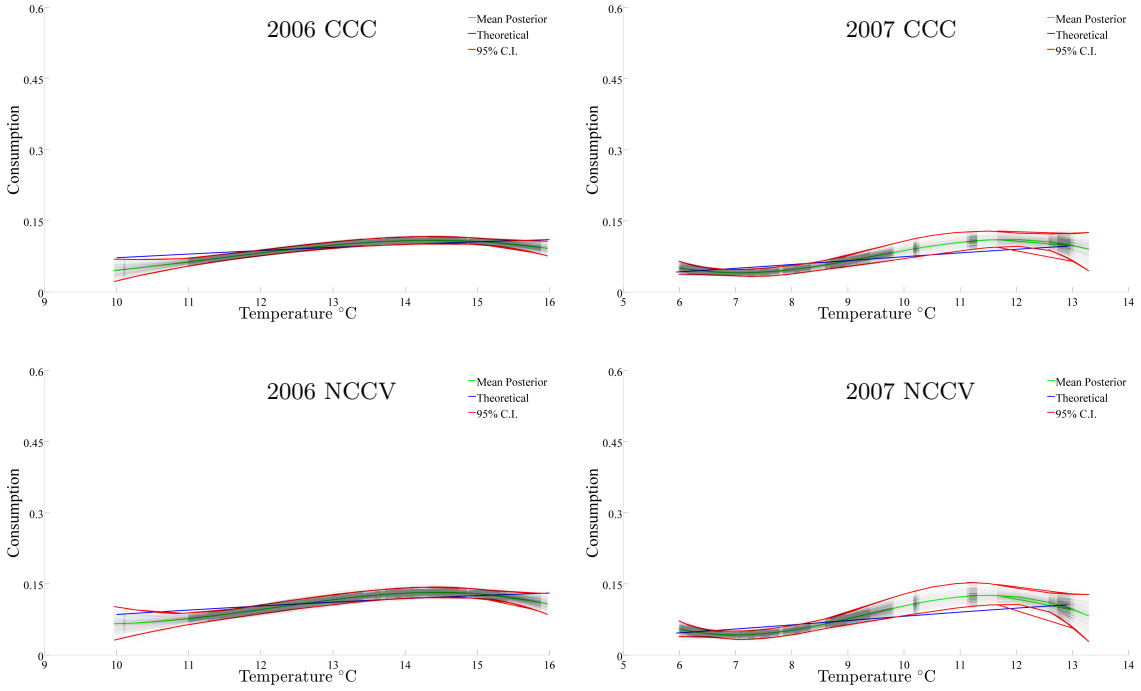

Figure C.1: Posterior estimates of the consumption-temperature relationship for the temperature ranges that were experienced by the individuals in the four different experimental treatments.

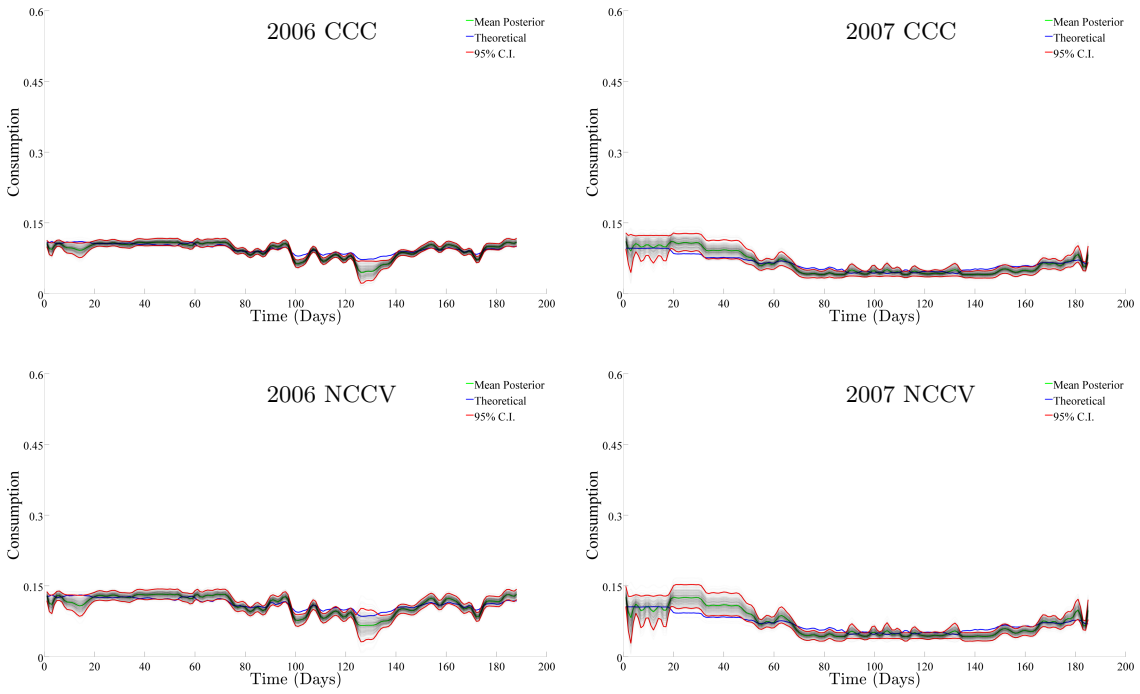

Figure C.2: Posterior estimates of the consumption of individuals as a function of time for the four different experimental treatments.

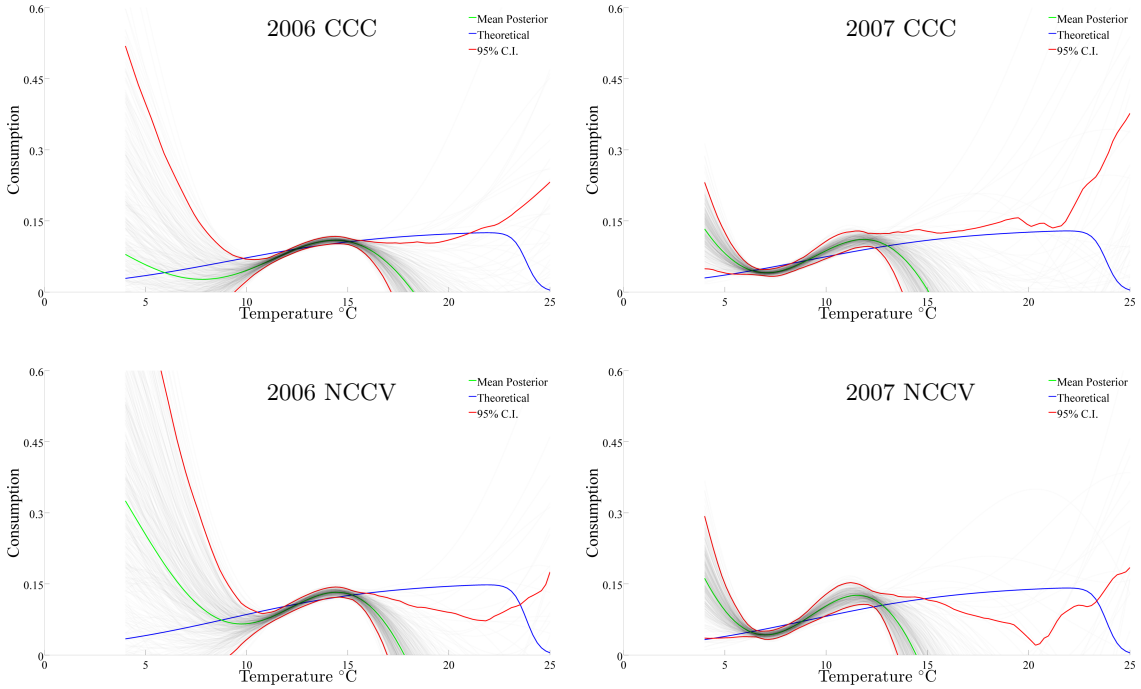

Figure C.3: Posterior predictive estimates of the consumption-temperature relationship for temperature ranges commonly experienced by steelhead in natural systems based on inference from the four different experimental treatments.

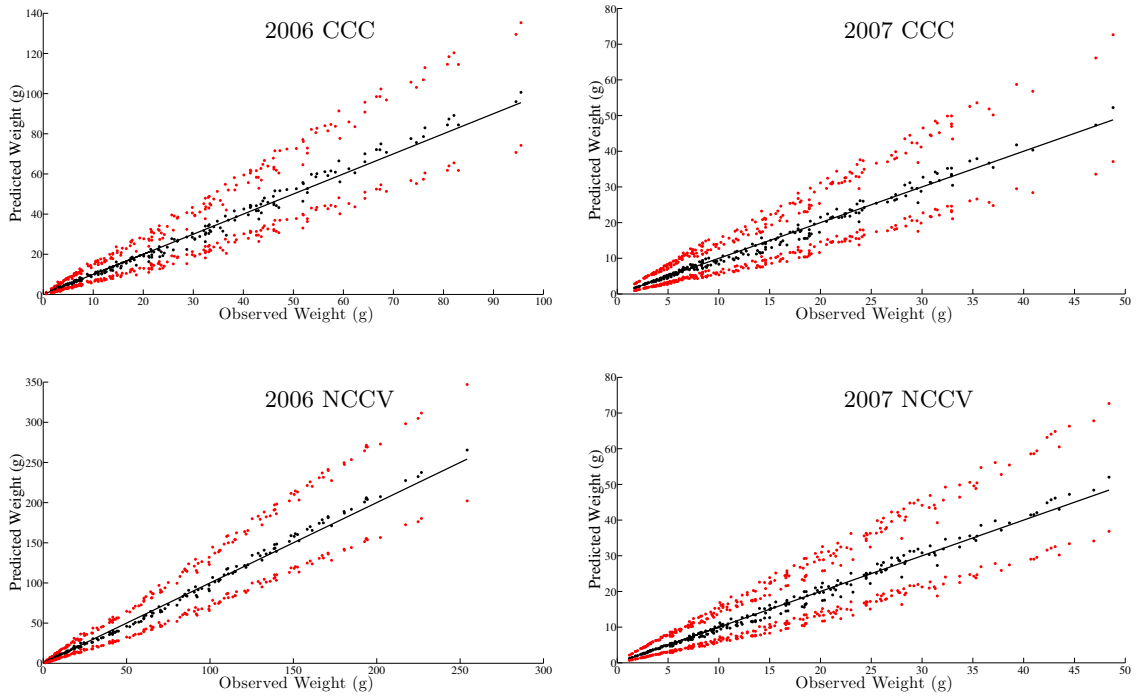

Figure C.4: Posterior predictive estimates of the consumption-temperature relationship for temperature ranges commonly experienced by steelhead in natural systems based on inference from the four different experimental treatments.

knowledge or the way in which i've incorporated it do not improve the predictions. Making judgment on the temperature-consumption relationship is a difficult task. The relationship derived from this analysis seems to have a different slope and be more curved in the region that temperature is experienced. Nonetheless the model is still able to capture the inference on individual growth.